TECHNISCHE UNIVERSITÄT MÜNCHEN

Lehrstuhl für Technische Chemie II

Formation and reactions of hydrogen-deficient species during the conversion of methanol and dimethyl ether on MFI zeolites

Felix Martin Kirchberger

Vollständiger Abdruck der von der Fakultät für Chemie der Technischen Universität München zur Erlangung des akademischen Grades eines

Doktors der Naturwissenschaften (Dr. rer. nat.)

genehmigten Dissertation.

Vorsitzender: Prof. Dr. Hubert A. Gasteiger

Prüfer der Dissertation:

1. Prof. Dr. Johannes A. Lercher

2. Prof. Dr. Klaus Köhler

3. Prof. Gary L. Haller, Ph.D.

Die Dissertation wurde am 12.06.2019 bei der Technischen Universität München eingereicht und durch die Fakultät für Chemie am 24.07.2019 angenommen.

Bevor der Mensch zu einer Wahrheit gelangt, geht er auf so vielen Umwegen, verfängt er sich in so vielen Widersprüchen, tut so viel Falsches, dass er sich nachher selbst über seinen Mangel an Scharfsinn wundert.

Nicolai Wassiljewitsch Gogol

Für meine Eltern

Acknowledgements

First of all, I want to thank Prof. Dr. Johannes A. Lercher for giving me the opportunity to be part of his group and to work on this interesting and highly inspiring project. You were always there when your creativity and sheer endless knowledge was needed and you left me on the long leash whenever you thought this was possible. And a special thanks for training me before the talks I gave on several occasions. I had a good time with you Johannes!

I furthermore want to thank Maricruz Sanchez-Sanchez and Yue Liu. You helped me immensely during the last years through scientific discussions, corrections of drafts and supporting me in all stages of my thesis.

A special thanks goes to:

My master thesis supervisor Peter Hintermeier and a group of “old hands” who helped me to integrate into the group and from whom I have learned a lot: Andreas Ehrmaier, Mathias Steib, Sebastian Eckstein, Stanislav Kasakov, Sylvia Albersberger, Moritz Schreiber, my predecessors Sebastian Müller and Jürgen Hajdo and especially Manuel Wagenhofer, who helped me with basically everything that broke or did otherwise malfunction in the lab during my first 1.5 years.

All my colleagues at TCll that accompanied and supported me till the end (or at least close to) of my thesis: Andreas Ehrmaier, Daniel Melzer, Ferdinand Vogelgsang, Manuel Weber, Martin Baumgärtl, Verena Höpfl, Teresa Schachtl, Roland Weindl, Edith Berger, Lara Milakovic, Laura Löbbert, Yang Zhang, Wanqiu Luo, Christoph Denk, Takaaki Ikuno, Ruixue Zhao, Alexander Wellmann, Niklas Pfriem, Mirjam Wenig, Insu Lee and Martina Aigner.

My colleagues from the LOC cluster and project partners from Clariant in the context of the MuniCat cooperation: Sebastian Standl, Philipp Donaubauer, Richard Fischer and Markus Tonigold.

All other employees on TC ll that keep the chair running: Franz-Xaver Hecht, Martin Neukamp, Andreas Marx, Bettina Federmann, Stefanie Seibold, Kateryna Kryvko, and Ulrike Sanwald.

The soccer crew: Sebastian Foraita, Bo Peng, Guoju Yang, Marco Peroni, Pilipp Pfauser, Korbi Huber, Sebastian “Ecki” Eckstein, Peter Hintermeier, Harry Rengus, Martin Baumgärtl, Andreas Ehrmaier, Laura Löbbert and especially all the players who helped me to achieve what I wanted to achieve since my first summer in Garching: Winning the trophy of the Fachschaft football tournament: Daniel Melzer, Daniel Hirche, Philipp Donaubauer, Thomas Burger, Ricardo Bermejo

Deval, Roland Weindl (in line with Rahn, Müller, Brehme and Götze), Ferdinand Vogelgsang, Thomas Kleiner, Manuel Weber and Matthias Stocker.

A long list of students I had the pleasure to work with: Laura Tebcharani, Greta Zambo, Hanna Türk, Batool Raza, Clara Eisebraun, Andres Jurzyk, Philipp Fischer, Duc Hien Nguyen and especially my master students Korbinian Huber and Moritz Eder.

Everybody who shared the experience of studding chemistry at the TUM with me. I would particularly like to mention the close friends that I have found: Markus Pschenitza, Pauline Fischer and Sebastian Helmbrecht. I would have not come that far without you.

All my friends outside of the faculty of chemistry you enabled me to relax apart from my work and studies and helped me to become the person that I am today.

Mein besonderer Dank gilt meiner Familie. Meinen Eltern Eva und Albert für ihre immerwährende Unterstützungen seit ich denken kann. Meiner Schwester Eva, besonders dafür, dass sie sich Zeit genommen hat, wenn ich Unterstützung brauchte während meines Studiums oder meiner Promotion. Meiner Freundin Anna für ihre Liebe und bedingungslosen Unterstützung während all meiner Launen und Zweifel während der letzten Jahre.

Felix

June, 2019

Abbreviations

BAS	**B**rønsted **A**cid **S**ite
BPD	**B**arrels **P**er **D**ay
CHA	**Cha**bazite
EFAl	**E**xtra **F**ramework **Al**uminum
Fig.	**Fig**ure
HC	**H**ydro**c**arbon
HT	**H**ydrogen **T**ransfer
LAS	**L**ewis **A**cid **S**ite
MFI	Framework type from Zeolite Socony **M**obil **Fi**ve
MIHT	**M**ethanol **I**nduced **H**ydrogen **T**ransfer
MTA	**M**ethanol **t**o **A**romatics
MTH	**M**ethanol **t**o **H**ydrocarbons
MTO	**M**ethanol **t**o **O**lefins
MTP	**M**ethanol **t**o **P**ropylene
OIHT	**O**lefin **I**nduced **H**ydrogen **T**ransfer
Rxn.	Reaction
SAPO-34	**S**ilico**a**lumino**p**h**o**sphate-34
SI	**S**upporting **I**nformation
ZSM-5	**Z**eolite **S**ocony **M**obil **5**
TOS	**T**ime **o**n **S**tream

Abstract

The formation of formaldehyde and CO from methanol is a key intermediate step for the generation of first C-C bond containing species in the zeolite catalyzed conversion of methanol. The intrinsic formation rate of HCHO from dimethyl ether is one order of magnitude higher than that from methanol. In subsequent reaction steps, formaldehyde enhances formation of aromatics via Prins type reactions. Introduction of dehydrogenation functionality in ZSM-5 by Ga ions selectively increases formation of aromatics without generation of undesired light alkanes.

Kurzzusammenfassung

Bei der sauer katalysierten Umsetzung von Methanol zu Kohlenwasserstoffen ist die Bildung von Formaldehyd und CO ein entscheidender Zwischenschritt für die Entstehung der ersten Moleküle mit C-C Bindung. Die intrinsische Rate der Formaldehydbildung aus Dimethylether ist um eine Größenordnung höher als die aus Methanol. In späteren Reaktionsschritten begünstigt Formaldehyd, über Prins Reaktionen, die Bildung von Aromaten. Werden Ga Kationen in ZSM-5 eingebracht, erhöht dies selektiv die Bildungsrate von Aromaten ohne kurzkettige Alkane zu bilden.

Table of contents

1. General introduction

1.1 Methanol to hydrocarbon technology

In our fast changing energy and resource landscape it is a necessity for the chemical industry to provide processes that cannot only produce the demanded substances, but are also flexible in the choice of feedstock. Long term predictions of which carbon feedstocks will be dominant over the next time period are highly difficult to make, therefore it would be even more beneficial to rely on technologies that can be easily adapted both in feedstock and product spectrum. The conversion of methanol to hydrocarbons (MTH) is one of these technologies.

The origins of this process lie in the 1970s when Chang and Silvestri managed to convert methanol to higher hydrocarbons at the Mobil research laboratories.[1] Driven by oil crisis and a generally growing demand for hydrocarbons, different processes were developed and further improved.[2] Initially, processes focusing on the formation of gasoline (methanol to gasoline, MTG) were developed and a first plant was commercially used in New Zealand by Mobil. The plant produced 14500 bpd of gasoline mainly containing C_{5+} paraffins, olefins, naphtenes and aromatics over an H-ZSM-5 catalyst.[3-4] Depending on the reaction conditions, short olefins can be produced in a large fraction in the MTG process. Consequently, Mobil developed a methanol to olefin (MTO) process, also based on H-ZSM-5 as catalyst, working at higher temperatures and lower pressure.[5-6] An improvement of this technology was the development of H-SAPO-34 by Union Carbide. This zeotype material enabled an increase of the selectivity of light olefins of up to 80%, even though it exhibits a higher tendency to coke formation than H-ZSM-5 and therefore needs a process design with continuous catalyst regeneration.[4] A further specification was the methanol to propylene (MTP) process implemented by Lurgi in the early 2000s utilizing H-ZSM-5.[7] The latest specification of the MTH process besides gasoline, olefins and propylene is the conversion into aromatics (MTA). According to forecasts, an increased amount of shale gas will be available, which might reduce the fraction of aromatics formed by the petrochemical industry.[8] MTA is considered to be a suitable alternative to react to this possible change in feedstocks. Therefore, also mainly medium pore size zeolites as ZSM-5 are tested in scientific studies, but often after additional modification with metals like gallium or zinc.[9]

Methanol as feed for all these processes can be produced from synthesis gas (a mix of H_2 and CO) over a $Cu/ZnO/Al_2O_3$ catalyst.[10] Thereby, a large variety of carbon sources, such as biomass, natural gas or coal can be utilized.[11-12] The choice of carbon resource has a significant influence on the resulting carbon footprint of the final product and strongly depends on the region where the process is applied. While China, the main methanol producer, mainly converts coal, the rest of the

world uses primarily natural gas as feedstock.[12] This has significant consequences for the environmental evaluation of the technology as a study of Yao et al. described in 2018: Based on the best practice technology, the quantity of carbon necessary for producing methanol is calculated as 889 kg carbon/ton MeOH based on coal, while it is only 378 kg carbon/ton MeOH if natural gas is used.[12]

Besides its lower CO_2 footprint, MTH technology offers the possibility of on purpose production of single products in the case that these are not fully provided by the conventional fossil-based fuel-oriented refineries. A current example for the need of an on purpose production method is the so called “propylene gap”: The already mentioned change in feed composition of steam crackers has led towards lighter feedstock during the last years. This has caused an increased ratio of produced ethylene to propylene, resulting in a propylene deficiency.[13] Furthermore, there has been an increasing demand for propylene,[7] which is the second most produced building block after ethylene with an estimated demand of 89 million tons (2014).[13] An MTH process optimized for propylene production could be able to fill this gap, together with other developing processes such as olefin metathesis and propane dehydrogenation.[13]

Overall, the usage of methanol as platform chemical obtained from different carbonaceous feedstocks and transformed into a wide range of HC products is expected to provide an interesting alternative to crude oil based processes. Consequently, several MTH plants have been launched for the last decade (mainly in China based on coal) focusing mostly on the formation of olefins.[14]

1.2 Zeolites as catalysts for the conversion of methanol to hydrocarbons

Zeolites as acidic, highly ordered porous frameworks are the backbone of modern day industrial hydrocarbon catalysis. They were first described in 1756 by the Swedish mineralogist Axel Frederick von Cronsted, who also named this new class of minerals by resorting to a combination of the greek words *zein* (to boil) and *lithos* (stone).[15-16] The term zeolite describes a silicon-aluminum mixed oxide consisting of defined crystalline building blocks. The main building unit is silica (SiO_2) with Si^{4+}-ions partly replaced by Al^{3+}. The resulting charge deficiency can either be balanced by metal-ions as Na^+ or Ca^{2+}, or by non-metallic counter ions like NH_4^+ or H^+. This characteristic of a charged framework with interchangeable counter ions provides a class of material that can be used for various applications. Thus, zeolites can be applied to soften water in laundry detergents by replacing unwanted Ca^{2+} with Na^+. If protonated they can also be used as strong solid acids, which opens up a wide field of applications.[17] Furthermore, their highly ordered channel structure and narrow pore size distribution in the range of 3 to 15 Å[15] enables different applications, for example as molecular sieves.[18]

Historically, the application of naturally obtained zeolites, which was the only method at that time, started in the early 20th century when their use as water softeners was established. As already mentioned, zeolites are heavily used in this field to this very day and are still object of recent studies.[19-20] From the 1920s onward zeolites were used based on their function as molecular sieves as described by Weigel on the example of a zeolite of the chabazite (CHA) framework for gas separation.[21] In 1948 Barrer successfully synthesized the first zeolite structures with no natural counterparts.[22] The first large scale applications as catalysts started at Union Carbide in 1957 when a zeolite type X was synthesized and brought to the protonated form with H^+-ions stabilizing the negative charge of the aluminosilicate by heat treatment. This new catalyst was tested in different reactions crucial for petroleum refining like cracking and isomerization, where it showed exceptional advantages compared to the so far commercially used amorphous silica-alumina gel catalysts.[18] Over the following decades the use of zeolites as catalysts has set the benchmark in most of the processes refining hydrocarbons to a point where an amount of 840000 metric tons per year is produced only for the application in fluid catalytic crackers around the world.[23]

Two main types of zeolites and zeotype materials are commercially applied for the conversion of methanol to hydrocarbons: H-ZSM-5 (Zeolite Socony Mobil 5) an MFI-type zeolite and Silicoaluminophosphate-34 (SAPO-34) with chabazite (CHA) framework structure (Fig. 1).[24] The MFI type consists of oxygen bridged pentasil units that build up 10-membered pores, forming both straight and zig-zag channels. In contrast, CHA has a maximum ring size of eight atoms forming only straight channels that connect significantly larger cavities.[15] The main consequence of the

different crystalline structures is that molecules of different pore size can be formed inside the zeolite and only molecules of a certain size can enter or leave the zeolite. Foster et al. calculated that in case of CHA, spheres with a maximum radius 0.737 nm can be formed in the pores, but only spheres with a radius of 0.372 nm can diffuse along the channels. In MFI only smaller molecules can be formed inside (up to 0.636 nm), but larger molecules are able to diffuse through the zeolite (up to 0.470 nm).[25]

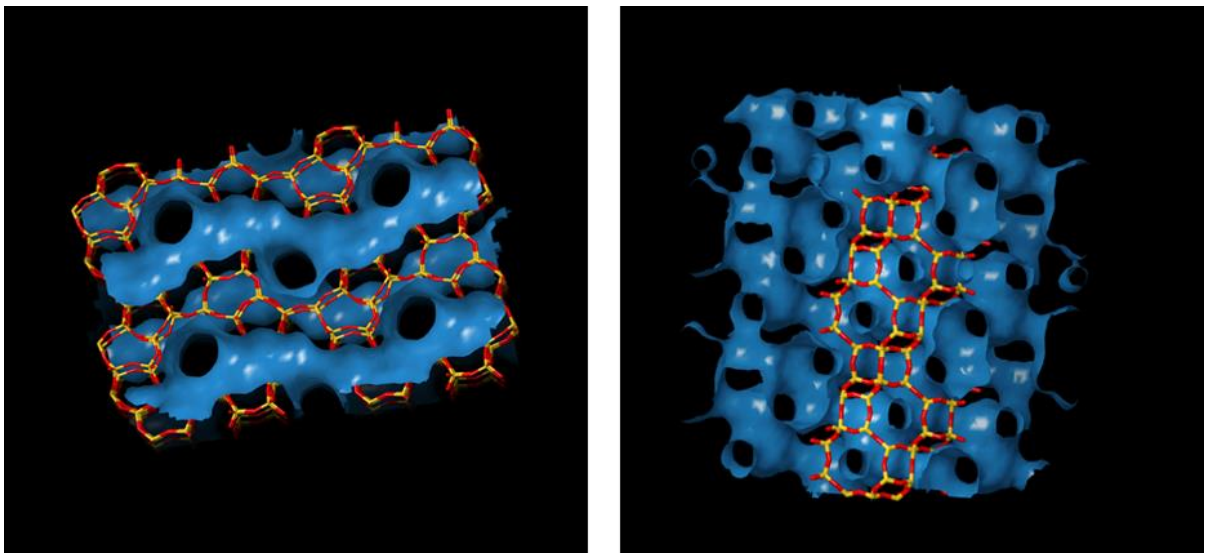

Figure 1: Framework structure of a MFI (left) and CHA (right) type, with marked silicon (yellow) and oxygen (red) atoms as well as schematic drawn channels through the pores (blue).[26]

Consequently, when applied in MTH processes, MFI zeolites are more stable with respect to coking followed by catalyst deactivation compared to CHA types, but produce a lower amount of short-chain olefins (C_3 and smaller).[5] In general, the choice of zeolite framework influences heavily the type of products formed during the conversion of MeOH or DME due to its influence on the hydrocarbon pool formed within the pores,[27] a fact that will be further described in section 1.5.

As already mentioned, the acidic nature of the zeolites is a result of the replacement of a Si^{4+} by an Al^{3+} in the framework (or, in the case of aluminophosphates of the replacement of P^{5+} by Si^{4+}). If the created charge in the lattice is balanced by a proton, a Brønsted acid site (BAS) is formed (Scheme 1).

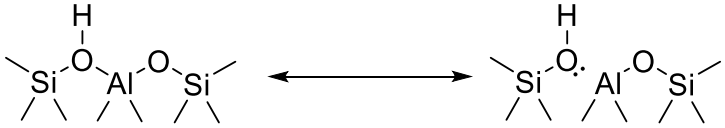

Scheme 1: Resonance structures of a Brønsted acid site (BAS) (adapted form ref.[28]).

Besides the BAS, also the formation of Lewis acid sites (LAS) occurs in zeolites. The chemical properties of LAS and BAS in zeolites are very similar to acids in solutions: While BAS are able to donate a proton, LAS are electrophilic and can attract an electron pair.[29] There are three main possibilities to form LAS in a zeolite: either by dehydration of BAS as proposed by Uytterhoeven et al. in 1965[30] (Scheme 2, I), by dehydration followed by Al leaving the zeolite framework forming an extra framework aluminum (EFAl) site[31] (Scheme 2, II) and by compensating the charge of the lattice with metal cation as for example Cu^{2+}.[32] (Scheme 2, III).

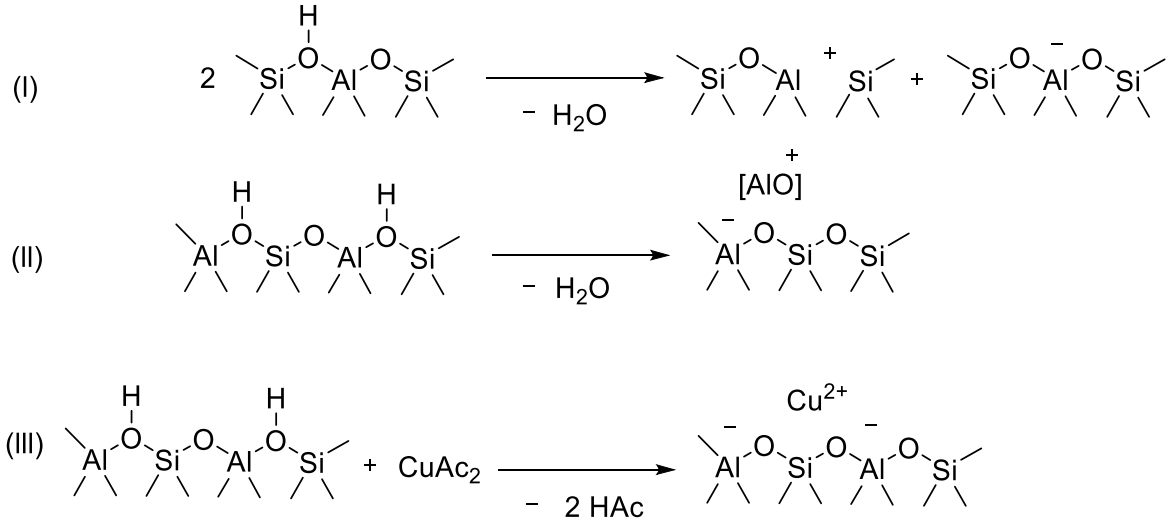

Scheme 2: Formation of Lewis acid sites (LAS) from protonated BAS. (I): Dehydration of the zeolite accompanied by the formation of a trigonal coordinated aluminum atom.[30] (II): Dehydration of the zeolite accompanied by the formation of an extra-framework aluminum species.[31] (III): Ion exchange of the H-form with copper(II)acetate forming lewis acidic copper ions balancing the charge deficiency of the zeolite framework.[32]

The overall acidity of a zeolite can be tuned by varying the Si/Al ratio, but there is an upper limit for the aluminum content given by the stability of the different framework types. An absolute maximum of Si/Al = 1 for certain frameworks is given by the *Löwenstein's rule* which states that each Al-atom has to be separated from the other Al-atom by at least one Si-bridge.[29] However, for example in the case of MFI only zeolites with a Si/Al ratio above 10 can be synthesized.[33]

1.3 Mechanistic concepts in the conversion of MeOH to hydrocarbons

The conversion of methanol to hydrocarbons over an acetic zeolite is an overall exothermic reaction, with the amount of heat released depending on the resulting product distribution.[1-2] It can be divided into several reaction steps as depicted in Scheme 3[34] based on the principles of the hydrocarbon pool mechanism proposed by Dahl and Kolboe.[35-37]

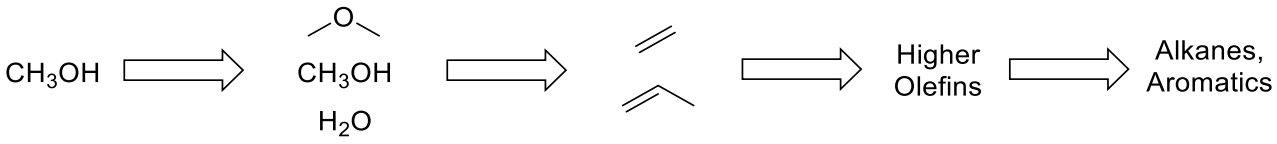

Scheme 3: Schematic of the conversion of methanol to hydrocarbons (adopted from ref.[34]).

In a first step a comparatively fast equilibration between methanol and DME is reached also forming an equimolar amount of water along with the ether. As this interconversion is also acid catalyzed and usually is faster than the subsequent reaction steps,[38] in many studies DME and methanol are considered in equilibrium and they are lumped together to determine the conversion of oxygenates.[5] The next step is the formation of the first C-C bonded products.[5] The nature of this first C-C bond coupling has been the subject of a large variety of studies over the last decade which will be discussed in the next chapter. All the approaches agree that the C-C bond coupling is slow, which results in a relatively long contact time in which the conversion of oxygenates is very low. As soon as olefins are available, methylation reactions can take place, which lead to a significantly faster consumption of MeOH and DME and the formation of higher olefins. Based on this formed pool of olefins, consecutive reactions between the hydrocarbons can take place, such as cracking reactions or hydrogen transfer (HT) reactions, which are expected to form alkanes and aromatics.[4-5] The nature of the slow C-C bond formation followed by a faster methylation of already formed olefins gives the whole reaction an autocatalytic character that was first described in the late 1970s by Chen et al.[39] Consequently, the evolution of the hydrocarbons (as well as the corresponding conversion of the oxygenates) follows a characteristic S-shape (Fig. 2).[4]

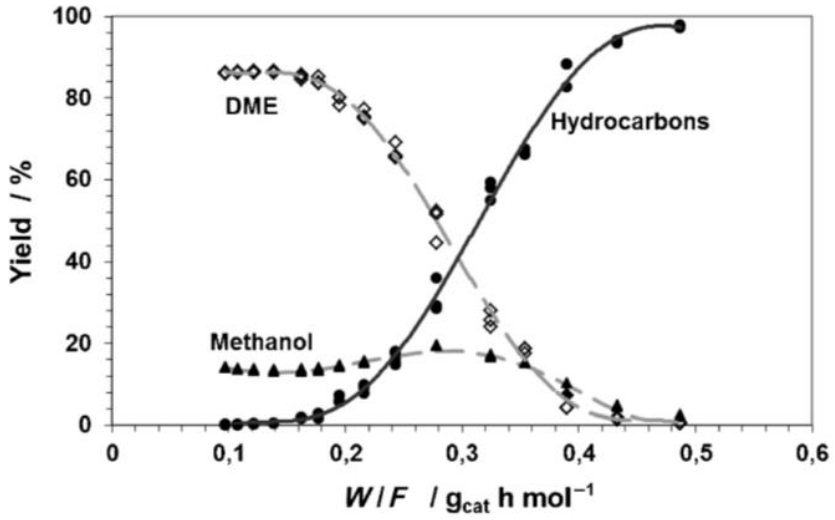

Figure 2: Hydrocarbon yield and carbon based concentrations of methanol and DME as a function of the contact time W/F.[4]

A characteristic of the MTH system is the different chemistries taking place at different contact times, such as mentioned olefin cracking and HT reactions once all the DME/MeOH has been converted. Consequently, the catalyst bed can be divided into three different sections based on the S-shape of the MeOH/DME conversion plot vs contact time: (i) The initiation zone at low contact times where MeOH/DME conversion is very low; (ii) the actual autocatalytic zone where the majority of the oxygenates are converted via methylation reactions, and (iii) the zone after total conversion has been reached, where hydrocarbon interconversions are dominant in the absence of MeOH and DME. This is of great importance as both in industrial applications and in academia plug flow reactors are often used to apply and study the MTH processes and the reaction is conducted at contact times well over the total conversion threshold.[40]

1.4 Formation of the first carbon-carbon bonds in the MTH process

Since its first description the MTH process has drawn a vast amount of scientific attention. A large fraction of the research tackled the question of how the first C-C bond starting from two MeOH molecules could be formed. Over 20 potential mechanism have been proposed until the beginning of the 21st century from radical based mechanisms[41] to oxonium-ylides,[42-43] carbenes[44] or carbocation based pathways[38] (Scheme 4).

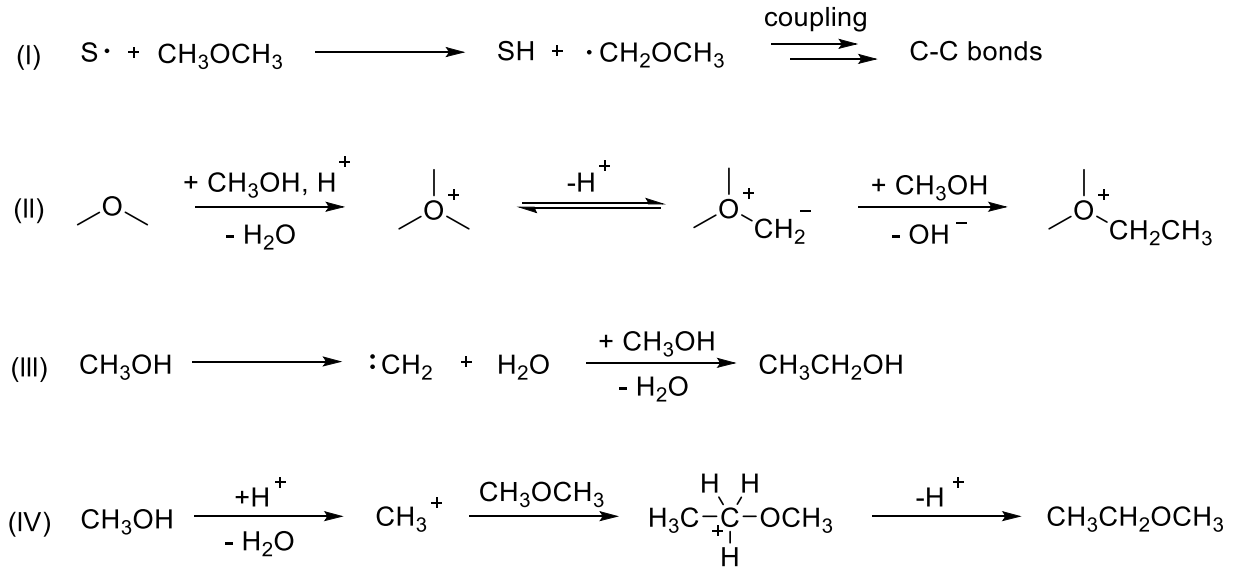

Scheme 4: Simplified reaction steps for the formation of the first C-C bond containing products from MeOH/DME. (I): Radical based surface mechanism with S• as a not further specified surface radical species. (II): An example for an oxonium-ylide based pathway. (III): A carbene-based route. (IV): One possible example for the C-C-bond formation via a carbocation. (adapted from Ref.[45])

None of these early hypothesis was proven to be a more plausible concept then the others over the decades and different computational studies found unrealistically high energy barriers for the majority of these pathways.[46] In recent years, renewed interest in the MTH process led to further mechanistic studies on the formation of C-C bond species.[47-50] The coupling of electrophilic and nucleophilic C_1-species has been proposed first by Liu et al. in 2016[49] (Scheme 5). It requires the preceding decomposition of MeOH/DME into hydrogen-poor species as CO and HCHO (formaldehyde) and hydrogen-rich methane.

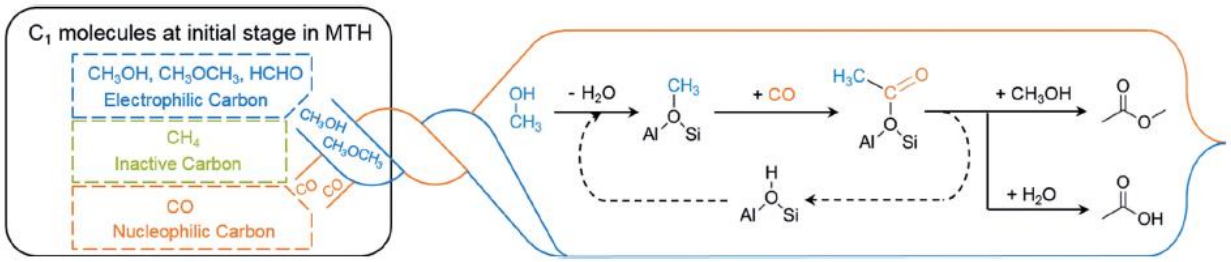

Scheme 5: First C-C bond formation pathway based on the coupling of nucleophilic and electrophilic C_1-species as proposed by Liu et al.[49]. After the insertion of a carbon monoxide molecule into a surface methoxy species the formed surface acetyl group is the first C-C bond product which is expected to desorb and be further converted providing the first olefins.

The C-C bond forming step is proposed to be the carbonylation of a surface methoxy group producing a surface acetyl group with an energy barrier of 80 kJ/mol.[49] This hypothesis has also found backing by computational studies assessing the activation barriers in correlation with the reaction rates found for the C-C-bond formation during the initiation period.[51] According to this proposal, the formation of HCHO (which subsequently produces CO) is the rate determining step in the overall pathway. Especially this formation of HCHO in the MTH catalyst has generated scientific attention recently as it is expected to play also a role in the formation of aromatics and the deactivation of the catalysts.[52-54] This proposal for a C-C bond formation pathway has been supported by the results and conclusions published by other research groups such as the study on SAPO-34 by Chowdhury et al.[50]

1.5 Mechanistic dependence of the products distribution in the MTH process

The widely accepted concept to explain the consumption of oxygenates after initial formation of the first C-C bonds and the correlation of zeolite framework and product distribution is the already mentioned hydrocarbon pool mechanism.[4, 27, 55] Based on the findings of Dahl and Kolboe[35-37] it could be shown that a hydrocarbon pool is adsorbed on the zeolite, which takes up the fed MeOH/DME and is converted to the range of products (Scheme 6). The central idea is that some species stay in the pores continuously incorporating MeOH and producing the whole spectrum of product molecules via terminating reactions such as dealkylation and hydrogen transfer.

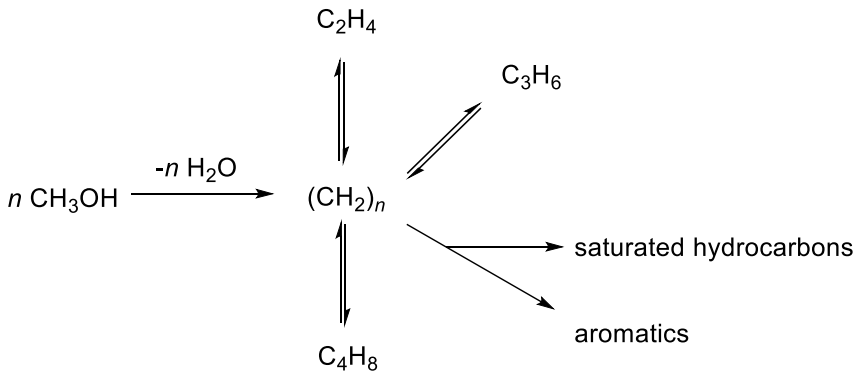

Scheme 6: Hydrocarbon-pool mechanism over SAPO-34 adapted from Dahl et al.[36]

The type of hydrocarbon species in the zeolite pores have a large influence on the products that can be formed. This is taken into account by the dual cycle concept, described in 2006 by Svelle et al.[56] Based on $^{12}C/^{13}C$ experiments in MFI an olefin - and an aromatic-based pathway were described (Scheme 7). In the olefinic cycle, linear or branched olefins are prolonged by subsequent methylation steps until their increasing thermodynamic instability results in cracking reactions producing again shorter olefins. Both cycles are linked via the possibility to form aromatics from larger alkenes by HT reactions producing alkanes as byproduct.

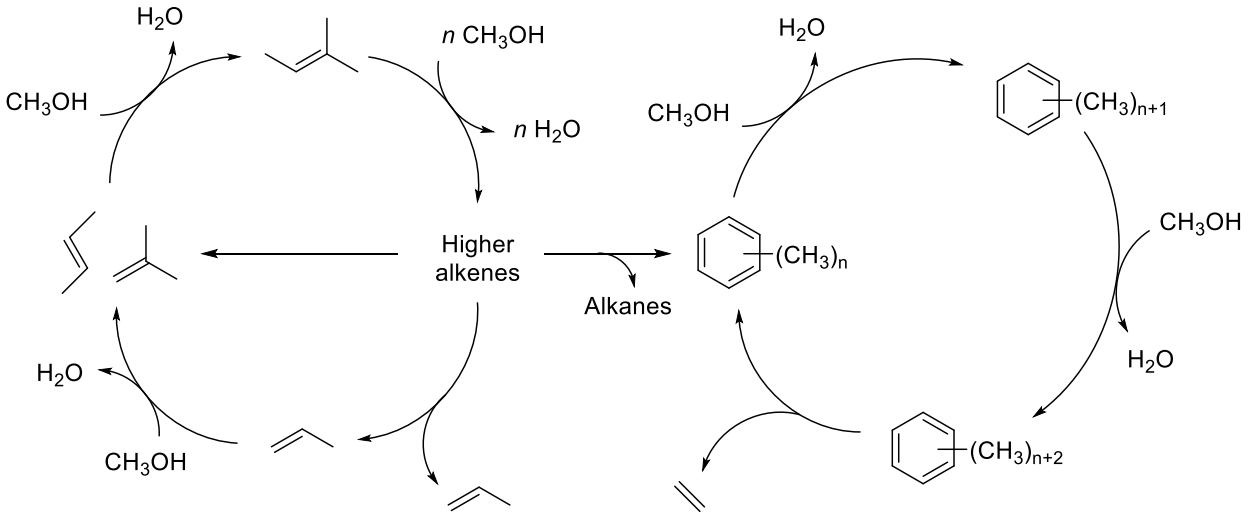

Scheme 7: Suggested dual cycle concept for the conversion of MeOH over MFI.[4] Olefinic cycle on the left aromatic cycle on the right.

In the aromatic cycle polymethylated cyclic hydrocarbons act as organic center for the formation of olefins, either methylbezenes[34] or methylated cyclopentenyl molecules[57]. These organic reaction centers further react and grow via combined paring and side-chain mechanisms.[58] Aromatics trapped or with slow diffusion in the zeolite are constantly methylated until the side chains are cleaved, producing aromatics and short olefins as soon as a certain size is reached (Scheme 8).

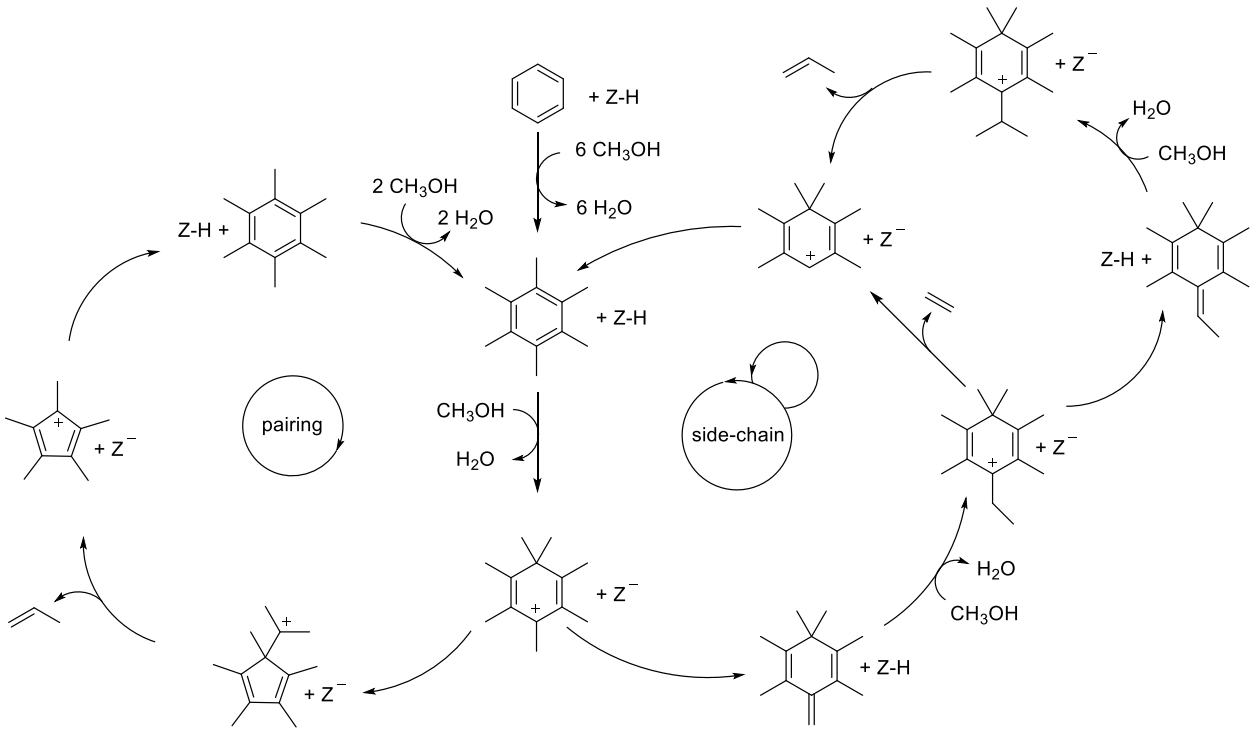

Scheme 8: Schematic of the pairing and side chain reaction mechanism adopted from Lesthaeghe et al.[58]

Distinct differences regarding the product selectivity of the two cycles could be shown: while the aromatic cycle is the main source of ethylene, the olefinic cycle produces more propylene.[56, 59] Consequently, catalysts with high HT activity which form comparatively large amounts of aromatics will also produce a larger fraction of ethylene compared to propylene[4]. Using the model of the so called dual-cycle, different attempts have been made to optimize the product distribution. If the aromatic cycle is suppressed, this leads to a maximization of the amount of propylene formed, while a dominance of the aromatic cycle leads to an increase yield of ethylene. Effective ways to favor one cycle above the other are the zeolite structure[60-63] and tuning the feed by co-feeding either olefins or aromatics together with the oxygenates.[64-65]

1.6 Hydrogen transfer reactions in the MTH process

Based on the initial reaction step of the MTH processes, the dehydrative condensation of MeOH/DME to CH_2 units, all reaction products should be hydrocarbons with an average hydrogen to carbon ratio of 2:1. As already mentioned in earlier sections hydrogen transfer (HT) processes are the reason why this is not the case and depending on the reaction conditions saturated alkanes and aromatics make a large fraction of the products. These two groups of products are often lumped as HT products. The HT steps are predominantly the combination of a hydride and a proton transfer step between two molecules in which the hydride transfer is thought to be the rate determining step.[66] Due to the fact that the tendency to donate hydrogen increases as the compounds get more unsaturated, e.g. Hazari et al. reported that the proficiency to donate hydrogen is 20 times higher in case of 1,4-cyclohexadiene as for a linear olefin,[67] the fraction of dienes and cyclic compounds in the product mix is relatively small and the hydrogen poor species are mainly aromatics and coke.[64, 66] The hydrogen transfer reactions predominant during the MTH process are different depending on the reaction zone of the catalytic bed, and they can be divided into two groups:

Hydrogen transfer between olefins and higher HCs

The hydrogen transfer reactions between olefins acting as hydrogen acceptors and other olefins or other unsaturated species as hydrogen donor (also referred to as olefin induced hydrogen transfer or OIHT[52]) (Scheme 9) is a pathway known in all types of zeolite catalyzed HC-conversion reactions.[68-69] It can occur during the conversion of MeOH/DME as soon as a certain amount of olefins has been produced and it is predominant in the last zone of the catalytic bed, once full MeOH/DME conversion has been reached.[52]

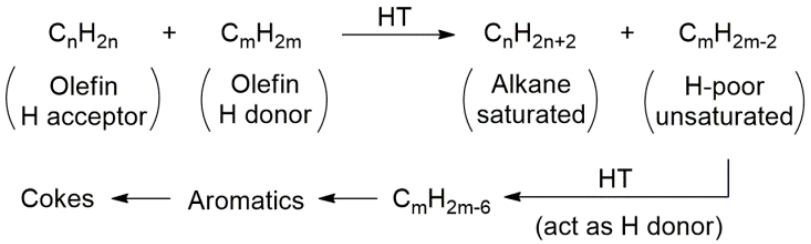

Scheme 9: Reaction scheme of HT reactions between olefins forming alkanes and aromatics (and finally coke).[52]

This reaction is considered to be catalyzed by BAS and takes place between an adsorbed alkoxide and a cyclic or acyclic alkane or alkene.[66]

Hydrogen transfer between methanol and higher HCs

In 2016, Müller et al. reported the methanol induced hydrogen transfer (MIHT)[52] in which methanol acts as hydrogen donor to an olefin, forming formaldehyde and an alkane. The formation of formaldehyde is considered to be the rate determining step and takes place on LAS while subsequent reactions of the mechanism are catalyzed by BAS and are comparatively fast.[52] Collectively, these reaction steps in combination with cyclization reactions will dominate the formation of alkanes and aromatics in the methylation zone of the catalyst (Scheme 10).[52]

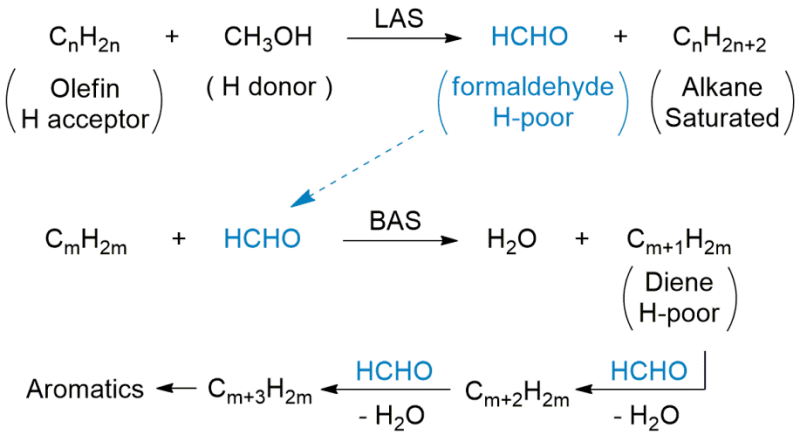

Scheme 10: Simplified reaction network of the methanol induced hydrogen transfer (MIHT) forming alkanes and aromatics with formaldehyde as hydrogen deficient intermediate.[52]

Based on its dependence on LAS in the zeolite it is possible to suppress or boost this HT pathway by modifying the zeolite and producing more or less HT products.[52] In general, the presence of formaldehyde and the MIHT pathway has gained a lot of attention in the last years[70-71] and different approaches were postulated to use this concept to minimize unwanted byproducts.[53-54]

1.7 Catalyst lifetime and deactivation in MTH process

Extending catalyst lifetime by minimizing deactivation of the zeolite is one of the main challenges in acid catalyzed hydrocarbon conversions and, in particular, in MTH, as the lifetime of the catalyst has a high impact on the economically successful application of the technology. The deactivation in MTH occurs mostly by formation of species that either block access of reactants and products to the micropores due to their size or that block the active sites by binding permanently to them. An often-used term therefore is “coke”, a loose expression for polyaromatics or HC residues in general, fulfilling at least one of the two stated characteristics. As mentioned before the main driving force for the formation of coke species are HT processes which in combination with acid catalyzed chain growth HC reactions form large polyaromatic species as shown in Scheme 12.[72]

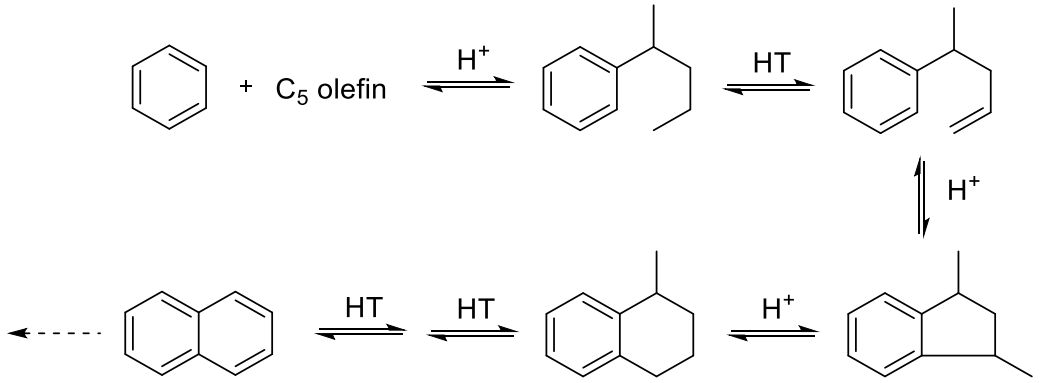

Scheme 7: Simplified scheme of the formation of a polyaromatic molecule from products from the MTH reaction via a combination of alkylation, cyclization, isomerization and hydrogen transfer steps (adopted from [72]).

Over the last decades a variety of studies has focused on the topic of coking in MTH pointing out that there are different sub-types of deactivating species and that the whole process is heavily depending on multiple parameters.[40, 54, 72-75] Schulz reported a differentiation into alkylated benzene molecules such as ethyltrimethylbenzene that are supposed to form at low reaction temperatures (<300 °C) and external coke formation over 350 °C.[40] Müller et al. proposed two types of coke, forming at comparatively high temperatures (450 °C) depending on the degree of MeOH conversion: In catalyst sections under high MeOH partial pressure oxygen containing HC species are formed that strongly attach to the acid sites while in later sections of the catalyst bed polyaromatic coke is formed.[73] Moreover, in 2017 Rojo-Gama et al. reported that the formation of coke species is also strongly depending on the type of zeolite framework used, as zeolites like SAPO-34 are more affected by HC-residues that can be dissolved in dichloromethane while frameworks with larger channels like MFI are deactivated by insoluble coke. There is no doubt that the formation of all these species lead to the decrease of accessible BAS for the conversion

MeOH/DME, resulting in a decreasing level of conversion with time on stream (TOS) as depicted in Figure 3.[76]

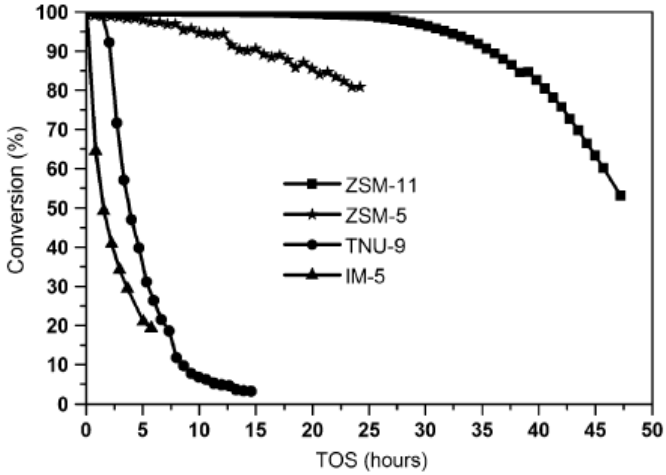

Figure 3: MeOH/DME conversion level over four different zeolite frameworks (ZSM-11, ZSM-5, TNU-9 and IM-5) versus TOS[76].

In summary, it is widely accepted that the coking process is very inhomogeneous and heavily depending on the process conditions, the type of zeolite used and the present mixture of HCs. Especially in a fixed bed reactor with a PFR configuration, this is problematic as an uneven deactivation of the catalyst bed occurs.[40, 73] It has been found that reducing the maximum local MeOH concentration in the catalytic bed has an overall positive effect on the catalyst lifetime.[73] Also many other strategies have been proposed in order to reduce catalyst deactivation as this is a vital topic to enhance the industrial applicability, like dehydrating MeOH to DME before reaching the zeolite[54] or the reduction of the amount of formaldehyde present during the process and thus reducing the amount of subsequently forming deactivation products.[53, 77]

1.8 Scope of the thesis

The main goal of this thesis is the elucidation of the formation of hydrogen-deficient species during the conversion of methanol and dimethyl ether over MFI zeolites and their role in the methanol to hydrocarbons (MTH) process. In the first section formaldehyde is identified as a central product of hydrogen transfer both during the initiation and the autocatalytic stages. Its role in the carbon-carbon bond formation and the formation of dienes, aromatics and coke species is investigated and its formation rate under MTH conditions is compared to hydrogen transfer between olefins and methylation reactions. In the second section of the thesis methanol and dimethyl ether are compared regarding their reactivity under MTH conditions. Especially their ability to act as a hydrogen donor during the initiation period is elucidated. The final chapter of this thesis focuses on the modification of MFI zeolites with gallium to increase their selectivity towards aromatics. The different pathways of hydrogen transfer and dehydrogenation are outlined and their dependence on the reactive sites of the catalysts are investigated. Furthermore, the stability of the modified catalysts under MTH conditions are tested.

1.9 References

1. Chang, C. D.; Silvestri, A. J., The conversion of methanol and other O-compounds to hydrocarbons over zeolite catalysts. *Journal of Catalysis* **1977,** *47* (2), 249-259.
2. Chang, C. D., Hydrocarbons from Methanol. *Catalysis Reviews* **1983,** *25* (1), 1-118.
3. Chang, C. D., The New Zealand Gas-to-Gasoline plant: An engineering tour de force. *Catalysis today* **1992,** *13* (1), 103-111.
4. Olsbye, U.; Svelle, S.; Bjørgen, M.; Beato, P.; Janssens, T. V. W.; Joensen, F.; Bordiga, S.; Lillerud, K. P., Conversion of Methanol to Hydrocarbons: How Zeolite Cavity and Pore Size Controls Product Selectivity. *Angewandte Chemie International Edition* **2012,** *51* (24), 5810-5831.
5. Stöcker, M., Methanol-to-hydrocarbons: catalytic materials and their behavior1. *Microporous and Mesoporous Materials* **1999,** *29* (1–2), 3-48.
6. Avidan, A., Gasoline and distillate fuels from methanol. In *Studies in Surface Science and Catalysis*, Elsevier: 1988; Vol. 36, pp 307-323.
7. Koempel, H.; Liebner, W., Lurgi's Methanol to Propylene (MTP): Report on a Successful Commercialisation. *Studies in Surface Science and Catalysis; Noronha, FB, Schmal, M., Sousa-Aguiar, EF Eds* **2007**, 261-267.
8. Allen, K., The shale revolution and its impacts on aromatics supply, pricing and trade flows. *Platts Special Report* **2013**.
9. Lai, P.-C.; Chen, C.-H.; Hsu, H.-Y.; Lee, C.-H.; Lin, Y.-C., Methanol aromatization over Ga-doped desilicated HZSM-5. *RSC Advances* **2016,** *6* (71), 67361-67371.
10. Hansen, J. B.; Højlund Nielsen, P. E., Methanol synthesis. *Handbook of Heterogeneous Catalysis: Online* **2008**, 2920-2949.
11. Mokrani, T.; Scurrell, M., Gas Conversion to Liquid Fuels and Chemicals: The Methanol Route - Catalysis and Processes Development. *Catalysis Reviews* **2009,** *51* (1), 1-145.
12. Yao, Y.; Chang, Y.; Huang, R.; Zhang, L.; Masanet, E., Environmental implications of the methanol economy in China: well-to-wheel comparison of energy and environmental emissions for different methanol fuel production pathways. *Journal of Cleaner Production* **2018,** *172*, 1381-1390.
13. Plotkin, J. S. The Propylene Gap: How Can It Be Filled? in *Cutting-Edge Chemistry,* ACS, https://www.acs.org/content/acs/en/pressroom/cutting-edge-chemistry/the-propylene-gap-how-can-it-be-filled.html (accessed 04. February 2019).
14. Teketel, S.; Erichsen, M. W.; Bleken, F. L.; Svelle, S.; Lillerud, K. P.; Olsbye, U., Shape selectivity in zeolite catalysis. The Methanol to Hydrocarbons (MTH) reaction. *Catalysis* **2014,** *26*, 179-217.
15. Masters, A. F.; Maschmeyer, T., Zeolites–From curiosity to cornerstone. *Microporous and Mesoporous Materials* **2011,** *142* (2-3), 423-438.
16. Cronstedt, A., Observation and description of an unknown kind of rock to be named zeolites. *Kongl Vetenskaps Acad Handl Stockh* **1756,** *17*, 120-123.
17. Tanabe, K.; Hölderich, W. F., Industrial application of solid acid–base catalysts. *Applied Catalysis A: General* **1999,** *181* (2), 399-434.
18. Rabo, J. A.; Schoonover, M. W., Early discoveries in zeolite chemistry and catalysis at Union Carbide, and follow-up in industrial catalysis. *Applied Catalysis A: General* **2001,** *222* (1-2), 261-275.
19. Loiola, A. R.; Andrade, J. C. R. A.; Sasaki, J. M.; da Silva, L. R. D., Structural analysis of zeolite NaA synthesized by a cost-effective hydrothermal method using kaolin and its use as water softener. *Journal of Colloid and Interface Science* **2012,** *367* (1), 34-39.
20. Ates, A.; Akgül, G., Modification of natural zeolite with NaOH for removal of manganese in drinking water. *Powder Technology* **2016,** *287*, 285-291.

21. Weigel, O.; Steinhoff, E., Adsorption of organic liquid vapors by chabazite. *Z. Kristallogr* **1925,** *61*, 125-154.
22. Barrer, R. M., 33. Synthesis of a zeolitic mineral with chabazite-like sorptive properties. *Journal of the Chemical Society (Resumed)* **1948**, 127-132.
23. Vogt, E.; Weckhuysen, B., Fluid catalytic cracking: recent developments on the grand old lady of zeolite catalysis. *Chemical Society Reviews* **2015,** *44* (20), 7342-7370.
24. Lefevere, J.; Mullens, S.; Meynen, V.; Van Noyen, J., Structured catalysts for methanol-to-olefins conversion: a review. *Chemical Papers* **2014,** *68* (9), 1143-1153.
25. Foster, M.; Rivin, I.; Treacy, M.; Friedrichs, O. D., A geometric solution to the largest-free-sphere problem in zeolite frameworks. *Microporous and mesoporous materials* **2006,** *90* (1-3), 32-38.
26. Structure Commission of the International Zeolite Association. Database of Zeolite Structures. http://www.iza-structure.org/databases/ (accessed 06. December 2018).
27. Shi, J.; Wang, Y.; Yang, W.; Tang, Y.; Xie, Z., Recent advances of pore system construction in zeolite-catalyzed chemical industry processes. *Chemical Society Reviews* **2015,** *44* (24), 8877-8903.
28. Rabo, J. A.; Gajda, G. J., Acid function in zeolites: recent progress. *Catalysis Reviews—Science and Engineering* **1989,** *31* (4), 385-430.
29. Weitkamp, J.; Puppe, L., *Catalysis and zeolites: fundamentals and applications*. Springer Science & Business Media: 2013.
30. Uytterhoeven, J. B.; Christner, L.; Hall, W. K., Studies of the hydrogen held by solids. VIII. The decationated zeolites. *The Journal of Physical Chemistry* **1965,** *69* (6), 2117-2126.
31. Jacobs, P. A.; Beyer, H. K., Evidence for the nature of true Lewis sites in faujasite-type zeolites. *Journal of Physical Chemistry* **1979,** *83* (9), 1174-1177.
32. Barrer, R. M.; Townsend, R. P., Transition metal ion exchange in zeolites. Part 1.—Thermodynamics of exchange of hydrated Mn 2+, Co 2+, Ni 2+, Cu 2+ and Zn 2+ ions in ammonium mordenite. *Journal of the Chemical Society, Faraday Transactions 1: Physical Chemistry in Condensed Phases* **1976,** *72*, 661-673.
33. Janda, A.; Bell, A. T., Effects of Si/Al ratio on the distribution of framework Al and on the rates of alkane monomolecular cracking and dehydrogenation in H-MFI. *Journal of the American Chemical Society* **2013,** *135* (51), 19193-19207.
34. Haw, J. F.; Marcus, D. M., Well-defined (supra)molecular structures in zeolite methanol-to-olefin catalysis. *Topics in Catalysis* **2005,** *34* (1), 41-48.
35. Dahl, I. M.; Kolboe, S., On the reaction mechanism for propene formation in the MTO reaction over SAPO-34. *Catalysis Letters* **1993,** *20* (3-4), 329-336.
36. Dahl, I. M.; Kolboe, S., On the reaction mechanism for hydrocarbon formation from methanol over SAPO-34: I. Isotopic labeling studies of the co-reaction of ethene and methanol. *Journal of Catalysis* **1994,** *149* (2), 458-464.
37. Dahl, I. M.; Kolboe, S., On the reaction mechanism for hydrocarbon formation from methanol over SAPO-34: 2. Isotopic labeling studies of the co-reaction of propene and methanol. *Journal of Catalysis* **1996,** *161* (1), 304-309.
38. Ono, Y.; Mori, T., Mechanism of methanol conversion into hydrocarbons over ZSM-5 zeolite. *Journal of the Chemical Society, Faraday Transactions 1: Physical Chemistry in Condensed Phases* **1981,** *77* (9), 2209-2221.
39. Chen, N.; Reagan, W., Evidence of autocatalysis in methanol to hydrocarbon reactions over zeolite catalysts. *Journal of catalysis* **1979,** *59* (1), 123-129.
40. Schulz, H., "Coking" of zeolites during methanol conversion: Basic reactions of the MTO-, MTP- and MTG processes. *Catalysis Today* **2010,** *154* (3–4), 183-194.
41. Clarke, J. K. A.; Darcy, R.; Hegarty, B. F.; O'Donoghue, E.; Amir-Ebrahimi, V.; Rooney, J. J., Free radicals in dimethyl ether on H-ZSM-5 zeolite. A novel dimension of heterogeneous catalysis. *Journal of the Chemical Society, Chemical Communications* **1986,** (5), 425-426.

42. van den Berg, J.; Wolthuizen, J., JHC van Hooff in Proceedings 5th International Zeolite Conference (Naples). *Heyden, London* **1980**, 649.
43. Olah, G. A., Higher coordinate (hypercarbon containing) carbocations and their role in electrophilic reactions of hydrocarbons. *Pure and Applied Chemistry* **1981,** *53* (1), 201-207.
44. Swabb, E. A.; Gates, B. C., Diffusion, reaction, and fouling in H-mordenite crystallites. The catalytic dehydration of methanol. *Industrial & Engineering Chemistry Fundamentals* **1972,** *11* (4), 540-545.
45. Haw, J. F.; Song, W.; Marcus, D. M.; Nicholas, J. B., The mechanism of methanol to hydrocarbon catalysis. *Accounts of chemical research* **2003,** *36* (5), 317-326.
46. Blaszkowski, S. R.; van Santen, R. A., Theoretical study of C− C bond formation in the methanol-to-gasoline process. *Journal of the American Chemical Society* **1997,** *119* (21), 5020-5027.
47. Yarulina, I.; Chowdhury, A. D.; Meirer, F.; Weckhuysen, B. M.; Gascon, J., Recent trends and fundamental insights in the methanol-to-hydrocarbons process. *Nature Catalysis* **2018,** *1* (6), 398.
48. Wu, X.; Xu, S.; Zhang, W.; Huang, J.; Li, J.; Yu, B.; Wei, Y.; Liu, Z., Direct Mechanism of the First Carbon–Carbon Bond Formation in the Methanol‐to‐Hydrocarbons Process. *Angewandte Chemie International Edition* **2017,** *56* (31), 9039-9043.
49. Liu, Y.; Müller, S.; Berger, D.; Jelic, J.; Reuter, K.; Tonigold, M.; Sanchez-Sanchez, M.; Lercher, J. A., Formation Mechanism of the First Carbon–Carbon Bond and the First Olefin in the Methanol Conversion into Hydrocarbons. *Angewandte Chemie* **2016,** *128* (19), 5817-5820.
50. Chowdhury, A. D.; Houben, K.; Whiting, G. T.; Mokhtar, M.; Asiri, A. M.; Al-Thabaiti, S. A.; Basahel, S. N.; Baldus, M.; Weckhuysen, B. M., Initial Carbon–Carbon Bond Formation during the Early Stages of the Methanol-to-Olefin Process Proven by Zeolite-Trapped Acetate and Methyl Acetate. *Angewandte Chemie* **2016,** *128* (51), 16072-16077.
51. Plessow, P. N.; Studt, F., Unraveling the Mechanism of the Initiation Reaction of the Methanol to Olefins Process Using ab Initio and DFT Calculations. *ACS Catalysis* **2017,** *7* (11), 7987-7994.
52. Müller, S.; Liu, Y.; Kirchberger, F. M.; Tonigold, M.; Sanchez-Sanchez, M.; Lercher, J. A., Hydrogen Transfer Pathways during Zeolite Catalyzed Methanol Conversion to Hydrocarbons. *Journal of the American Chemical Society* **2016,** *138* (49), 15994-16003.
53. Hwang, A.; Bhan, A., Bifunctional Strategy Coupling Y2O3-Catalyzed Alkanal Decomposition with Methanol-to-Olefins Catalysis for Enhanced Lifetime. *ACS Catalysis* **2017,** *7* (7), 4417-4422.
54. Martinez-Espin, J. S.; Mortén, M.; Janssens, T. V.; Svelle, S.; Beato, P.; Olsbye, U., New insights into catalyst deactivation and product distribution of zeolites in the methanol-to-hydrocarbons (MTH) reaction with methanol and dimethyl ether feeds. *Catalysis Science & Technology* **2017**.
55. Liang, T.; Chen, J.; Qin, Z.; Li, J.; Wang, P.; Wang, S.; Wang, G.; Dong, M.; Fan, W.; Wang, J., Conversion of methanol to olefins over H-ZSM-5 zeolite: Reaction pathway is related to the framework aluminum siting. *ACS Catalysis* **2016,** *6* (11), 7311-7325.
56. Svelle, S.; Joensen, F.; Nerlov, J.; Olsbye, U.; Lillerud, K.-P.; Kolboe, S.; Bjørgen, M., Conversion of methanol into hydrocarbons over zeolite H-ZSM-5: Ethene formation is mechanistically separated from the formation of higher alkenes. *Journal of the American Chemical Society* **2006,** *128* (46), 14770-14771.
57. Goguen, P. W.; Xu, T.; Barich, D. H.; Skloss, T. W.; Song, W.; Wang, Z.; Nicholas, J. B.; Haw, J. F., Pulse-quench catalytic reactor studies reveal a carbon-pool mechanism in methanol-to-gasoline chemistry on zeolite HZSM-5. *Journal of the American Chemical Society* **1998,** *120* (11), 2650-2651.
58. Lesthaeghe, D.; Horre, A.; Waroquier, M.; Marin, G. B.; Van Speybroeck, V., Theoretical Insights on Methylbenzene Side‐Chain Growth in ZSM‐5 Zeolites for Methanol‐to‐Olefin Conversion. *Chemistry – A European Journal* **2009,** *15* (41), 10803-10808.

59. Bjorgen, M.; Svelle, S.; Joensen, F.; Nerlov, J.; Kolboe, S.; Bonino, F.; Palumbo, L.; Bordiga, S.; Olsbye, U., Conversion of methanol to hydrocarbons over zeolite H-ZSM-5: On the origin of the olefinic species. *Journal of Catalysis* **2007,** *249* (2), 195-207.
60. Teketel, S.; Svelle, S.; Lillerud, K. P.; Olsbye, U., Shape‐Selective Conversion of Methanol to Hydrocarbons Over 10‐Ring Unidirectional‐Channel Acidic H‐ZSM‐22. *ChemCatChem* **2009,** *1* (1), 78-81.
61. Teketel, S.; Olsbye, U.; Lillerud, K.-P.; Beato, P.; Svelle, S., Selectivity control through fundamental mechanistic insight in the conversion of methanol to hydrocarbons over zeolites. *Microporous and Mesoporous Materials* **2010,** *136* (1-3), 33-41.
62. Li, J.; Wei, Y.; Liu, G.; Qi, Y.; Tian, P.; Li, B.; He, Y.; Liu, Z., Comparative study of MTO conversion over SAPO-34, H-ZSM-5 and H-ZSM-22: Correlating catalytic performance and reaction mechanism to zeolite topology. *Catalysis today* **2011,** *171* (1), 221-228.
63. Olsbye, U.; Svelle, S.; Lillerud, K.; Wei, Z.; Chen, Y.; Li, J.; Wang, J.; Fan, W., The formation and degradation of active species during methanol conversion over protonated zeotype catalysts. *Chemical Society Reviews* **2015,** *44* (20), 7155-7176.
64. Sun, X.; Mueller, S.; Shi, H.; Haller, G. L.; Sanchez-Sanchez, M.; van Veen, A. C.; Lercher, J. A., On the impact of co-feeding aromatics and olefins for the methanol-to-olefins reaction on HZSM-5. *Journal of Catalysis* **2014,** *314*, 21-31.
65. Ilias, S.; Bhan, A., Tuning the selectivity of methanol-to-hydrocarbons conversion on H-ZSM-5 by co-processing olefin or aromatic compounds. *Journal of Catalysis* **2012,** *290*, 186-192.
66. Ilias, S.; Bhan, A., Mechanism of the Catalytic Conversion of Methanol to Hydrocarbons. *ACS Catalysis* **2013,** *3* (1), 18-31.
67. Hazari, N.; Labinger, J. A.; Scott, V. J., A mechanistic explanation for selectivity in the conversion of methanol to 2, 2, 3-trimethylbutane (triptane): Moderate acidity allows kinetic control to operate. *Journal of Catalysis* **2009,** *263* (2), 266-276.
68. Kotrel, S.; Knözinger, H.; Gates, B., The Haag–Dessau mechanism of protolytic cracking of alkanes. *Microporous and Mesoporous Materials* **2000,** *35*, 11-20.
69. Feller, A.; Guzman, A.; Zuazo, I.; Lercher, J. A., On the mechanism of catalyzed isobutane/butene alkylation by zeolites. *Journal of Catalysis* **2004,** *224* (1), 80-93.
70. Martinez-Espin, J. S.; De Wispelaere, K.; Erichsen, M. W.; Svelle, S.; Janssens, T. V.; Van Speybroeck, V.; Beato, P.; Olsbye, U., Benzene co-reaction with methanol and dimethyl ether over zeolite and zeotype catalysts: Evidence of parallel reaction paths to toluene and diphenylmethane. *Journal of Catalysis* **2017,** *349*, 136-148.
71. Martínez-Espín, J. S.; De Wispelaere, K.; Janssens, T. V. W.; Svelle, S.; Lillerud, K. P.; Beato, P.; Van Speybroeck, V.; Olsbye, U., Hydrogen Transfer versus Methylation: On the Genesis of Aromatics Formation in the Methanol-To-Hydrocarbons Reaction over H-ZSM-5. *ACS Catalysis* **2017**, 5773-5780.
72. Guisnet, M.; Magnoux, P., Organic chemistry of coke formation. *Applied Catalysis A: General* **2001,** *212* (1-2), 83-96.
73. Müller, S.; Liu, Y.; Vishnuvarthan, M.; Sun, X.; van Veen, A. C.; Haller, G. L.; Sanchez-Sanchez, M.; Lercher, J. A., Coke formation and deactivation pathways on H-ZSM-5 in the conversion of methanol to olefins. *Journal of Catalysis* **2015,** *325*, 48-59.
74. Rojo-Gama, D.; Signorile, M.; Bonino, F.; Bordiga, S.; Olsbye, U.; Lillerud, K. P.; Beato, P.; Svelle, S., Structure–deactivation relationships in zeolites during the methanol–to-hydrocarbons reaction: Complementary assessments of the coke content. *Journal of Catalysis* **2017,** *351*, 33-48.
75. Bleken, F. L.; Barbera, K.; Bonino, F.; Olsbye, U.; Lillerud, K. P.; Bordiga, S.; Beato, P.; Janssens, T. V.; Svelle, S., Catalyst deactivation by coke formation in microporous and desilicated zeolite H-ZSM-5 during the conversion of methanol to hydrocarbons. *Journal of catalysis* **2013,** *307*, 62-73.

76. Bleken, F.; Skistad, W.; Barbera, K.; Kustova, M.; Bordiga, S.; Beato, P.; Lillerud, K. P.; Svelle, S.; Olsbye, U., Conversion of methanol over 10-ring zeolites with differing volumes at channel intersections: comparison of TNU-9, IM-5, ZSM-11 and ZSM-5. *Physical Chemistry Chemical Physics* **2011,** *13* (7), 2539-2549.
77. Arora, S. S.; Nieskens, D. L.; Malek, A.; Bhan, A., Lifetime improvement in methanol-to-olefins catalysis over chabazite materials by high-pressure H 2 co-feeds. *Nature Catalysis* **2018**, 1.

2. Critical role of formaldehyde during methanol conversion to hydrocarbons

Abstract: Formaldehyde is an important intermediate product in the catalytic conversion of methanol to olefins (MTO). Here we show that formaldehyde is present during MTO with an average concentration of ~ 0.2 C% across the ZSM-5 catalyst bed up to a MeOH conversion of 70 %. It condenses with acetic acid or methyl acetate, the carbonylation product of MeOH and DME, into unsaturated carboxylate or carboxylic acid, which decarboxylates into the first olefin. By tracing its reaction pathways using ^{13}C-labeled formaldehyde, it is shown that formaldehyde reacts with alkenes via Prins reaction into dienes and finally to aromatics. Because its rate is one order of magnitude higher than that of hydrogen transfer between alkenes on ZSM-5, the Prins reaction is concluded to be the major reaction route to produce dienes and aromatics and, in consequence, increases the yield of ethene by enhancing the contribution of aromatic cycle.

2.1 Introduction

The conversion of methanol to hydrocarbons (MTH) is considered as a promising route of converting gas and coal to fuels and chemicals via methanol.[1-3] By adjusting catalysts and reaction conditions, the product distribution shifts from gasoline-range (methanol to gasoline; MTG) to lower olefin-range products (methanol to olefins; MTO).[1] As a consequence, methanol conversion has been commercialized in different variants.[1, 4] The central mechanism consists of two catalytic cycles[5-7] interconverting surface species (hydrocarbon pool).[8-9] One is called olefin-cycle and it is dominated by methylation of light alkenes, followed by cracking of the larger alkenes. The other is called aromatic-cycle catalyzing methylation of aromatic molecules followed by cracking of a sidechain. The fast propagation of these two cycles is responsible for the autocatalytic nature of the MTH reaction. The relative contribution of each cycle depends on the local concentrations of hydrocarbon species within the zeolite.[10]

A mechanistic description focused solely on hydrocarbons as key compounds may lead, however, to a rather incomplete description of the interlinked processes. As far back as 1984, evidence of formaldehyde formation under the conditions of methanol conversion was given. Kubelková et al.[11] reported formaldehyde and methane formed by methanol disproportionation on H-ZSM-5 at 670 K and low methanol pressures (1-3 Pa). Hutchings et al. observed methane before C_{2+} hydrocarbons formation at low methanol coverage, supporting these results.[12-13] On the basis of these results a methane-formaldehyde mechanism leading to first C-C bond was proposed by Tajima et al.[14] In spite of these first reports, formaldehyde in methanol conversion did not attract much attention until recently. Theoretical calculations[15-17] and dedicated experiments[15, 17-18] showed possible pathways forming the first C-C bond and first olefin from HCHO in a subtle interplay with Brønsted acid and extra-framework Al sites. Experimental observations of strong deactivation in presence of HCHO[19-20] and of the O-containing surface species, were attributed to reaction products of HCHO, strongly adsorbed on the zeolite acid sites.[21-23] While always being present during MTO conversion at least in very low concentrations, it promotes the formation of non-olefinic byproducts[24-25] and accelerates deactivation.[19-21, 26-27] The recognition of the importance of HCHO in MTO makes it imperative to quantify its concentration in the reaction and distribution over the catalyst bed. However, the very low concentration of HCHO and its high reactivity on acid sites set obstacles in such quantitative studies.

Generation of HCHO under MTO conditions occurs via several pathways, including hydride transfer between two methanol molecules (Rxn 1),[10-13, 15] thermal or reactor-wall catalyzed decomposition of methanol (Rxn 2)[18] and hydrogen transfer from methanol to alkenes on Lewis acid sites (LAS) (Rxn 3).[24]

$$2\ CH_3OH \longrightarrow HCHO + CH_4 + H_2O \quad (1)$$

$$CH_3OH \longrightarrow HCHO + H_2 \quad (2)$$

$$CH_3OH + Olefin \xrightarrow{LAS} HCHO + Alkane \quad (3)$$

The present study quantifies the concentration level of HCHO and its distribution along the catalyst bed in MTO and explores the role of formaldehyde as intermediate in two critical stages of methanol conversion. We examine rigorously the participation of formaldehyde in the formation of the first olefinic product on the one hand and its impact on product distribution and deactivation of an H-ZSM-5 catalyst on the other hand. Insight into these elementary steps will help to tailor catalysts to higher alkene selectivity, while extending the useful lifetime of the catalysts.

2.2 Results

Formaldehyde detection in MTO

Methanol decomposes into HCHO under typical reaction conditions employed in this study (MTO conditions).[18, 21-24] The concentration of the intermediately formed HCHO has not been discussed until now, because the combination of low concentrations and high reactivity makes this very challenging under typical reaction conditions reported. To achieve quantification, we turn to very low conversions. A blank test shows only a conversion of MeOH to 0.01 C% methane and 0.01 C% HCHO, while with H-ZSM-5 a higher conversion was observed. Table 1 shows a typical effluent composition at a methanol (+ DME) conversion of only 0.24 C% on H-ZSM-5 at 475 °C. Methane is the dominant product with a yield of 0.12 C%, and HCHO has a yield of 0.06 C%. The rest are CO and CO_2, with a yield of 0.06 C%. The olefin yield was very low at these conditions, and only a trace concentration of ethene, below 0.01 C%, was detected. The amount of H_2 was below the detection limit. This shows that MeOH/DME is converted to HCHO with a selectivity as high as 25 % before alkenes are formed in appreciable amounts and the hydrocarbon pool has evolved. In Fig. 1 it is shown that by increasing the residence time the yield of HCHO increased to a yield maximum of 0.27 C% at ~ 20 % conversion of MeOH, and then it decreased gradually with higher conversions to levels below the detection limit. These results directly establish the presence of HCHO in H-ZSM-5 under MTO reaction conditions and its concentration evolution with the conversion of MeOH. We investigate next in which steps of the complex reaction network of methanol to olefins does HCHO participate.

Table 1: Stream composition in methanol reaction over H-ZSM-5 at a conversion of 0.24 %.[a]

Effluent molecules	Effluent composition (C%)	Selectivity (C%)
MeOH + DME	99.76	
CH_4	0.12	50
HCHO	0.06	25
CO + CO_2	0.06[b]	25
C_2H_4	< 0.01	< 4
H_2	< 0.01 (H%)[c]	-

[a] Conditions: 475 °C, DME 90 mbar, H-ZSM5 (Si/Al 90 steamed), W/F 0.076 $h \cdot g_{(cat)} \cdot mol_C^{-1}$.

[b] estimated based on C balance.

[c] below detection limit.

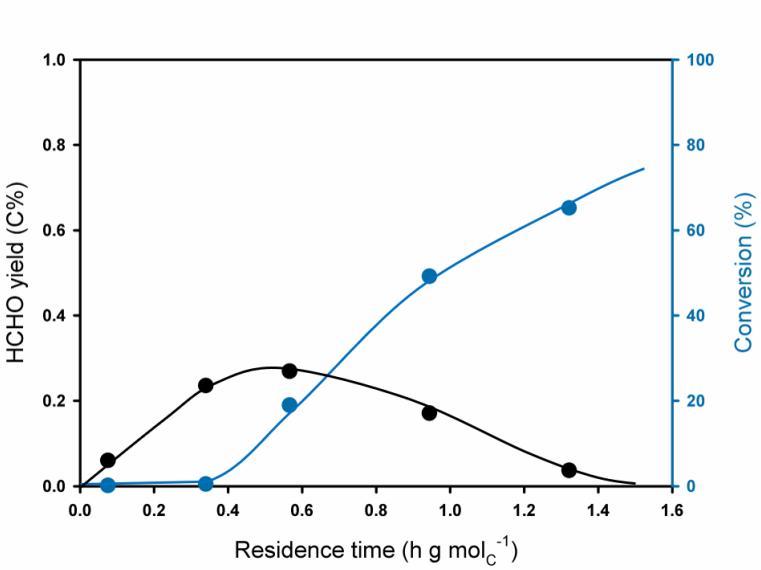

Figure 1: Methanol conversion and the yield of HCHO as a function of residence time. Reaction conditions: DME 90 mbar, H-ZSM5 (Si/Al 90 steamed) 475 ºC.

Role of formaldehyde in the formation of first alkenes

Having established that HCHO is a main product at low MeOH/DME conversions before alkenes are detected in significant concentrations in the products, we use surface reactions of adsorbed MeOH on H-ZSM-5 to better understand the possible reaction pathways. Fig. 2 shows the evolution of gaseous products and surface species from H-ZSM5 saturated with 3 mbar MeOH as a function of temperature. With increasing temperature, MeOH desorption reached a maximum at 120 °C, while DME had maximum at 180 °C with formation extending to 300 °C (Fig. 2a). Decomposition and disproportionation products from MeOH, including CH_4, HCHO and CO, were detected from 220 °C to 400 °C with maxima at 290 °C, forming a mixture of C_1 species. Alkenes appeared at 300 °C and reached a maximum at 380 °C. This agrees with previously reported results, linking the formation of first C-C bond in MTH to the presence of small concentrations of CO.[18] In a recent report, Wu *et al.* observed a simultaneous appearance of ethene and propene with CH_4 and HCHO, hence proposing a direct C-C formation from MeOH, DME, surface methoxy or trimethyloxonium ion.[28-29] While we cannot establish the experimental differences the present study unequivocally identified that olefin appeared after CH_4, HCHO and CO strongly suggesting that olefin formation follows a different pathway than that Wu *et al.* proposed. Noticeably, CO_2 was also observed after MeOH decomposition and before the onset of olefin desorption. The formation of CO_2 prior to the formation of alkenes in the early stages of the MTH reaction has been attributed to ketonic decarboxylation of two acetic acid molecules into acetone and CO_2.[18] The present results suggest, however, that this pathway is minor, because acetone was not detected under the present reaction conditions.

IR spectra recorded during this process show the formation and evolution of carbonyl-containing species during the MeOH surface reactions (Fig. 2b). At 260 °C, four bands were observed between 1800 and 1400 cm^{-1}: (i) bands of the deformation vibration of water at 1630 cm^{-1}, (ii) bands of C-H deformation vibrations at 1460-1470 cm^{-1} (O-CH_3),[30] and (iii) two bands of C=O stretching vibrations at 1700 cm^{-1} attributed to acetate (O-CO-CH_3)[31-32] and at 1734 cm^{-1} to formate (O-CO-H) groups,[33] respectively. At this temperature, gas phase analysis showed that DME, HCHO, CO and CH_4 evolved. We hypothesize, therefore, that these C_1 species are involved in the formation of the surface species observed in the IR spectra.

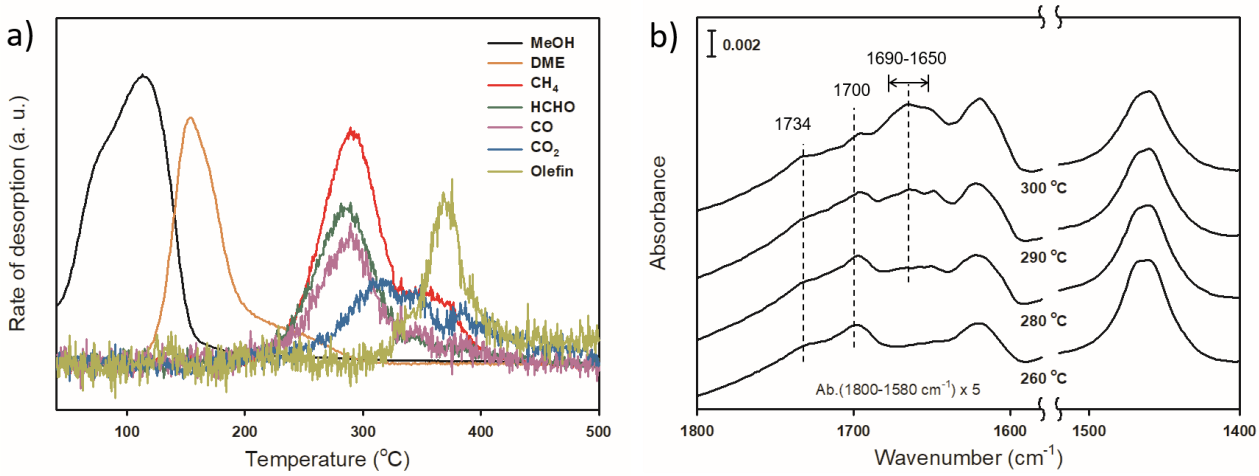

Figure 2: Surface reaction of MeOH adsorbed on H-ZSM-5 with linearly increasing temperature. (a) Desorbed products in gas phase; (b) IR spectrum of corresponding surface species on H-ZSM-5 taken *in situ*. Reaction conditions: H-ZSM-5 (Si/Al 15) 25 mg saturated under 3 mbar MeOH subsequently outgassed under vacuum, afterwards ramping temperature with 3 °C min^{-1} under vacuum.

The methoxy group is formed by dissociative adsorption of MeOH/DME on Brønsted acid sites. Acetate groups are formed by CO insertion into the O-CH_3 bond of methoxy groups;[32, 34-38] while formate groups are attributed to be the products of the disproportionation of HCHO under hydrothermal conditions.[39] With reaction progress (here observed when temperature increased from 280 ˚C to 300 ˚C), the acetate C=O stretching vibrations at 1700 cm^{-1} shifts to 1690-1650 cm^{-1}. This red shift is attributed to the transformation of acetate groups into unsaturated carboxylates, i.e. acrylate, making conjugated carbonyl groups. This reaction went through the condensation of HCHO at the acetate methyl group (Fig. 3).[40] The unsaturated carboxylates have also been proposed to convert, via stepwise condensations with HCHO, to O-containing species, strongly interacting with BAS.[21] Note that formation of this unsaturated carboxylates occurred in parallel with the CO_2 evolution at 280 °C, indicating that partial decarboxylation took place. The evolution of alkenes was then observed at 300 °C (Fig. 2a). This strongly suggests that decarboxylation of unsaturated carboxylic acids plays a role in the formation of the first olefinic products (Fig. 3). An alternative pathway, the methylation of acetate-derived ketene to propionate followed by

decarbonylation,[36-38] may also occur in parallel, but is less important under the applied condition here, because neither ketene nor propionate were observed.

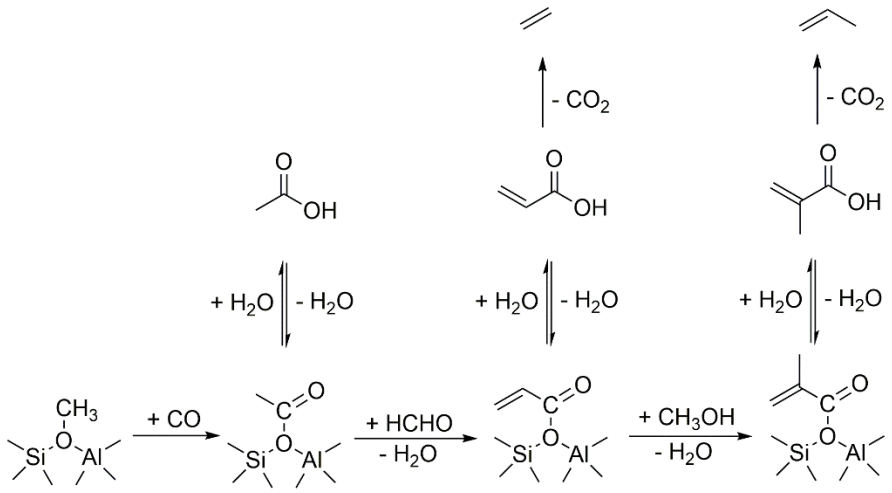

Figure 3: Schematic illustration of the proposed reaction pathways for the formation of alkenes.

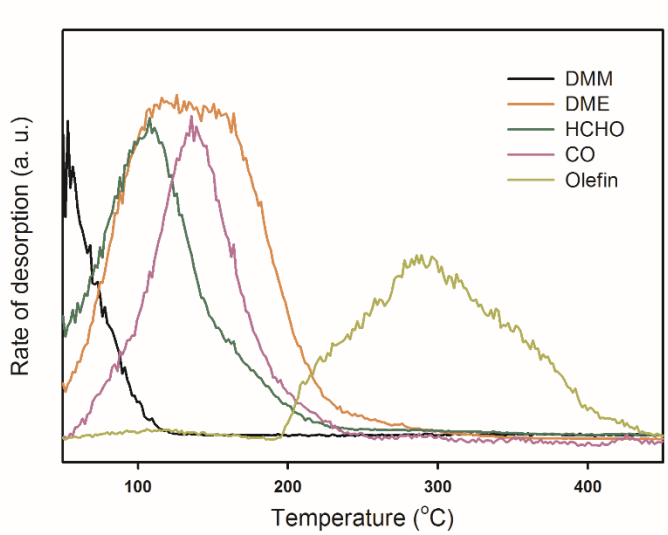

Figure 4: Surface reaction of DMM adsorbed on H-ZSM-5 with linearly increasing temperature. Reaction conditions: H-ZSM-5 (Si/Al 15) 25 mg saturated under 1 mbar DMM, subsequently outgassed under vacuum, afterwards ramping temperature with 3 °C min^{-1} under vacuum.

A similar temperature-programmed surface reaction was performed with dimethoxymethane (DMM) instead of MeOH (Fig. 4). On H-ZSM-5, DMM decomposes into equimolar concentration of HCHO and DME below 100 °C. Thus, the surface reaction of DMM at T > 100 °C represents the reaction of a mixture of HCHO and DME on H-ZSM-5. The evolution of alkenes started in this case at ~ 200 °C, while in pure MeOH alkenes did not appear until 300 °C (Fig. 2a). Converting MeOH required temperatures above 200 °C to generate HCHO and CO. In presence of HCHO and CO the reaction started already below 200 °C, facilitating the initiation of the hydrocarbon pool at low temperatures.

Participation of formaldehyde in the dual-cycle mechanism

Having shown how HCHO participates in the formation of first olefin, we investigate next its participation in the dual-cycle mechanism. Because HCHO is H-poor, incorporation into products must increase the selectivity to aromatic molecules,[20, 24] and in turn the selectivity to ethene, formed in the aromatic cycle.[20] As the formation of aromatic molecules has been associated to deactivation of the zeolite catalysts, we hypothesize that the higher concentration of HCHO in the reacting mixture leads to faster deactivation of the catalyst.[20]

In order to show the most relevant conversion pathways of HCHO, ^{13}C-labeled HCHO was co-fed with MeOH. Table 2 shows the selectivity to hydrocarbon products when feeding pure MeOH and MeOH with 5 C% HCHO at comparable conversion levels (88.8 C% and 75.8 C%, respectively). For pure MeOH feed, propene and butene were the major products, with selectivities of 36.9 C% and 20.3 C%, respectively. Ethene selectivity was only 3.0 C%, in good agreement with the low yield of aromatics (2.4 C%). The products indicate that under the selected reaction conditions the aromatic cycle was less important than the olefin cycle. The selectivity to C_{1-4} alkanes was at the same low level as aromatics, indicating low rate of hydrogen transfer reactions.

Table 2. Conversion and product selectivity in MTO reaction with and without H^{13}CHO.[a]

Feed composition	MeOH	MeOH + 5 C% H^{13}CHO
Conversion (C%)	88.8	75.8
Product selectivity (C%)		
Ethene	3.0	8.6
Propene	36.9	28.1
Butene	20.3	15.8
Dienes[b]	0.4	0.7
Aromatics	2.4	12.2
C_{1-4} alkanes	3.1	2.8
C_{5+} aliphatics	20.2	20.1

[a] Reaction conditions: H-ZSM-5 (Si/Al 90 steamed), W/F 1.82 $h \cdot g_{cat} \cdot mol_{(MeOH+HCHO)}^{-1}$, MeOH 180 mbar, H_2O 60 mbar, or MeOH 171 mbar, H^{13}CHO 9 mbar, H_2O 60 mbar, 475 °C;
[b] Butadiene and pentadiene

When HCHO was co-fed with MeOH, the selectivity to H-poor products, i.e., dienes and aromatics, increased drastically. The selectivity to aromatic molecules increased five-fold from 2.4 C% to 12.2 C%. The ethene selectivity increased from 3.0 C% to 8.6 C%. In parallel, the selectivities to propene and butene decreased from 36.9 C% to 28.1 C% and from 20.3 C% to 15.8 C%, respectively. These changes indicate that in presence of HCHO the olefin cycle decreased in importance. The selectivity to C_{1-4} alkanes did not change, which indicates that the hydrogen

transfer rate was not affected by the presence of HCHO. Thus, the increase of dienes and aromatics is concluded to be the result of a direct reaction between alkenes and HCHO.

The distribution of ^{13}C in the products can be used to deduce the reaction pathways in which HCHO is preferentially incorporated into hydrocarbons. Fig. 5a shows the fraction of each hydrocarbon product containing ^{13}C. All hydrocarbon products had a similar percentage of ^{13}C incorporated, within 5 % to 6 %, corresponding to the total ^{13}C content of the feed. Only methane showed a significantly lower fraction of 2.7 %. This uniform distribution of ^{13}C in the product mixture and particularly the value close to ^{13}C fraction in the feed (accounting for the natural abundance of 1 % ^{13}C in MeOH) indicates a fast scrambling of ^{13}C during reaction.

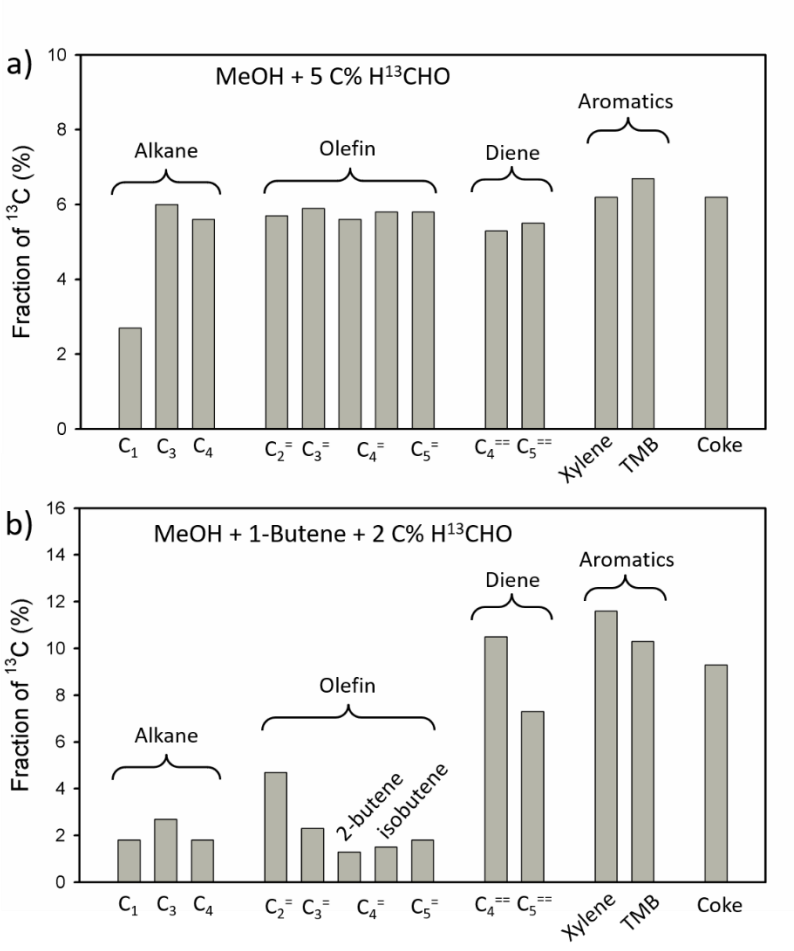

Figure 5: Fraction of ^{13}C in hydrocarbon products in the reaction of MeOH cofed with $H^{13}CHO$. (a) MeOH cofed with 5 C% $H^{13}CHO$, MeOH conversion 75 %; (b) MeOH cofed with 1-butene and 2 C% $H^{13}CHO$; MeOH conversion 100 %, butene decreased from 57% in the feedstock to 24% in the gas products. Reaction conditions: (a) W/F 1.82 $h \cdot g_{(cat)} \cdot mol_{(MeOH+HCHO)}^{-1}$, MeOH 171 mbar, $H^{13}CHO$ 9 mbar, H_2O 60 mbar, 475 °C; (b) W/F 1.30 $h \cdot g_{(cat)} \cdot mol_{(MeOH+HCHO)}^{-1}$, MeOH 171 mbar, $H^{13}CHO$ 9 mbar, H_2O 60 mbar, 1-butene 60 mbar, 475 °C. See Supplementary Methods 1 and 2 for the determination of ^{13}C fraction.

The scrambling is hypothesized to result from the fast interconversion of MeOH with $H^{13}CHO$ via hydride transfer from MeOH to a protonated $H^{13}CHO$ on a BAS, which generates a ^{13}C-labeled MeOH ($^{13}CH_3OH$) and an unlabeled HCHO (Rxn 4).

$$CH_3OH + H^{13}CHO \longrightarrow HCHO + {}^{13}CH_3OH \quad (4)$$

This hypothesis is supported by the detection of 5.5 % of ^{13}C labelled MeOH and concurrently HCHO with only 8.7 % ^{13}C at MeOH conversions as low as 5 C%. The low ^{13}C fraction in methane indicates that it is formed mainly in reactions during the initiation stage of the methanol conversion to hydrocarbons (Rxn 1), occurring before and in parallel to the MeOH/HCHO scrambling in Rxn 4. Thus, the fast scrambling of MeOH with $H^{13}CHO$ before the appearance of alkenes does not allow tracking the conversion pathway of $H^{13}CHO$.

It has been reported that co-feeding alkenes, such as propene and butene quickly initiates the olefin cycle and subsequently also the aromatic cycle.[4] Although under such conditions the hydrogen transfer from MeOH to $H^{13}CHO$ still exist, the extent of scrambling is hypothesized to be significantly reduced, because of the accelerated rate of MeOH (or HCHO) consumption in forming C-C bonds by alkylation. Therefore, 1-butene was co-fed with MeOH and $H^{13}CHO$ (Fig. 5b). A higher incorporation of ^{13}C was observed in dienes and aromatics: 10.5 % in butadiene, 7.4 % in pentadiene, 11.6 % in xylene and 10.3 % in trimethylbenzene (TMB). In contrast, alkanes had only about 2 % of ^{13}C. Within alkenes, ethene had the highest ^{13}C fraction (4.7 %); for propene it was 2.3 % and for butene and pentene even lower (1.3 % for 2-butene, 1.6 % for isobutene and 1.8 % for pentene). The total ^{13}C content in the gas products was 2.9 %, very close to the 3.1 % ^{13}C in the feedstock (2 % from $H^{13}CHO$ and 1.1 % from natural abundance in MeOH and butene), in which the 0.2 % difference could be those incorporated in ^{13}CO, $^{13}CO_2$ or coke. These results show that HCHO participates in both cycles as a C_1 source. Ethene is formed in the aromatic cycle and the high incorporation of ^{13}C in ethene and aromatic molecules indicates a high involvement of $H^{13}CHO$ in the aromatic cycle. Both pentene and isobutene are products and intermediates in olefin cycle. Although the direct skeletal isomerization of the cofed 1-butene to isobutene is possible, this pathway has only a minor contribution on H-ZSM-5 and most isobutene is generated from cracking of higher olefins.[41-42] Therefore, their low incorporation of ^{13}C indicates a minor participation of $H^{13}CHO$ in the olefin cycle.

Isobutene is chosen as indicator of the olefin cycle, because the other two butene isomers are either the co-fed reactant (1-butene) or can be formed by 1-butene isomerization on BAS without passing the olefin cycle (2-butene). Propene is generated in both the aromatic and the olefin cycle,[1-2, 4] showing in consequence a ^{13}C incorporation level intermediate between ethene and isobutene. The preferred ^{13}C enrichment of dienes and aromatics supports earlier conclusions that

HCHO leads to H-poor products at a rate that is higher than that of hydrogen transfer between hydrogen poor and hydrogen rich hydrocarbon intermediates.

$$C_4H_8 + C_4H_8 \longrightarrow C_4H_6 + C_4H_{10} \quad (5)$$

$$C_4H_8 + HCHO \longrightarrow C_5H_8 + H_2O \quad (6)$$

An alkene, e.g., butene, can react into a diene in MTO via two pathways, hydrogen transfer with another alkene (Rxn 5) and Prins reaction with a formaldehyde (Rxn 6). Unlike hydrogen transfer, the Prins reaction has not attracted much attention until recently. Earlier reports have, however, noted the possibility of Prins type reaction for the formation of dienes and aromatics without experimental evidence.[20, 24] Comparing the isotope distribution allows now unequivocally establishing the importance of the two routes. If hydrogen transfer were the dominant path of diene formation (Rxn 5), butadiene and pentadiene would have a ^{13}C labelling similar to that of butene and pentene, respectively. The fact that eight times more ^{13}C was found in butadiene (10.5 %) than in n-butene (1.3 %) and over four times more ^{13}C in pentadiene (7.4 %) than in pentene (1.8 %) when MeOH was reacted together with 1-butene and 2 C% $H^{13}CHO$, allowed us to rule out hydrogen transfer as the main pathway to dienes. Moreover, the rate of hydrogen transfer has been reported to increase by one order of magnitude by the simultaneous presence of MeOH and alkenes, attributed to the reaction pathway involving hydrogen transfer from MeOH to an alkene.[24] Such reaction generates formaldehyde in situ, which, as discussed above, reacts subsequently by Prins reaction converting a second alkene to a diene (Rxn 7). Therefore, we conclude that the Prins reaction is the dominant pathway for diene formation.

$$\begin{aligned} C_3H_6 + CH_3OH &\longrightarrow HCHO + C_3H_8 \\ C_4H_8 + HCHO &\longrightarrow H_2O + C_5H_8 \end{aligned} \quad (7)$$

This conclusion is further supported by an additional experiment in which 1-butene was reacted with $H^{13}CHO$ in absence of MeOH. The resulting pentadiene from this reaction had a labelling of ~ 20 % ^{13}C (Supplementary Fig. 1), indicating an incorporation of one ^{13}C in each pentadiene molecule via a Prins type reaction (Rxn 8). In the reaction of MeOH with butene and $H^{13}CHO$, the incorporation of ^{13}C in pentadiene was much lower (7.4 % ^{13}C, Fig. 5b). We speculate that this is caused by $H^{13}CHO$ being partially interconverted with unlabeled HCHO generated in situ from MeOH via Rxn 4 and Rxn 7.

$$C_4H_8 + H^{13}CHO \longrightarrow {}^{13}C_1C_4H_8 + H_2O \quad (8)$$

After showing the participation of HCHO in the dual cycle via Prins reaction, we discuss the importance of this reaction pathway in typical MTO reaction for the non-olefinic byproduct formation. In order to do so, we compare the reaction rates of Prins reaction and hydrogen transfer between alkenes in H-ZSM-5. To avoid the interference of products directly formed via MeOH

routes, we examine these reactions by studying the reaction of 1-butene – chosen as representative of the olefin pool – with HCHO on H-ZSM-5. Fig. 6a shows the product yield in the reaction of 45 mbar 1-butene with 0.32 mbar HCHO. The HCHO concentration was chosen as 0.18 C% in the total feed, corresponding to the average concentration derived from the yield of HCHO during MTO reaction at different contact times (as shown in Fig. 1). Butene dimerization and cracking were the dominant reactions leading to a 0.72 C% yield of propene, 1.2 C% yield of pentene and 0.17 C% yield of higher aliphatic products at 0.17 h g_{cat} mol_C^{-1} residence time (Fig. 6a). In addition, small concentrations of pentadiene, butadiene and butane were formed (Fig. 6a). Pentadiene is the product from Prins reaction of butene with HCHO (Rxn 6) while butane is formed via hydrogen transfer reaction (Rxn 5). Butadiene can be formed both from Prins reaction of propene with HCHO and from hydrogen transfer reaction.

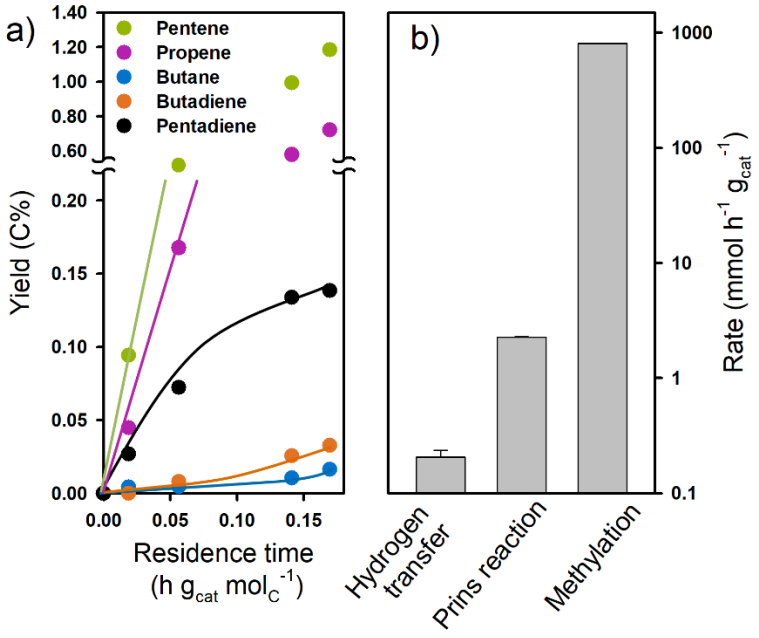

Figure 6: Reaction of 1-butene with HCHO over H-ZSM-5. (a) Product yield as a function of residence time. Reaction condition: 1-butene 45 mbar, HCHO 0.32 mbar, H_2O 22.5 mbar, 475 °C; (b) Reaction rates obtained for hydrogen transfer, Prins reaction (initial rates of formation of butane and pentadiene respectively under reaction conditions shown in Fig. 6a) and methylation (represented by the DME/MeOH conversion rate at ~ 40 % conversion shown in Fig. 1) on H-ZSM-5. Error bar represents the standard error of the reactions rates.

Therefore, the rates of pentadiene and butane formation represent the rates of Prins reaction and hydrogen transfer, respectively. As it can be seen in Fig. 6b, the rate of Prins reaction is one order of magnitude higher than that of hydrogen transfer, even though the concentration of HCHO was two orders of magnitude lower than that of butene. These results provide unequivocal evidence for previous speculations that the Prins reaction is the major route of HCHO being converted to H-poor products in the MTO process, i.e., dienes and aromatics.[18, 20] As a reference, the rate of

methylation, which represents the rate of the dual cycles, derived from a standard MTO feed (Fig. 1) is also included in Fig. 6b. It can be concluded that the reactions in the dual cycle are dominant in MTO, because the methylation rate is two orders of magnitude higher than the rate of Prins reaction. However, formaldehyde forms aromatics and H-poor products selectively, even if present only in low concentrations. Thus, it impacts the product distribution of the overall MTO process. The presence of HCHO acts in analogy to the established effect of co-feeding small concentrations of aromatics with MeOH on H-ZSM-5,[4] which leads to enhancement of the aromatic cycle, shifting the selectivity of the process towards aromatics and ethene.

Role of formaldehyde in deactivation

Aromatic molecules are coke precursors in MTO.[21-22, 25] The higher yield of aromatics induced by the presence of HCHO will, thus, cause a higher coking and deactivation rates. This is supported by the sharp decline of conversion with time on stream for the reactions of MeOH with 5 C% cofed $H^{13}CHO$ in contrast to pure MeOH feeds (Fig. 7). It is shown in Section 2.1 that the presence of HCHO would promote reactivity by facilitating the first olefin formation. However, because of the strong deactivation induced when 5 C% of MeOH is replaced by $H^{13}CHO$, under the same reaction conditions, the conversion dropped below 80 % after only 10 min time on stream and to approximately 5 % after 100 min. Conversely, when butene was co-fed with MeOH and HCHO, the fast consumption of MeOH and HCHO via alkylation and Prins reaction with butene lead to their full conversion at the contact time studied. The conversion only dropped slightly to 98.5 % after 100 min time on stream (Supplementary Fig. 2). This agrees well with previous conclusions that the presence of alkenes drastically prolongs catalyst lifetime.[10, 21]

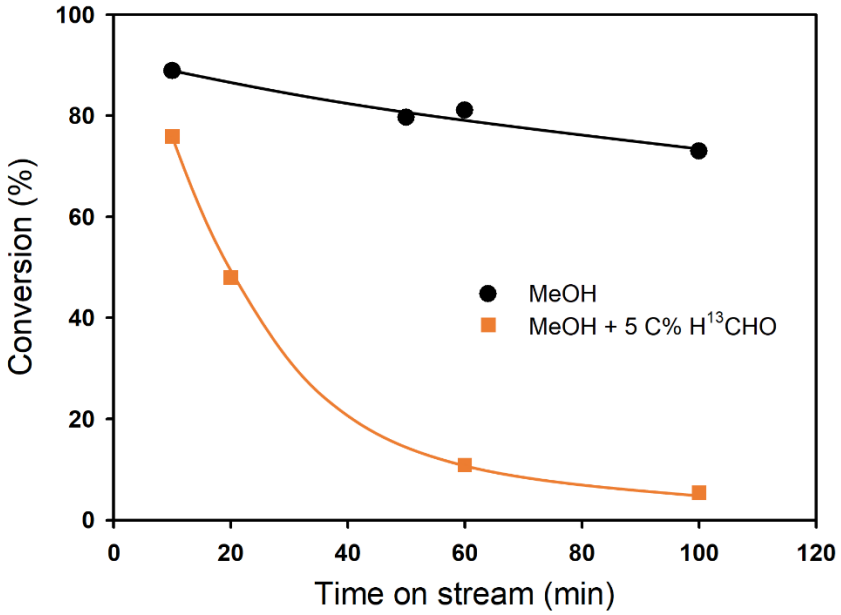

Figure 7: Evolution of MeOH conversion during MTO reaction with time on stream. The reactions in presence and absence of cofed $H^{13}CHO$ were compared. Reaction conditions: H-ZSM-5 (Si/Al 90 steamed), W/F 1.82 $h \cdot g_{cat} \cdot mol_{(MeOH+HCHO)}^{-1}$, MeOH 180 mbar, H_2O 60 mbar, or MeOH 171 mbar, $H^{13}CHO$ 9 mbar, H_2O 60 mbar, 475 °C.

The carbon deposits on H-ZSM-5 using different feeds were analyzed after 100 min time on stream and results are compiled in Table 3. The reaction of pure MeOH feed for 100 min accumulated 1.0 wt.% of coke on catalyst. In contrast, co-feeding 5 C% $H^{13}CHO$ increased the deposited coke to 5.2 wt.%. Normalizing the coke concentration to the converted MeOH showed that only 0.084 C% of pure MeOH feed are converted to coke, but 1.3 C% for MeOH co-fed with 5 C% $H^{13}CHO$. We conclude that the high rate of coke formation in presence of HCHO is attributed to the observed higher yield towards H-poor products.

When butene was co-fed to MeOH and HCHO, 7.7 wt.% coke was deposited, corresponding to 0.37 C% of the total converted MeOH. This lower coke formation per converted MeOH in the presence of butene, is attributed to the successful competition of methylation of butene, decreasing the local concentration of MeOH along the catalyst bed and, as a consequence, the concentration of HCHO (formed by MeOH hydrogen transfer).

The ^{13}C content of coke was analyzed by measuring the fraction of ^{13}CO and $^{13}CO_2$ in total CO and CO_2 during its combustion in temperature-programmed oxidation. The fast scrambling of ^{13}C in $H^{13}CHO$ with MeOH (Rxn 4) under MTO conditions causes an almost equal distribution of ^{13}C (5 – 6 %) in all products, including coke (6.2 % ^{13}C) in the reaction of MeOH with 5 C% $H^{13}CHO$. When the ^{13}C content of coke was analyzed after co-feeding butene with MeOH and 2 C% $H^{13}CHO$, coke contained 10 % ^{13}C, which is comparable to the ^{13}C percentage found in aromatics (11.6 % ^{13}C for xylene and 10.3 % ^{13}C for TMB). This amount of ^{13}C in coke corresponds to 0 72 C% of

total converted $H^{13}CHO$, which is twofold higher than the percentage of converted MeOH that ended up in coke (0.37 %), showing that HCHO has a higher fraction incorporated than MeOH.

Table 3: Coke concentration and extent of labelling after 100 min time on stream.

Reactants	Coke concentration on catalyst (wt.%)	Coke amount per total converted MeOH (C%)	^{13}C fraction in coke (%)
MeOH[a]	1.0	0.084	1.1[c]
MeOH + 5 C% $H^{13}CHO$[a]	5.2	1.3	6.2
MeOH + 1-Butene + 2 C% $H^{13}CHO$[b]	7.7	0.37	10.0

[a] W/F 1.82 $h \cdot g_{(cat)} \cdot mol_{(MeOH+HCHO)}^{-1}$, MeOH 171 mbar, $H^{13}CHO$ 9 mbar, H_2O 60 mbar, 475 °C;
[b] W/F 1.30 $h \cdot g_{(cat)} \cdot mol_{(MeOH+HCHO)}^{-1}$, MeOH 171 mbar, $H^{13}CHO$ 9 mbar, H_2O 60 mbar, 1-butene 60 mbar, 475 °C.
[c] Natural abundance of ^{13}C.

2.3 Discussion

The present experiments show unequivocally that formaldehyde, methane and CO are generated from MeOH under MTO conditions in H-ZSM-5. We have been able to identify key reaction intermediates in the mechanism of formation of alkenes from a C_1 reacting mixture containing MeOH, CO and HCHO. MeOH and DME react with CO into methyl acetate and acetic acid as the first species containing a C-C bond.[18, 35-38] Formaldehyde condenses with surface methyl acetate and acetic acid to form unsaturated carboxylic acids, which then are converted into the first olefin species via decarboxylation. Once the concentration of these olefins in the catalyst surpasses a threshold value, the fast methylation activity of Brønsted acid sites allows for the full development of the MTO dual-cycle reaction network.

Formaldehyde reacts with olefins into dienes via Prins reaction. The Prins reaction is one order of magnitude faster than the hydrogen transfer between two alkenes, which makes it the dominant reaction towards H-poor byproducts, i.e., dienes, aromatics and coke. Even in small concentrations, the presence of HCHO increases the selectivity to aromatics, enhancing the importance of the aromatic cycle in the dual cycle and in turn shifting the process towards a higher selectivity to ethene at expenses of the selectivity to propene and butenes. As an additional consequence, the high yield of aromatics induced by HCHO leads to a high rate of coke formation and to a high rate of deactivation.

Strategies to extend catalyst lifetime should aim, therefore, to minimize the HCHO concentration during the MTO reactions. This could be conceptually achieved by inhibiting its formation or by its fast decomposition. Indeed, many of the improvements in catalyst lifetime reported in the literature can be attributed to reaction conditions in which the chemical potential of MeOH – and thus of HCHO - is reduced in the reactor (via dilution of MeOH,[20, 26]co-feeding alkenes,[10] back-mixing products[10, 21] or replacing MeOH by DME[19]).

2.4 Methods

Catalysts

H-ZSM-5 catalyst with Si/Al 90 was synthesized according to the procedure described by Ong et al.[43] In brief, Na-ZSM-5 was first synthesized by mixing colloidal silica, $Al(NO_3)_3$ $9H_2O$, NaOH and tetrapropylammonium bromide (TPABr) with a composition of 100 SiO_2: 0.2 Al_2O_3: 5 Na_2O: 10 TPABr: 4000 H_2O. After aging, the obtained gel was transferred to an autoclave and kept at 180 °C for 48 h. Then the solid was separated by filtration and washed until pH 8. Afterwards, the powder was dried at 100 °C overnight and calcined with the following sequential steps: (1) rising with 1 °C/min to 200 °C in flowing He and kept for 3 h; (2) rising with 1 °C/min to 520 °C in flowing air and kept for 3 h. The obtained Na-ZSM-5 was then transformed into H-ZSM-5 via ion-exchange with NH_4NO_3 solution and calcination in flowing air at 520 °C for 3 h. It has a Si/Al ratio of 90 according to atomic absorption spectroscopic analysis. For some experiments, the H-ZSM-5 was steamed at 753 K for 24 h at water vapor pressure of 1 bar prior to usage. Accordingly, the samples are denoted as H-ZSM-5 (Si/Al 90) and H-ZSM-5 (Si/Al 90, steamed). For the TPSR/IR spectroscopy experiment an H-ZSM-5 with Si/Al 15 was used (named as H-ZSM-5 (Si/Al 15)) which was purchased from Zeolyst. Methanol (≥99.9%) and dimethoxymethane (99 %) were supplied by Sigma-Aldrich. ^{13}C-labeled HCHO (99 atom % ^{13}C) was purchased from Sigma-Aldrich as aqueous solution (20 wt. %).

TPSR/IR spectroscopy

Temperature programmed surface reactions (TPSR) of MeOH and DMM were performed in a home-made IR-cell connected to a mass spectrometer. A self-supporting wafer of 25 mg H-ZSM-5 (Si/Al 15) was loaded in the cell center and perpendicular to the IR beam. The H-ZSM-5 (Si/Al 15) has a high acid site concentration and high adsorption capacity of MeOH and DMM, and led, thus, to higher intensities of the bands in the IR spectra. The wafer was first activated at 723 K in vacuum for 1 h. After cooling down to 40 °C, 3 mbar MeOH or 1 mbar DMM was introduced into the cell and kept for 15 min followed by desorption for 30 min under vacuum. Then, the wafer temperature was increased to 40 °C with a rate of 3 °C min^{-1}. Desorbed molecules were detected on line using mass spectrometry: m/e 31 for MeOH, m/e 75 for DMM, m/e 45 for DME (after subtracting fragment ion signal of m/e 45 from DMM), m/e 16 for methane, m/e 30 for HCHO (after subtracting fragment ion signal of m/e 30 from MeOH), m/e 44 for CO_2, m/e 28 for CO (after subtracting fragment ion signal of m/e 28 from CO_2), m/e 27 for olefins. In-situ IR spectra of the wafer were collected on a Bruker Vertex 70 FTIR spectrometer.

Temperature-programmed oxidation of coke on spent catalysts

Thermogravimetric analysis (TGA) on a SETARAM Sensys Evo TGA-DSC was utilized to analyze coke deposited on deactivated catalysts. Typically, 10-20 mg of powdered sample was loaded and treated at 200 °C in 16 mL/min He flow until weight stabilization. Afterwards, the temperature was raised to 650 °C at 5 °C/min in 16 mL/min 10 vol% O_2 in He flow and kept for 1 h. The coke amount was obtained from the loss of weight and the formed H_2O, CO and CO_2 were detected online with an MS.

Catalytic testing

Catalytic measurements were performed in a fixed bed quartz reactor with an internal diameter of 6 mm at 475 °C and ambient pressure. The H-ZSM-5 catalysts (200-280 µm) were homogeneously diluted with silicon carbide (ESK-SiC) in the range of 355-500 µm to ensure temperature uniformity. Catalysts were activated at 475 °C for 1 h under He atmosphere before reaction. Methanol and water were introduced into the reactor by an HPLC-pump combine with a direct evaporator. For cofeeding experiments, 1-butene was fed by MFC (Bronkhorst) and ^{13}C-formaldehyde solution (20 wt%) was introduced into reactor by mixing with MeOH and the pump-evaporator combination. Via adjusting mixing ratio and liquid flow as well as the butene and He gas flow, the feeding ratio and partial pressures of 1-butene and ^{13}C-formaldehyde were varied, and the partial pressure of water was kept constant at 60 mbar. Products were analyzed online on a gas chromatograph (HP 5890) equipped with a HP-PLOTQ capillary column and an FID detector. A mass spectrometer is used to analyze H_2. Formaldehyde is detected by solving the reaction effluent in water at 2 °C with subsequent stoichiometric Hantzsch reaction as described by Nash[44] and quantification by a Varian Cary 50 UV-Vis Spectrophotometer. The product yield and selectivity were given on a carbon basis and DME was treated as unconverted methanol. For the quantification of ^{13}C fraction in the products, a certain volume of product stream was collected and analyzed on a GC-MS (Agilent Technologies 7890 B GC, column: Agilent HP-PLOT Q, 30 m, 0.32 mm, 20.00 µm). The analysis of ^{13}C incorporation is described in Supporting Information Methods part.

2.5 References

1. Olsbye, U.; Svelle, S.; Bjorgen, M.; Beato, P.; Janssens, T. V. W.; Joensen, F.; Bordiga, S.; Lillerud, K. P., Conversion of Methanol to Hydrocarbons: How Zeolite Cavity and Pore Size Controls Product Selectivity. *Angew Chem Int Ed* **2012,** *51* (24), 5810-5831.
2. Ilias, S.; Bhan, A., Mechanism of the Catalytic Conversion of Methanol to Hydrocarbons. *ACS Catal* **2013,** *3* (1), 18-31.
3. Yarulina, I.; Chowdhury, A. D.; Meirer, F.; Weckhuysen, B. M.; Gascon, J., Recent trends and fundamental insights in the methanol-to-hydrocarbons process. *Nat Catal* **2018,** *1* (6), 398-411.
4. Sun, X. Y.; Mueller, S.; Shi, H.; Haller, G. L.; Sanchez-Sanchez, M.; van Veen, A. C.; Lercher, J. A., On the impact of co-feeding aromatics and olefins for the methanol-to-olefins reaction on HZSM-5. *J Catal* **2014,** *314*, 21-31.
5. Dahl, I. M.; Kolboe, S., On the Reaction-Mechanism for Propene Formation in the Mto Reaction over Sapo-34. *Catal Lett* **1993,** *20* (3-4), 329-336.
6. Dahl, I. M.; Kolboe, S., On the Reaction-Mechanism for Hydrocarbon Formation from Methanol over Sapo-34 .1. Isotopic Labeling Studies of the Co-Reaction of Ethene and Methanol. *J Catal* **1994,** *149* (2), 458-464.
7. Dahl, I. M.; Kolboe, S., On the reaction mechanism for hydrocarbon formation from methanol over SAPO-34 .2. Isotopic labeling studies of the co-reaction of propene and methanol. *J Catal* **1996,** *161* (1), 304-309.
8. Bjorgen, M.; Svelle, S.; Joensen, F.; Nerlov, J.; Kolboe, S.; Bonino, F.; Palumbo, L.; Bordiga, S.; Olsbye, U., Conversion of methanol to hydrocarbons over zeolite H-ZSM-5: On the origin of the olefinic species. *J Catal* **2007,** *249* (2), 195-207.
9. Svelle, S.; Joensen, F.; Nerlov, J.; Olsbye, U.; Lillerud, K. P.; Kolboe, S.; Bjorgen, M., Conversion of methanol into hydrocarbons over zeolite H-ZSM-5: Ethene formation is mechanistically separated from the formation of higher alkenes. *J Am Chem Soc* **2006,** *128* (46), 14770-14771.
10. Sun, X. Y.; Mueller, S.; Liu, Y.; Shi, H.; Haller, G. L.; Sanchez-Sanchez, M.; van Veen, A. C.; Lercher, J. A., On reaction pathways in the conversion of methanol to hydrocarbons on HZSM-5. *J Catal* **2014,** *317*, 185-197.
11. Kubelková, L.; Nováková, J.; Jírů, P., Reaction of Small Amounts of Methanol on HZSM-5, HY and Modified Y Zeolites. *Stud Surf Sci Catal* **1984,** *18*, 217-224.
12. Hutchings, G. J.; Gottschalk, F.; Hunter, R., Kinetic-Model for Methanol Conversion to Olefins with Respect to Methane Formation at Low Conversion - Comment. *Ind Eng Chem Res* **1987,** *26* (3), 635-637.
13. Hutchings, G. J.; Gottschalk, F.; Hall, M. V. M.; Hunter, R., Hydrocarbon Formation from Methylating Agents over the Zeolite Catalyst ZSM-5 - Comments on the Mechanism of Carbon Carbon Bond and Methane Formation. *J Chem Soc Faraday Trans* **1987,** *83*, 571-583.
14. Tajima, N.; Tsuneda, T.; Toyama, F.; Hirao, K., A new mechanism for the first carbon-carbon bond formation in the MTG process: A theoretical study. *J Am Chem Soc* **1998,** *120* (32), 8222-8229.
15. Comas-Vives, A.; Valla, M.; Coperet, C.; Sautet, P., Cooperativity between Al Sites Promotes Hydrogen Transfer and Carbon-Carbon Bond Formation upon Dimethyl Ether Activation on Alumina. *Acs Central Sci* **2015,** *1* (6), 313-319.
16. Chu, Y.; Yi, X.; Li, C.; Sun, X.; Zheng, A., Brønsted/Lewis acid sites synergistically promote the initial C–C bond formation in the MTO reaction. *Chem Sci* **2018**.
17. Wang, C.; Chu, Y.; Xu, J.; Wang, Q.; Qi, G.; Gao, P.; Zhou, X.; Deng, F., Extra-framework Aluminum-Assisted First C-C Bond Formation in Methanol-to-Olefins Conversion on Zeolite H-ZSM-5. *Angew Chem Int Ed Engl* **2018**.

18. Liu, Y.; Müller, S.; Berger, D.; Jelic, J.; Reuter, K.; Tonigold, M.; Sanchez-Sanchez, M.; Lercher, J. A., Formation Mechanism of the First Carbon-Carbon Bond and the First Olefin in the Methanol Conversion into Hydrocarbons. *Angew Chem Int Ed* **2016,** *55* (19), 5723-5726.
19. Martinez-Espin, J. S.; Morten, M.; Janssens, T. V. W.; Svelle, S.; Beato, P.; Olsbye, U., New insights into catalyst deactivation and product distribution of zeolites in the methanol-to-hydrocarbons (MTH) reaction with methanol and dimethyl ether feeds. *Catal Sci Technol* **2017,** *7* (13), 2700-2716.
20. Arora, S. S.; Bhan, A., The critical role of methanol pressure in controlling its transfer dehydrogenation and the. corresponding effect on propylene-to-ethylene ratio during methanol-to-hydrocarbons catalysis on H-ZSM-5. *J Catal* **2017,** *356*, 300-306.
21. Müller, S.; Liu, Y.; Vishnuvarthan, M.; Sun, X. Y.; van Veen, A. C.; Haller, G. L.; Sanchez-Sanchez, M.; Lercher, J. A., Coke formation and deactivation pathways on H-ZSM-5 in the conversion of methanol to olefins. *J Catal* **2015,** *325*, 48-59.
22. Liu, Z. H.; Dong, X. L.; Liu, X.; Han, Y., Oxygen-containing coke species in zeolite-catalyzed conversion of methanol to hydrocarbons. *Catal Sci Technol* **2016,** *6* (22), 8157-8165.
23. Zhao, X. B.; Wang, L. Y.; Li, J. Z.; Xu, S. T.; Zhang, W. N.; Wei, Y. X.; Guo, X. W.; Tian, P.; Liu, Z. M., Investigation of methanol conversion over high-Si beta zeolites and the reaction mechanism of their high propene selectivity. *Catal Sci Technol* **2017,** *7* (4), 5882-5892.
24. Müller, S.; Liu, Y.; Kirchberger, F. M.; Tonigold, M.; Sanchez-Sanchez, M.; Lercher, J. A., Hydrogen Transfer Pathways during Zeolite Catalyzed Methanol Conversion to Hydrocarbons. *J Am Chem Soc* **2016,** *138* (49), 15994-16003.
25. Martinez-Espin, J. S.; De Wispelaere, K.; Erichsen, M. W.; Svelle, S.; Janssens, T. V. W.; Van Speybroeck, V.; Beato, P.; Olsbye, U., Benzene co-reaction with methanol and dimethyl ether over zeolite and zeotype catalysts: Evidence of parallel reaction paths to toluene and diphenylmethane. *J Catal* **2017,** *349*, 136-148.
26. Hwang, A.; Kumar, M.; Rimer, J. D.; Bhan, A., Implications of methanol disproportionation on catalyst lifetime for methanol-to-olefins conversion by HSSZ-13. *J Catal* **2017,** *346*, 154-160.
27. Hwang, A.; Bhan, A., Bifunctional Strategy Coupling Y2O3-Catalyzed Alkanal Decomposition with Methanol-to-Olefins Catalysis for Enhanced Lifetime. *ACS Catal* **2017,** *7* (7), 4417-4422.
28. Wu, X. Q.; Xu, S. T.; Zhang, W. N.; Huang, J. D.; Li, J. Z.; Yu, B. W.; Wei, Y. X.; Liu, Z. M., Direct Mechanism of the First Carbon-Carbon Bond Formation in the Methanol-to-Hydrocarbons Process. *Angew Chem Int Ed* **2017,** *56* (31), 9039-9043.
29. Wu, X.; Xu, S.; Wei, Y.; Zhang, W.; Huang, J.; Xu, S.; He, Y.; Lin, S.; Sun, T.; Liu, Z., Evolution of C–C Bond Formation in the Methanol-to-Olefins Process: From Direct Coupling to Autocatalysis. *ACS Catal* **2018,** *8* (8), 7356-7361.
30. Forester, T. R.; Howe, R. F., In situ FTIR studies of methanol and dimethyl ether in ZSM-5. *J Am Chem Soc* **1987,** *109* (17), 5076-5082.
31. Kresnawahjuesa, O.; Gorte, R. J.; White, D., Characterization of acylating intermediates formed on H-ZSM-5. *J Mol Catal A Chem* **2004,** *208* (1-2), 175-185.
32. Chen, X. Y.; Neidig, M. L.; Tuinstra, R.; Malek, A., Direct Observation of Acetyl Group Formation from the Reaction of CO with Methylated H-MOR by in Situ Diffuse Reflectance Infrared Spectroscopy. *J Phys Chem Lett* **2010,** *1* (20), 3012-3015.
33. Celik, F. E.; Kim, T.; Mlinar, A. N.; Bell, A. T., An investigation into the mechanism and kinetics of dimethoxymethane carbonylation over FAU and MFI zeolites. *J Catal* **2010,** *274* (2), 150-162.
34. Cheung, P.; Bhan, A.; Sunley, G. J.; Law, D. J.; Iglesia, E., Site requirements and elementary steps in dimethyl ether carbonylation catalyzed by acidic zeolites. *J Catal* **2007,** *245* (1), 110-123.
35. Chowdhury, A. D.; Houben, K.; Whiting, G. T.; Mokhtar, M.; Asiri, A. M.; Al-Thabaiti, S. A.; Basahel, S. N.; Baldus, M.; Weckhuysen, B. M., Initial Carbon-Carbon Bond Formation during the Early Stages of the Methanol-to-Olefin Process Proven by Zeolite-Trapped Acetate and Methyl Acetate. *Angew Chem Int Ed* **2016,** *55* (51), 15840-15845.

36. Chowdhury, A. D.; Paioni, A. L.; Houben, K.; Whiting, G. T.; Baldus, M.; Weckhuysen, B. M., Bridging the Gap between the Direct and Hydrocarbon Pool Mechanisms of the Methanol-to-Hydrocarbons Process. *Angew Chem Int Ed* **2018,** *57* (27), 8095-8099.
37. Plessow, P. N.; Studt, F., Theoretical Insights into the Effect of the Framework on the Initiation Mechanism of the MTO Process. *Catal Lett* **2018,** *148* (4), 1246-1253.
38. Plessow, P. N.; Studt, F., Unraveling the Mechanism of the Initiation Reaction of the Methanol to Olefins Process Using ab Initio and DFT Calculations. *ACS Catal* **2017,** *7* (11), 7987-7994.
39. Morooka, S.; Matubayasi, N.; Nakahara, M., Kinetic study on disproportionations of C1 aldehydes in supercritical water: Methanol from formaldehyde and formic acid. *J Phys Chem A* **2007,** *111* (14), 2697-2705.
40. Wang, A. L.; Hu, J.; Yin, H. B.; Lu, Z. P.; Xue, W. P.; Shen, L. Q.; Liu, S. X., Aldol condensation of acetic acid with formaldehyde to acrylic acid over Cs(Ce, Nd) VPO/SiO2 catalyst. *RSC Adv.* **2017,** *7* (76), 48475-48485.
41. HouŽViČKa, J.; Ponec, V., Skeletal Isomerization ofn-Butene. *Catalysis Reviews* **1997,** *39* (4), 319-344.
42. Klepel, O., Oligomerization as an important step and side reaction for skeletal isomerization of linear butenes on H-ZSM-5. *Applied Catalysis A: General* **2003,** *255* (2), 349-354.
43. Ong, L. H.; Domok, M.; Olindo, R.; van Veen, A. C.; Lercher, J. A., Dealumination of HZSM-5 via steam-treatment. *Micropor Mesopor Mat* **2012,** *164*, 9-20.
44. Nash, T., The colorimetric estimation of formaldehyde by means of the Hantzsch reaction. *Biochem. J.* **1953,** *55*, 416-421.

2.6 Supporting information

Supplementary Method 1. Analysis of ^{13}C incorporation in gas products.

The degree of ^{13}C incorporation in gas products in MTO was determined by analyzing the MS spectra of each gas product in GC-MS. The normal procedure of analyzing the shift of the molecular ion towards m/e +1 and +2 is hardly applicable in this work because the ^{13}C incorporation is very low and the molecular ions of a few products are less abundant than fragment ions. Therefore, we used a different approach as follow:

(1) For a certain product, we take its MS spectra and find all the fragment ions that have the same number of carbons as the molecular ion in the MS spectra.
(2) Define and calculate “mean weight (m/e) of fragment ions” as intensity weighted fragment ion weight:

$$W_{\text{frag}} = \frac{\sum_{j=m}^{n} j \cdot I_{\text{j}}}{\sum_{j=m}^{n} I_{\text{j}}} \qquad \text{(Eq. 1)}$$

The *m* and *n* are the lowest m/e and highest m/e in the fragment ions mentioned in (1); I_{j} is the MS peak intensity of the fragment ion with m/e of *j*.

(3) The unlabeled product has the mean weight of fragment ions, $W_{\text{frag,unlabel}}$; the ^{13}C incorporated sample has $W_{\text{frag,samp}}$. Then the fraction of ^{13}C in the product, X_{13C}, is calculated by:

$$X_{13C} = \frac{W_{\text{frag,samp}} - W_{\text{frag,unlabel}}}{N} + 1.1\% \qquad \text{(Eq. 2)}$$

in which *N* is the number of carbon atoms in the product molecule; 1.1 % is the natural abundance of ^{13}C.

The derivation of equation (2):

The product sample is a mixture of unlabeled and ^{13}C labeled molecules. It contains x_0 mole of unlabeled molecule, x_1 mole of one ^{13}C labeled molecule, x_{j} mole of *j* (number) ^{13}C labeled molecule, till x_{N} mole of *N* ^{13}C labeled molecule. *N* is the number of carbon atoms in the product molecule. The unlabeled molecule has the mean weight of fragment ions, $W_{\text{frag,unlabel}}$. The one ^{13}C labeled molecule has the mean weight of fragment ions, $W_{\text{frag,unlabel}} + 1$. The *j* (number) ^{13}C labeled

molecule has the mean weight of fragment ions, $W_{frag,unlabel} + j$. Then the product sample has a mean weight of fragment ions of $W_{frag,samp}$.

$$W_{frag,samp} = \frac{\sum_{j=0}^{N} x_j \left(W_{frag,unlabel} + j\right)}{\sum_{j=0}^{N} x_j} = W_{frag,unlabel} + \frac{\sum_{j=0}^{N} x_j j}{\sum_{j=0}^{N} x_j} \quad \text{(Eq. 3)}$$

The second term on the right in equation (3) is virtually the number of more ^{13}C atoms per product molecule compared to that in unlabeled molecule. Since each product molecule contains *N* number of carbon atoms, the fraction of ^{13}C in the product, X_{13C}, is thus given by Equation 4. The natural abundance (1.1 % ^{13}C) of unlabeled molecule is accounted.

$$X_{13C} = \frac{\sum_{j=0}^{N} x_j j}{\sum_{j=0}^{N} x_j} \cdot \frac{1}{N} + 1.1\% = \frac{W_{frag,samp} - W_{frag,unlabel}}{N} + 1.1\% \quad \text{(Eq. 4)}$$

Supplementary Method 2. Analysis of ^{13}C incorporation in cokes.

The quantification of ^{13}C fraction in cokes was carried by analyzing the generated CO_2 on a mass spectrometer in the temperature programmed oxidation (TPO) of cokes. With the obtained spectra, the intensity ratio of $^{13}CO_2$ (m/e 45) to the sum of the intensity of $^{12}CO_2$ (m/e 44) and $^{13}CO_2$ (m/e 45) was used as the ^{13}C fraction in coke.

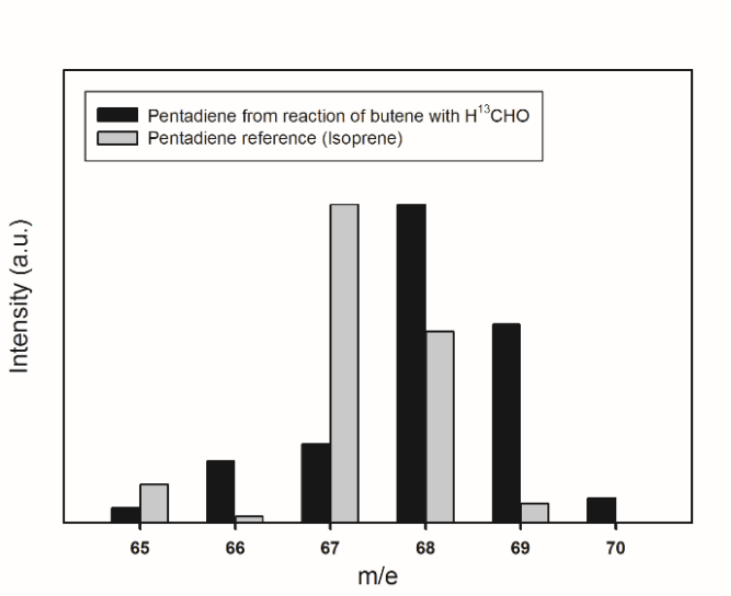

Supplementary Figure 1: MS of pentadiene from the reaction of butene with $H^{13}CHO$. Reaction conditions: $H^{13}CHO$ 3.8 mbar, butene 1.5 mbar ($H^{13}CHO$/Butene 2.5/1), 35 mL/min N_2 flow, H-ZSM-5 (Si/Al 90 steamed) 35 mg, 475 ^oC, butene conversion 26 %.

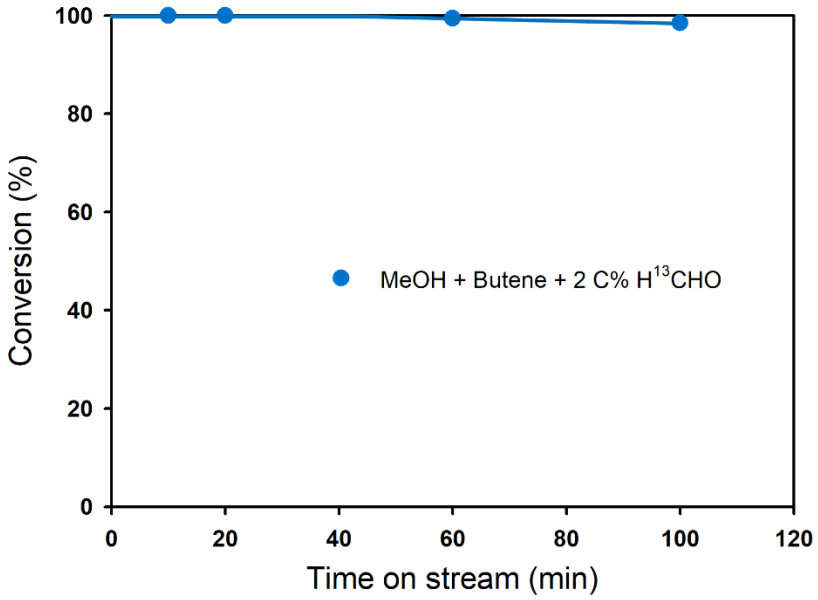

Supplementary Figure 2: Evolution of MeOH conversion during MTO reaction with time on stream under the feeding of MeOH, 1-butene and 2 C% $H^{13}CHO$. Reaction conditions: W/F = 0.96 $h \cdot g_{(cat)} \cdot mol_{(MeOH+HCHO)}^{-1}$, MeOH 171 mbar, $H^{13}CHO$ 9 mbar, H_2O 60 mbar, butene 60 mbar.

2.7 Associated Content

Publication

This chapter is based on a peer reviewed article (Yue Liu, Felix M. Kirchberger, Sebastian Müller, Moritz Eder, Markus Tonigold, Maricruz Sanchez-Sanchez, Johannes A. Lercher; "*Critical role of formaldehyde during methanol conversion to hydrocarbons*" Nature Communications 2019, 10, 1462.

Minor changes on the layout have been made.

Contributions

F.M.K. did the quantification of HCHO, the deactivation test and the ^{13}C-HCHO cofeeding and tracing experiments; F.M.K., S.M. and M.E. carried out the catalytic reactions and analyzed the conversion and product selectivity; Y.L. prepared the catalysts, performed the surface reactions, collected infrared spectra and analyzed the cokes; Y.L., M.T., M.S.-S. and J.A.L. conceived the research; The manuscript was written through contributions of all authors. All authors have given approval to the final version of the manuscript.

Acknowledgements

The authors acknowledge the support of the Bavarian Ministry of Economic Affairs and Media, Energy and Technology and Clariant Produkte (Deutschland) GmbH. S.M. is thankful to Elisabeth Hanrieder for helpful discussions. Y.L. and F.M.K. are thankful to Manuel Wagenhofer for discussion of ^{13}C quantification.

3. Difference in the reactivity of methanol and dimethyl ether in ZSM-5 and its role in the autocatalytic formation of olefins

Abstract: Hydride transfer is the rate determining step in the initiation of the conversion of methanol to higher hydrocarbons. Surface methoxy species formed by dissociative adsorption of methanol are the main H acceptors with methane as end-product and formaldehyde and related C_1 species as reactive intermediates for the formation of first C-C bond products. Thus, the methane formation rate linearly correlates with the formation of hydrocarbons at low methanol conversions. Dimethyl ether decomposes as well into methane and formaldehyde leading to a C_1 reacting mixture similar to the mixture obtained from methanol. However, the hydrogen transfer rate from DME to methoxy species is one order of magnitude faster than from methanol. The net hydrocarbon methylation rates, once larger hydrocarbons are formed are similar for both reactants. The presence of H_2O decreases the overall coverage of methoxy species and shifts the equilibrium between methanol and dimethyl ether, affecting so both, initiation and methylation rates.

3.1 Introduction

The catalytic conversion of methanol in lower olefins (MTO), gasolines (MTG) or aromatic compounds (MTA), is the key flexible synthetic alternative route to crude oil based production pathways. Methanol as a platform chemical enables the use of less conventional hydrocarbon sources like coal, natural gas and biomass.[1-4] Two types of molecular sieve catalysts, aluminasilicate MFI and the silicoaluminophosphate of CHA, SAPO-34, are commercialized in the majority of processes, producing propene and ethene with different selectivities due to their different shape selectivity induced by the framework structures and depending on operation conditions.[5]

It is a characteristic of the MTO reaction that the feedstock is introduced as a mixture of MeOH, dimethyl ether (DME) and water, in ratios determined by the reversible dehydration of MeOH to DME and water. Even when only DME is introduced, its conversion to hydrocarbons forms water and MeOH. It is common practice in industrial applications to utilize water to dilute hydrocarbons and to promote heat transfer, modulating inevitably the interconversion between MeOH and DME. Therefore, the differences in the reactivity between MeOH and DME to both olefin products and non-olefinic byproducts as well as the influence of the presence of water in MTO have been studied.[6-9] The different reactivity of MeOH and DME would be less important, if they were equilibrated under reaction conditions, but several reports showed that concentrations of MeOH, DME and water deviate from equilibrium.[5, 10]

The conversion of MeOH/DME on zeolites proceeds via three stages: (1) an initiation stage, for which conversion is very low, but the first C-C bond is formed and the resulting species are gradually converted to a hydrocarbon pool[11-13] (Fig. 1, Stage I); (2) as soon as a certain concentration of hydrocarbons in the hydrocarbon pool is reached, methylation begins to dominate and MeOH and DME are rapidly converted by a dual-cycle mechanism[14-15] in an autocatalytic manner (Fig. 1, Stage II); (3) after complete conversion of methanol and DME, the interconversions between hydrocarbons, including mainly short olefins, aromatics, and short alkanes, determine the final product distribution (Fig. 1, Stage III). In a fixed bed reactor, this zoning leads to the characteristic S-shape of conversion versus contact time (Fig. 1).

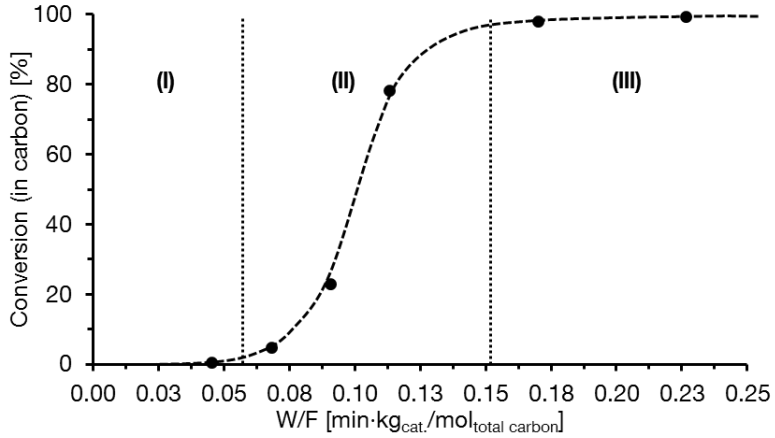

Figure 1: Conversion as a function of contact time during the MTH process. The characteristic S-shape curve is divided into three sections: (I): initiation period, (II): autocatalytic period and (III): hydrocarbon interconversion in the absence of MeOH or DME. T = 748 K, 180 mbar MeOH in N_2 dilution over H-ZSM-5. DME is treated as unconverted MeOH.

DME was reported to be more reactive than MeOH.[16-17] However, regarding the formation of non-olefinic byproducts, MeOH was speculated to be more reactive.[8] Olsbye et al. postulated that only MeOH could be converted to formaldehyde, the critical intermediate inducing strong deactivation.[8] In spite of these qualitative comparisons, a precise quantitative evaluation of the reactivity differences between DME and MeOH is experimentally challenging, because MeOH, DME, and water always coexist in the reaction due to a rapid interconversion making it difficult to evaluate the influence of each single component separately. Moreover, the key mechanistic intermediates in the reaction pathways leading to non-olefinic byproducts and catalyst deactivation are highly reactive and, therefore, challenging to detect and quantify.[18-20]

In this work, we evaluate the equilibrium of DME, MeOH and H_2O over a whole H-ZSM-5 catalyst bed in MTO reaction and compare the reactivity of DME and MeOH in different reaction steps; i.e., the initiation of the hydrocarbon pool and the dual-cycle. We provide evidence of a higher reactivity of DME for the formation of CH_4 and HCHO compared to MeOH, which leads to differences in overall rates and in the deactivation of the catalyst. In contrast, the study shows that methylation rates in the production of olefins by the dual-cycle are similar for DME and MeOH feeds.

3.2 Results and discussion

3.2.1 Equilibrium between MeOH and DME

The reversible intermolecular dehydration of MeOH to DME is a primary reaction in MTH (Rxn. 1).

$$CH_3OCH_3 + H_2O \rightleftharpoons 2\ CH_3OH \qquad \text{(Rxn. 1)}$$

As a consequence, under typical MTH conditions, not only MeOH but also the presence of DME and H_2O in the feed has to be considered. Thus, in a mechanistic study it is necessary to understand the interactions of MeOH, DME and H_2O with active sites (i.e., competitive adsorption) and their different reactivity towards surface intermediates.

In order to study the influence of the different feed components during the MTH reaction, it is necessary to know how DME and MeOH partial pressures evolve along the catalytic bed. The gas phase composition is affected by the initial composition of the feed and the MeOH dehydration equilibrium (Rxn. 1), but also (as the MTH reaction progresses) by the different rate of consumption of MeOH and DME in the formation of hydrocarbons. Fig. 2A shows the concentrations of MeOH, H_2O and DME measured for a reaction with initial feed of 90 mbar DME and 90 mbar water on H-ZSM-5. It can be seen that MeOH, DME and H_2O quickly reached steady concentrations at short contact times (before the onset of olefins), with a calculated pseudo-equilibrium constant of $(P_{MeOH})^2/(P_{DME}\cdot P_{H2O}) = 0.201 \pm 0.004$. The P_{MeOH}, P_{DME} and P_{H_2O} here refer to measured partial pressures of MeOH, DME and H_2O in the contact time range 0.02 - 0.05 $min\cdot kg_{cat}\cdot mol_{total\ carbon}^{-1}$. Similar ratios were obtained with different MeOH, DME, and water mixtures at 475 °C (Supporting information, S1), indicating that the pseudo-equilibrium constant at 475 °C for Reaction 1 is 0.22 ± 0.03. It should be noted that this experimental value deviates from the theoretical value of K_{eq} 0.30.[21] The discrepancy is likely due to deviations from ideal gas behavior of MeOH, DME and H_2O in the zeolite micropores at reaction conditions. For the sake of clarity, in this work we use K_{eq} notation to refer to the experimental value.

After the onset of alkene formation, MeOH and DME are rapidly consumed, while H_2O is produced due to the fast conversion either via alkene (olefin pathway) or arene (aromatics pathway) methylation. If these reactions are faster than the rates leading to interconversion of MeOH, DME and H_2O, their concentrations in the outlet are no longer equilibrated. The deviation from equilibrium from the side of dimethyl ether can be better examined by the use of the approach-to-equilibrium value η_{eq} of Rxn. 1. (Fig. 2B)

$$\eta_{eq} = \frac{(P_{MeOH})^2}{P_{DME}\cdot P_{H2O}} / K_{eq} \qquad \text{(Eq. 1)}$$

In Equation 1, MeOH, DME, and H_2O are assumed to behave ideally. The MeOH/DME conversion in Fig. 2B follows the characteristic S-shape curve with contact time, with an initiation zone ranging from 0 to 0.05 $min \cdot kg_{cat} \cdot mol_{total\ carbon}^{-1}$ and autocatalysis zone from 0.05 to 0.15 $min \cdot kg_{cat} \cdot mol_{total\ carbon}^{-1}$. The equilibration of DME, H_2O and MeOH ($\eta_{eq} \approx 1$) is reached within the initiation stage at a contact time of ca. 0.025 $min \cdot kg_{cat} \cdot mol_{total\ carbon}^{-1}$, as mentioned above. At conversions above 5 C% of MeOH/DME, η_{eq} increases sharply up to a value of 2.0, indicating that the methylation rate in the dual-cycle is faster than the interconversion of MeOH and DME (Rxn 1) under these conditions. The same trend was observed with other feed compositions, as long as the water/DME feed ratios were below 2. Under excess of H_2O, the partial pressures of MeOH, DME and H_2O are equilibrated over the whole contact time range explored (Supporting Information S5).

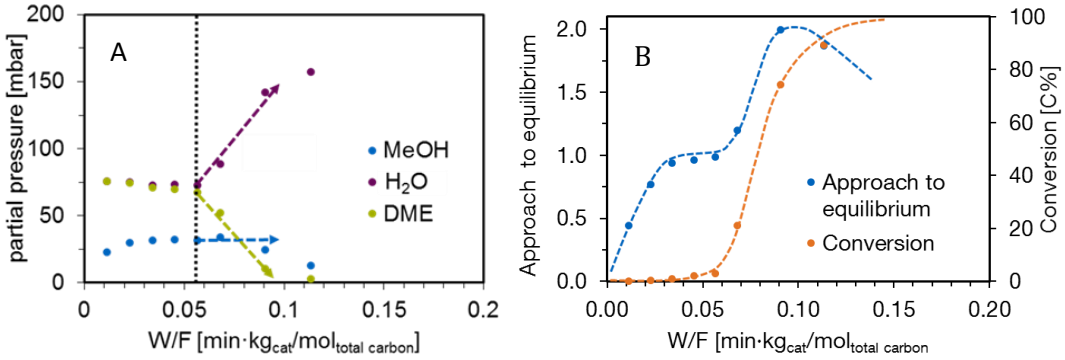

Figure 2: Equilibrium between the DME and MeOH during their conversion to hydrocarbons versus the W/F value. A depicts the partial pressure of DME, MeOH and H_2O (calculated for atmospheric pressure and an average C-number of formed HCs of four). B gives approach to equilibrium defined as $c(MeOH)^2/(c(DME) \cdot c(water) \cdot Keq)$ as well as the overall conversion of DME and MeOH the molar fractions of DME, MeOH and H_2O. The dotted line in Fig. A marks the onset of olefins where ~ 0.02 C% propene is formed.

3.2.2 Hydrogen transfer reactions with MeOH and DME as H-donors

Besides the interconversion of MeOH and DME via dehydration and hydration, MeOH transfers a hydrogen to chemisorbed methanol, a methoxy group, leading to the formation of CH_4 and HCHO (Rxn. 2).[22-23]

$$2\ CH_3OH \longrightarrow CH_4 + HCHO + H_2O \qquad \text{(Rxn. 2)}$$

The reaction forms formaldehyde and methane in equimolar quantities. This reaction, even though it occurs at very low rates, is an essential step in the initiation zone, as it provides key intermediates for the formation of the first olefins that subsequently are transformed to higher hydrocarbons of the hydrocarbon pool.[11]

Fig. 3 shows the reaction of dry DME on H-ZSM-5 at very short contact times (up to 0.007 $min \cdot kg_{cat} \cdot mol_{total\ carbon}^{-1}$) and low conversions (< 0.3 C%). Under these conditions, the presence of MeOH is ruled out. It can be seen that methane and formaldehyde are formed as primary products, in good agreement with the decomposition of DME into methane and formaldehyde proposed in Reaction 3, which has been so far only reported by computational catalysis.[24]

$$CH_3OCH_3 \longrightarrow CH_4 + HCHO \qquad \text{(Rxn. 3)}$$

A very small amount of C_2+C_3 olefins appeared at ~ 0.005 $min \cdot kg_{cat} \cdot mol_{total\ carbon}^{-1}$, which are the main C-C bond containing products under those conditions. The methane yield increased linearly from the beginning of the reaction, until the formation rate of olefins started to increase significantly (from 0.007 min $kg_{cat} \cdot mol_{total\ carbon}^{-1}$ on). This indicates a constant formation rate of methane in the initiation period. Based on Reactions 2 and 3, HCHO should be formed in stoichiometric amounts to methane. However, measured HCHO formation rates were lower than CH_4 formation rates. This difference is attributed to the high reactivity of HCHO, which leads to its rapid consumption in consecutive reactions, such as the decomposition to CO or the condensation with surface species to build the hydrocarbon pool.[12, 19-20, 24-26]

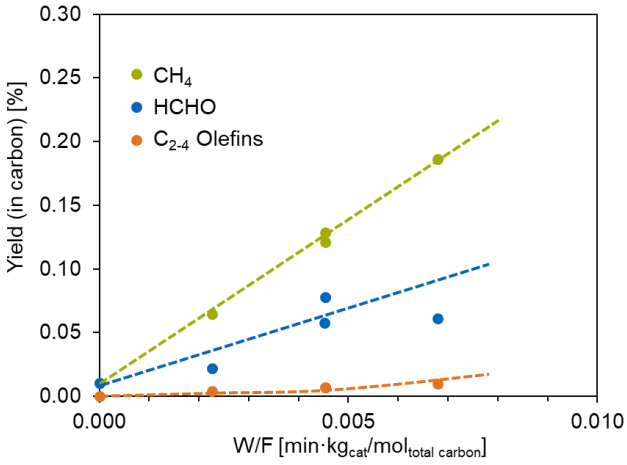

Figure 3: Yield of methane, formaldehyde and C_2+C_3 olefins at short contact times. Reaction conditions: T=748K, Feed: N_2/DME, p (DME) =90 mbar; $\dot{n}$ (C-based) = 14 mmol/h.

In contrast to the high reactivity of HCHO in secondary reactions, methane is quite stable on H-ZSM-5 under the applied MTO conditions (see Supporting Information, S2) and can be considered as end-product. Therefore, the methane formation rate at low conversions is a suitable quantitative descriptor of the extent of hydrogen transfer involving MeOH and DME surface species in the initiation zone of MTO conversion. Thus, we used the methane formation rates at short contact times under different DME/H_2O feeds to evaluate the activity of DME and MeOH in hydrogen transfer reactions in the initiation stage.

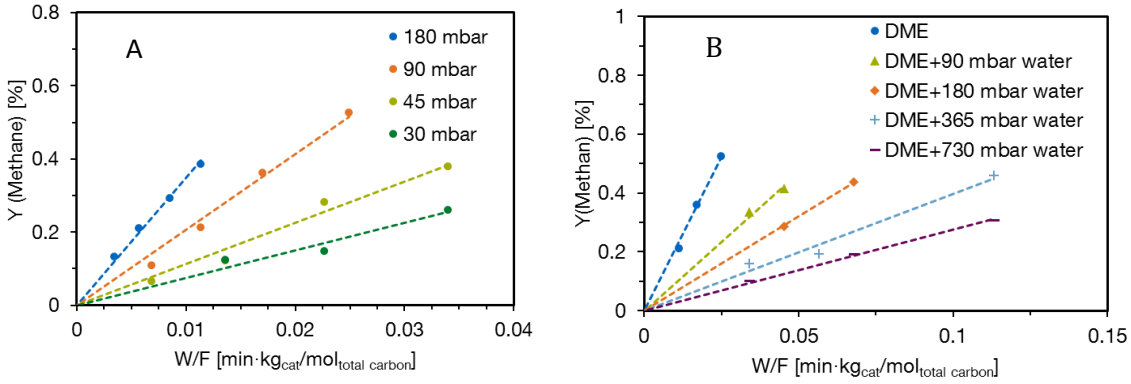

Figure 4: Evolution of the methane yield with contact time (weight over feed, W/F) for different DME partial pressures in dry feed (A) and for different H_2O/MeOH/DME compositions (B), in both cases N_2 is used as dilutant. (A): DME pressure is varied from 30 to 180 mbar. (B): DME is intruduced with a partial pressure of 90 mbar, while different water partial pressures from 90 to 730 mbar are added. In both plots W/F is defined by the total molar amount of introduced carbon, which is kept constant in between the measurements, while the catalyst loadings are varied.

Fig. 4 shows the evolution of methane yield with contact times in the initiation stage of MTO with different feed compositions (conditions at which olefin yields are below 0.8 C%). In all cases, a linear increase of the methane yield with contact time was observed, the slope representing CH_4 formation rates.

Determining the reaction kinetics with respect to the three feed components (DME, methanol and water) for the methane formation rate is the basis for a further understanding of the reaction mechanism of hydrogen transfer in the initiation stage. However, due to fast equilibration of the interconversion between MeOH, DME and water (Rxn. 2), it is not possible to vary independently the partial pressure of the three involved components. However, by adjusting the overall flow with an inert gas (N_2), one of the components partial pressure can be kept constant, while the other two vary accordingly to the equilibrium.

The reaction with pure DME is the simplest case. In the absence of H_2O, hydration of DME to MeOH (Rxn. 1) is excluded and the formation rate of methane is only related to reactions from DME. The CH_4 formation rate increased proportionally with increasing DME pressure (Fig. 5, black line), indicating a first order reaction with respect to DME (Supporting Information S3). This indicates a direct conversion of DME into methane and formaldehyde (Scheme 1). Although subsequent reactions of the growing hydrocarbon pool might produce additional methane,[2, 27] the amount of CH_4 originating from these routes was negligible at this low DME conversions.

Next, we co-fed DME and H_2O in a N_2 flow under reaction conditions similar to the experiments in absence of water. Under these conditions MeOH, DME and H_2O rapidly equilibrated. Based on this equilibration, we adjusted the DME and H_2O concentrations in the feed in order to reach constant MeOH partial pressure for all measurements in Fig. 5. The measured CH_4 formation rate (Fig. 5 blue line and Supporting Information Table S3) was significantly lower than the rate obtained with dry DME. The reaction order of approximately 1 with respect to DME was preserved (Fig. S5-A in Supporting Information).

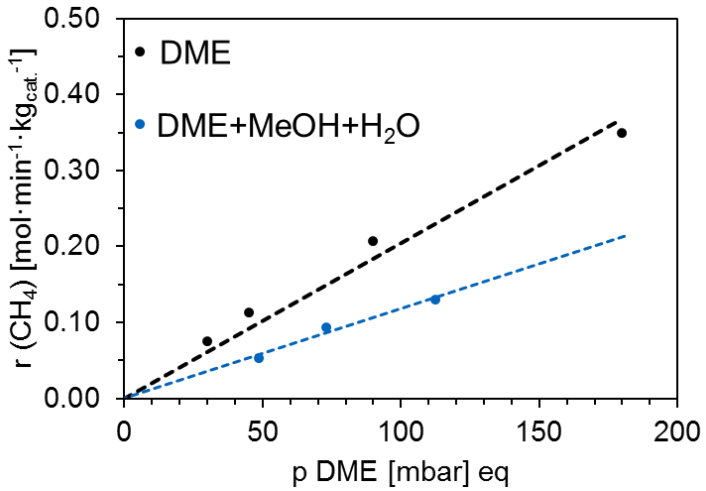

Figure 5: Methane formation rate as a function of DME pressure in pure DME feedings (black) and in mixtures of DME, MeOH and water (blue). Reaction at 748 K with a W/F of 0 to 0.05 $min \cdot kg_{cat} \cdot mol_{total\ carbon}^{-1}$ and partial pressures of the feed as shown in (Supporting Information S3). In the latter case a constant MeOH partial pressure is reached during the equilibrium while the water partial pressure increases parallel to the DME partial pressure.

We hypothesize that two possible reaction pathways of DME lead to a first order rate dependence for CH_4 formation: (1) direct decomposition of DME on BAS, or (2) hydrogen transfer from DME to methoxy groups at high coverage of BAS with methoxy species (Scheme 1). The pathway 1 is unlikely to happen, because the protonation of DME usually occurs at the oxygen atom, forming $CH_3O(H^+)CH_3$. The pathway 2, in contrast, has been described by Plessow et al. for H-SSZ-13 as catalyst.[24]

We have observed that the presence of MeOH and/or water decreased the methane formation rate (Fig. 5) with respect to dry DME. When the DME pressure was constant (Supporting Information S5B), the methane rate decreased with increasing MeOH and H_2O partial pressures. Even though MeOH itself can lead to methane formation by reaction with methoxy species (Scheme 1, Pathway 3), the rate for that reaction seems to be significantly lower than for DME. Thus, increasing concentration of H_2O leads to a lower fraction of DME in the reactive mixture and in turn to an overall lower rate of hydride transfer.

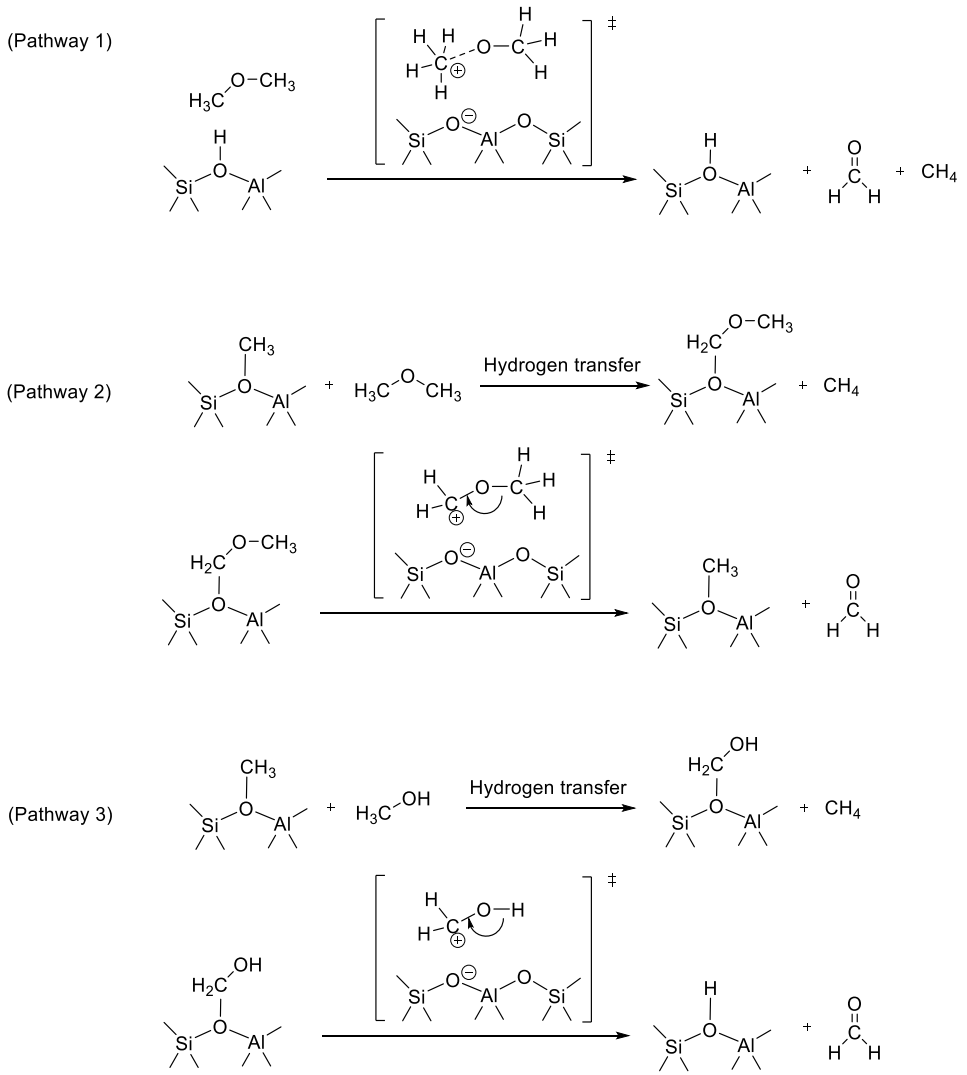

Scheme 1: Postulated reaction steps necessary for decomposition of DME and MeOH into methane and formaldehyde.

Thus, we conclude that both DME and MeOH form CH_4 via hydrogen transfer to surface methoxy species, the latter with a lower rate than the former (pathways 2 and 3 in Scheme 1). Therefore, the reaction of methoxy groups with methanol lead either reversibly to DME (Scheme 2, reaction II) or quasi-irreversibly to formaldehyde and methane via hydrogen transfer (Scheme 2, reaction III). It should be noted that the reaction of methoxy species with H_2O forms methanol and restores a BAS (Scheme 2, reaction I). Thus, the water partial pressure influences not only the partial pressure of MeOH and DME by Rxn 1, but also the available concentration of reactive surface methoxy species. The reactions I and II in Scheme 2 are the elementary steps in the interconversion of DME, MeOH and water, which is readily equilibrated in gas phase (Fig. 2). At the reaction conditions used here (T = 748 K, conversions < 1 C%), it can be assumed that the coverage of BAS with methoxy species is determined by the reaction equilibria I and II.[28] Thus,

hydrogen transfer from DME or MeOH to surface methoxy species is concluded to be the rate determining step (Scheme 2, reaction III and IV) for CH_4 formation. Note that the rate of these reactions also depends on the concentration of surface methoxy species.

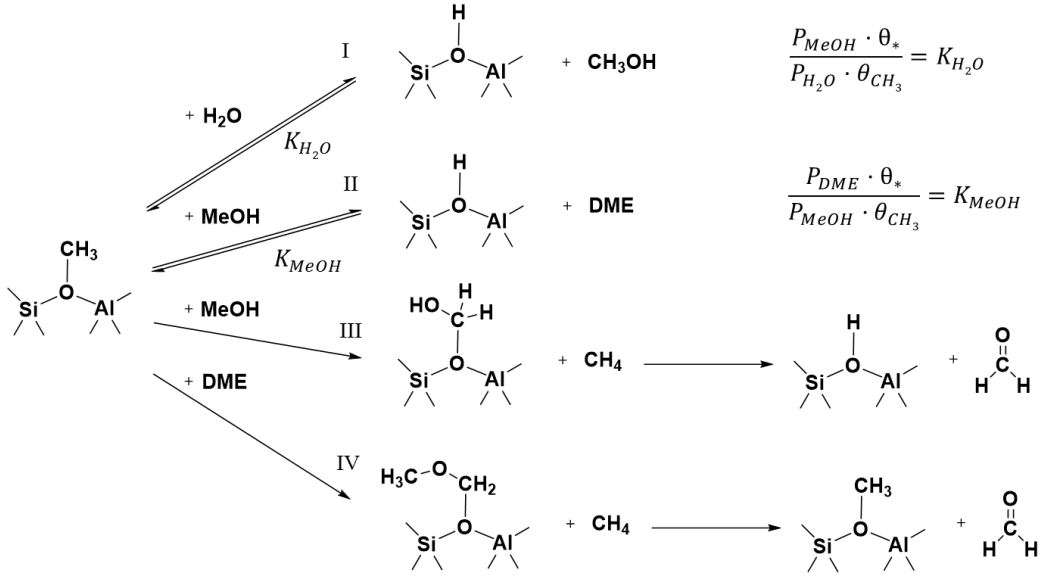

Scheme 2: Reaction pathways starting from surface methoxy species and the feed components MeOH and H_2O.

Based on the reaction network in Scheme 2, we derive a rate equation for the formation of methane and formaldehyde depending on the partial pressures of DME, MeOH and water. Because reactions (I) and (II) are the elementary steps for the interconversion of DME and MeOH (Rxn 1), they have the correlation shown in Equation 2.

$$\frac{K_{H2O}}{K_{MeOH}} = \frac{{P_{MeOH}}^2}{P_{H2O} \cdot P_{DME}} = K_{Eq} \qquad \text{(Eq. 2)}$$

Based on the adsorption entropy and enthalpy values reported by Pope et. al.[29] and Piccini et al.[30] for H_2O and MeOH respectively, the coverage of BAS by H_2O, MeOH and DME can be regarded as negligible at 748 K (Supporting Information S6). Thus, only the coverage of BAS by methoxy species has to be taken into account:

$$\Theta_{CH3} + \Theta_* = 1 \qquad \text{(Eq. 3)}$$

From the reaction constants of I and II, the ratio of the coverage of the methoxy species (θ_{CH3}) and empty BAS sites (θ_*) can be expressed as a function of MeOH and H_2O partial pressures.

$$\frac{\Theta_{CH3}}{\Theta_*} = \frac{P_{MeOH}}{P_{H2O}} \cdot \frac{1}{K_{H2O}} \qquad \text{(Eq. 4)}$$

The rate of formation of methane has contributions of both the reaction of DME and MeOH with surface methoxy species (reactions III and IV):

$$r_{CH4} = k_{DME} \cdot \Theta_{CH3} \cdot P_{DME} + k_{MeOH} \cdot \Theta_{CH3} \cdot P_{MeOH} \quad \text{(Eq. 5)}$$

Here, k_{DME} refers to the reaction rate constant for the methane formation from DME and k_{MeOH} to the reaction rate constant for the CH_4 formation from MeOH. Finally, with the Equations 3 and 4, the methane formation rate r_{CH4} can be expressed as a function of the partial pressures of DME, MeOH and water (see SI for details):

$$r_{CH4} = \frac{P_{MeOH}}{P_{H2O} \cdot K_{H2O} + P_{MeOH}} \cdot (k_{DME} \cdot P_{DME} + k_{MeOH} \cdot P_{MeOH}) \quad \text{(Eq. 6)}$$

For the case of the reaction of dry DME at low conversion levels ($P_{H_2O} \approx 0$ and $P_{MeOH} \approx 0$), Equation 6 is simplified into:

$$r_{CH4} \approx k_{DME} \cdot P_{DME} \quad \text{(Eq. 7)}$$

Which implies that the BAS are fully covered by methoxy groups ($\theta_{CH3} \rightarrow 1$) under these conditions (see SI for details). This approximation is in good agreement with the proportional increase of methane rate with the pressure of DME, with a calculated reaction order of 1. Regression of the data with Equation 7 gives a value of k_{DME} of 2.1 ± 0.1 mmol·min^{-1}·kg$_{cat}^{-1}$·mbar $_{DME}^{-1}$.

To determine the values of k_{MeOH} and K_{H_2O}, Equation 6 is rearranged into

$$P_{MeOH} \cdot (r_{CH4} - k_{DME} \cdot P_{DME}) = k_{MeOH} \cdot {P_{MeOH}}^2 - K_{H2O} \cdot r_{CH4} \cdot P_{H2O} \quad \text{(Eq. 8)}$$

With the measured rates at different MeOH, DME and H_2O pressure (Table S3), a 3D plot for P_{MeOH}·(r_{CH4}-k_{DME}·P_{DME}), ${P_{MeOH}}^2$ and r_{CH4} P_{H2O} is shown in Fig. 6. The experimental data fall into a 2D surface indicating a good correlation with the proposed Equation 8. Regression of the experimental data by Equation 8 gave an R value of 0.96 and allowed calculating values for reaction rate constant k_{MeOH} and equilibrium constants K_{H_2O} and, based on the rearranged Equation 2, K_{MeOH} (Table 1).

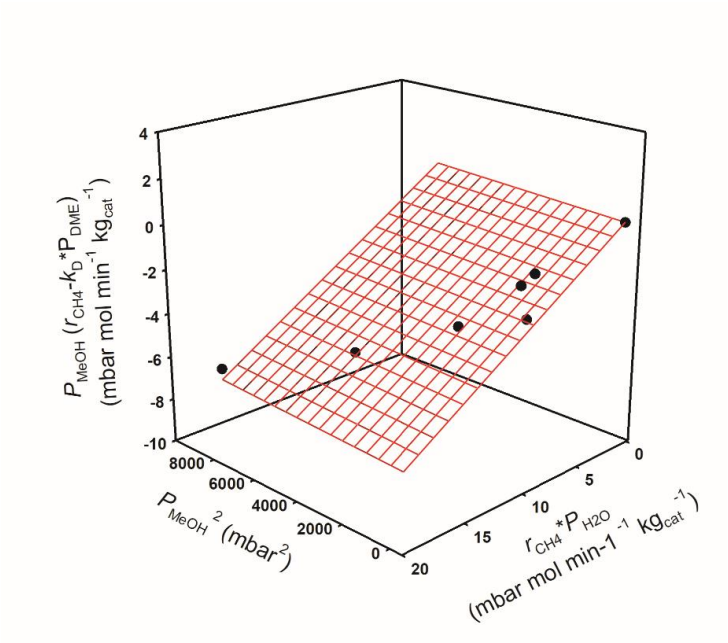

Figure 6: 3D Plot of the DME and MeOH partial pressures and the formation rate of methane. Constant T of 748 K, conversion below 1 C%, DME, MeOH and water partial pressures in the range of 0-180, 0-90 and 0-684 mbar.

Table 1: Rate constants for the formation of methane from DME (k_{DME}) and MeOH (k_{MeOH}) and equilibrium constants K_{MeOH} and K_{H2O}.

Equilibrium or rate constant	
k_{DME}	2.1 ± 0.1 mmol·min^{-1}·kg$_{cat}^{-1}$·mbar $_{DME}^{-1}$
k_{MeOH}	0.15 ± 0.15 mmol·min^{-1}·kg$_{cat}^{-1}$·mbar $_{MeOH}^{-1}$
K_{MeOH}	1.7 ± 0.5
K_{H2O}	0.37 ± 0.08
K_{eq}	0.22 ± 0.04

The equilibrium and rate constants involved in the reaction network in Scheme 2 are compiled in Table 1. The rate constant k_{DME} is at least one order of magnitude higher than k_{MeOH}. This shows that DME is a stronger hydrogen donor than MeOH toward surface methoxy groups. This observation is in contrast to the report by Martinez-Espin et al.[31] in which it is proposed that only MeOH may lead to formaldehyde under MTO conditions. On the other hand, Plessow et al.[24] calculated the activation barrier for the HT from DME to a methoxy species to be 226 kJ/mol at 400 °C on H-SSZ-13, while the barrier for the subsequent decomposition of the resulting methoxymethyl species into methoxy species and formaldehyde is only 141 kJ/mol. According to their calculations, the energy barrier of the HT step with MeOH as H-donor via reaction III in Scheme 2 is 17 kJ/mol higher than with DME,[24] which agrees well with the differences in reaction rate constants derived from our experiments at 475 °C.

3.2.3 Consequences of HT rates for the formation of the hydrocarbon pool

Fig. 7 shows the conversion of DME/MeOH under different DME and water cofeeding compositions. A higher concentration of DME induces a faster formation of the hydrocarbon pool, triggering the dual-cycle, and, hence, reducing the contact time required to reach the onset of olefins. The rate of hydrogen transfer from DME or MeOH to methoxy groups is also the rate of formation of formaldehyde (Scheme 2, III and IV), which is a key intermediate in the initiation reactions for the formation of hydrocarbons.[19]

The formation rate of the hydrocarbon pool cannot be directly measured, but an indirect quantification can be given by examining the contact time necessary to generate 0.02 C% of propene. We designate this minimum contact time as “critical contact time”. The critical contact time increases with increasing water content in the feed. For the highest tested H_2O partial pressure (730 mbar), the critical contact time is about 4 times larger than for dry DME.

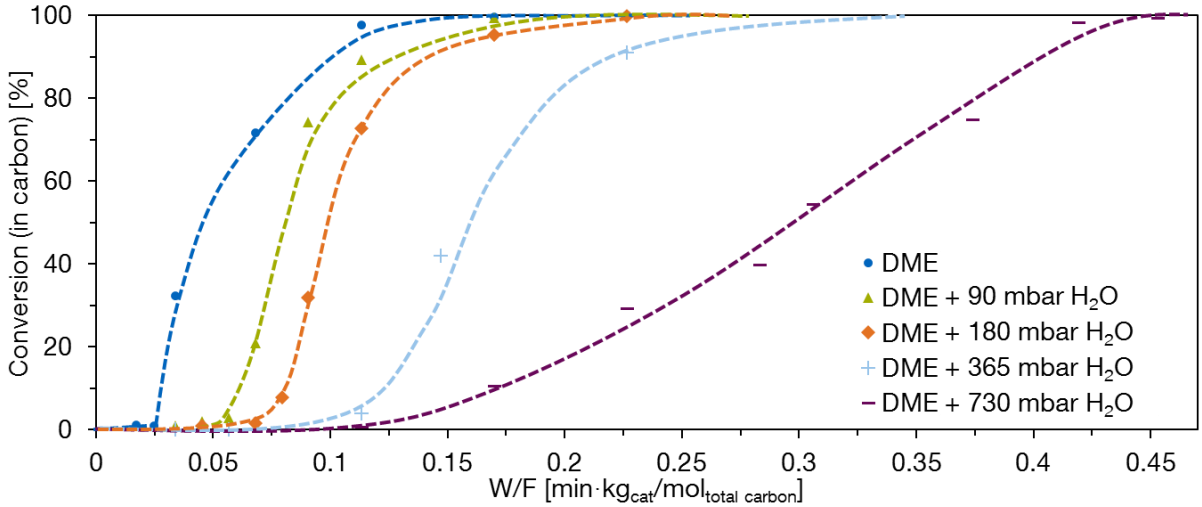

Figure 7: Conversion of MeOH and DME under different feed compositions versus the contact time. DME partial pressure is kept constant at 90 mbar, while different water partial pressures from 90 to 730 mbar are added. W/F is defined by the total molar amount of introduced carbon, which is kept constant during all measurements, while the catalyst loadings are varied. Constant T of 748 K.

In Fig. 8A it can be seen that the critical contact time is inversely related to the hydrogen transfer rate (methane formation rate) (Fig. 8A). A short critical contact time indicates fast formation of the hydrocarbon pool. It is conceptually not possible to define a rate for the hydrocarbon pool formation, because it involves complex reactions and surface-only products. Therefore, for quantitative comparisons we have calculated a pseudo rate of hydrocarbon pool formation by dividing the 0.02 C% propene yield at the end of the initiation period by the critical contact time (Eq. 9).

$$r_{Hydrocarbon\ pool\ formation} = \frac{0.02\ C\%}{Critical\ contact\ time} \qquad \text{(Eq. 9)}$$

This pseudo rate of hydrocarbon pool formation increases linearly with the CH_4 formation rate (Fig. 8B). Based on previous reports, CH_4 and HCHO are involved in several pathways to trigger the hydrocarbon pool[11-12, 24, 32-33]. The correlation depicted in Fig. 8 supports these proposals, showing that the kinetically relevant step in the hydrocarbon pool formation is the hydrogen transfer between DME or MeOH and surface methoxy species.

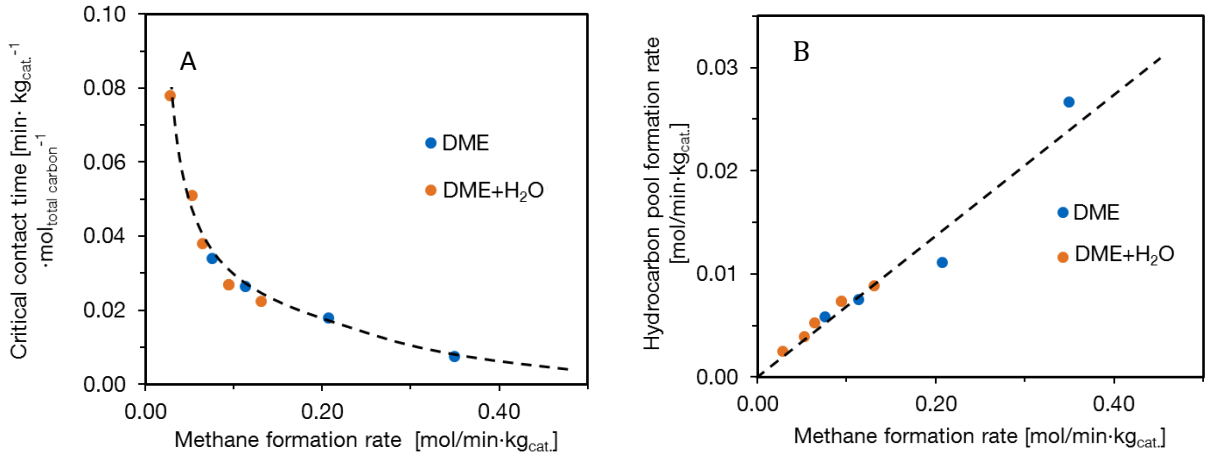

Figure 8: Correlation between the methane formation rate and the critical contact time to initiate the methylation state (defined by the formation of 0.02 carbon % of $C_3^=$) (A), and (B) the pseudo rate for the hydrocarbon pool formation based on apparent $C_3^=$ formation rate. "DME" marks measurements where the feed is dry DME in N_2 dilution, while "DME+H_2O" denotes measurements where DME/water mixtures in N_2 were used as feed. Constant T of 748 K.

3.2.4 Methylation rates for MeOH and DME in the dual-cycle mechanism

As a critical concentration of alkenes is formed, the continuous propagation of the dual (olefin and aromatics) cycle sets in. In the dual-cycle, DME and MeOH are rapidly consumed by methylation of alkenes and of arenes in the olefin and aromatic cycle, respectively. The rates of these methylation reactions are orders of magnitude faster than the reactions initiating the hydrocarbon pool, which results in the S-shape of the MeOH/DME-conversion curves in Fig. 1 and 7. The methylation of an olefin (e.g., butene) or an arene with MeOH generates a H_2O molecule per MeOH consumed (Rxn. 4). Conversely, methylation via DME stochiometrically generates a molecule of MeOH (Rxn. 5). Assuming that the interconversion between DME and MeOH is negligible once the hydrocarbon pool chemistry sets in, the formation rate of H_2O and the consumption rate of DME approximate the rates of methylation with MeOH and DME, respectively.

$$\mathbf{DME} + \mathbf{C_4H_8} \longrightarrow \mathbf{C_5H_{10}} + \mathbf{MeOH} \quad \text{(Rxn. 4)}$$

$$\mathbf{MeOH} + \mathbf{C_4H_8} \longrightarrow \mathbf{C_5H_{10}} + \mathbf{H_2O} \quad \text{(Rxn. 5)}$$

Fig. 9 shows the evolution of DME, MeOH and H_2O with contact time under two different feed compositions, i.e., DME/H_2O = 1/1 (Fig. 9A) and DME/H_2O = 1/2 (Fig. 9B). In both reactions, DME, MeOH and H_2O reached equilibrium at the end of the initiation period. As soon as the dual-cycle propagates (indicated by the dashed vertical line in Fig. 9), H_2O concentration in the gas phase increases and DME decreases, whereas MeOH concentration remains approximately constant (only decreasing at long contact times). The initial rate of H_2O formation and DME consumption should be predominantly caused by the MeOH and DME methylation reaction in the dual-cycle. The absolute values of slopes for increasing concentration of H_2O (Fig. 11, purple arrow) and decreasing concentration of DME (Fig. 11, green arrow) are identical. On the other hand, the almost zero rate of MeOH (Fig. 9, blue arrow) indicates that the amount of MeOH consumed by methylation (Rxn. 5) is identical to the amount of MeOH produced by DME-methylation (Rxn. 4). These observations indirectly show that the methylation rates in Rxn. 4 and Rxn. 5 are similar. Therefore, we concluded that, contrary to previous proposals,[5, 10] DME and MeOH are equally reactive with respect to methylation of olefins and arenes in the dual cycle. This is consistent with a stepwise methylation mechanism[34-35] where methoxy species has been proposed as the key surface intermediate. It should be noted that, even though MeOH and DME are equally reactive in the dual cycle, a lower absolute methylation rate is nevertheless observed, if a higher concentration of MeOH is present in the feed. This is because MeOH leads to a higher concentration of water via shifting the dehydration equilibrium. Accordingly, when H_2O content is systematically increased in the feed, a decrease in the slope of the curve in the range of 10-90 %

conversion is observed (Fig. 7). This lower methylation rate at high H_2O (and MeOH) concentrations is attributed to a lower concentration of surface methoxy species.

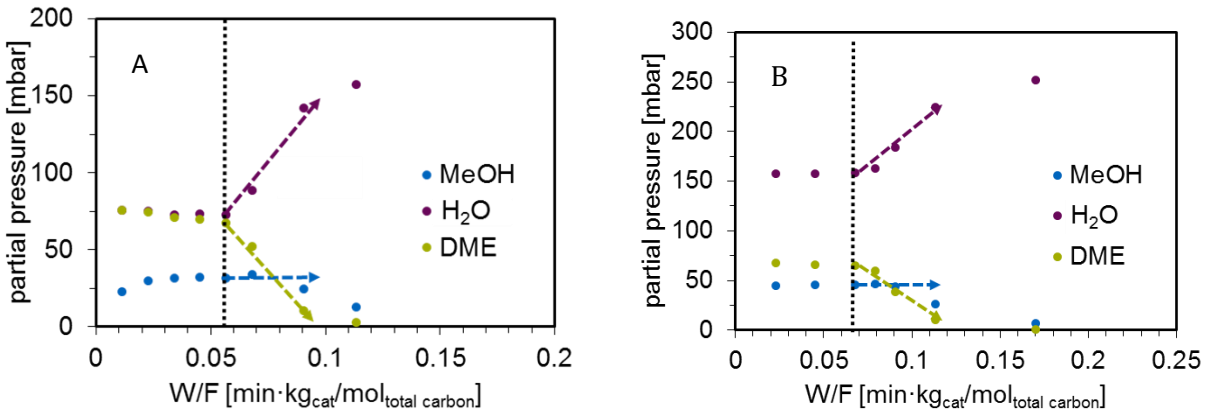

Figure 9: Evolution of DME, MeOH and water partial pressures during their conversion to hydrocarbons versus the W/F value. A depicts the initial DME to water ratio of 1:1, B of 1:2. The dotted line marks the beginning of the autocatalytic period (calculated for atmospheric pressure and an average C-number of formed HCs of four). The slope of the eye-guiding arrows represents the consumption respectively formation rates of the three components at the beginning of the dual cycle. Constant T of 748 K.

Fig. 10 exemplifies the decrease in methylation rates with the increasing water partial pressure. The presence of water reduces the surface concentration of methoxy groups on BAS (Scheme 4, I) and consequently lowers the observed overall methylation rate, because the olefin or arene methylation occur via nucleophilic attack of methoxy groups by an olefin or an arene.[34-35] The decrease of the reaction rate with increasing H_2O partial pressure has also an impact on the product selectivity during the autocatalytic period, which has been widely reported.[6-9] In particular, at high water partial pressures, e.g. 329 and 684 mbar, the methylation rate becomes lower than the interconversion rate of H_2O, DME and MeOH. In this way, the equilibrated DME, MeOH and H_2O composition is reached in the gas phase in the whole range of conversions (Supporting Information S7).

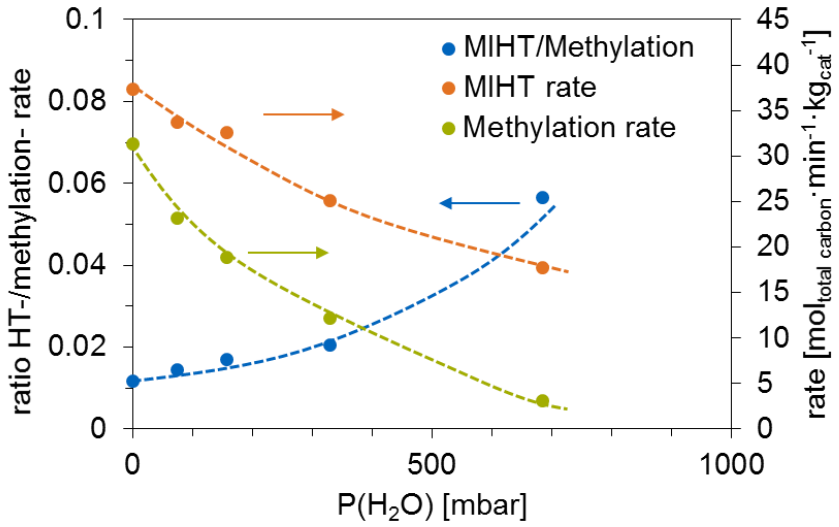

Figure 10: Correlation of the ratio between the MIHT rate and the methylation rate with the water partial pressure in the equilibrium. All rates are determined between 5 and 30 C% conversion. Constant T of 748 K.

As the water partial pressure increases, the rate of formation of aromatics and alkanes decreases. At these conversion levels, it has been demonstrated that alkane and aromatic products generated in the dual cycle on H-ZSM-5 are formed by HT between MeOH/DME and olefins via the methanol induced hydrogen transfer (MIHT) pathway.[36] However, the effect of H_2O partial pressure on the rate of MIHT reactions is not as significant as the effect on methylation rates. As a consequence, the ratio between MIHT rate and methylation rate increases with water partial pressure (Fig. 10). This leads to higher selectivities to alkanes and aromatics, when high H_2O concentrations are present in the feed. This is in good agreement with other studies that have reported lower alkane and aromatic yields, when DME was used as reactant instead of MeOH.[8]

The rate determining step of the MIHT pathway involves formaldehyde formation on LAS.[36] In view of the results presented in Fig. 10, we hypothesize that water adsorption on LAS competes with the HT from MeOH/DME to olefins. This competitive adsorption effect is, however, weaker than the H_2O effect on methylation rates, where H_2O reacts with active surface methoxy species and restores BAS, decreasing the coverage of methoxy groups available for the reaction.

3.3 Conclusions

Both DME and MeOH are viable reactants in the MTO reaction on H-ZSM-5. They react with methoxy groups formed on zeolite BAS to produce HCHO and CH_4 via hydrogen transfer. Such hydrogen transfer from MeOH and DME to surface methoxy species is the rate determining step for the initiation of the autocatalytic conversion of methanol, as it forms formaldehyde, the key reactant for the initial C-C bond formation. Dimethyl ether is a stronger hydrogen donor to methoxy species than MeOH, with a rate one order of magnitude faster than methanol.

Once a threshold concentration of hydrocarbon pool species is formed, methylation reactions become dominant and both DME and MeOH are rapidly consumed by reacting with olefins and arenes. In this stage, DME and MeOH react with identical rates via intermediately formed methoxy groups. As the concentration of this intermediate is involved in the rate determining step, the overall rate of methylation decreases sharply with increasing H_2O partial pressures. Thus, the presence of high partial pressures of H_2O leads to a decrease of all reaction rates involving surface methoxy species, as H_2O reduces the coverage of methoxy species via hydrolysis, restoring Brønsted acid sites. The rate of formation of non-olefinic byproducts, i.e., alkanes and aromatics, also decreases with water partial pressure for medium conversions, however, to a lower extent compared to methylation. Here, a competitive adsorption of H_2O on LAS - where the rate determining step of hydride transfer takes place at partial MeOH conversions - is hypothesized to cause the lower rates.

The results highlight the role of surface methoxy species as main active species in H-ZSM-5 in the reactions occurring in presence of oxygenates. The better understanding of the elementary steps involved in the MTH reaction and their dependence on the feed composition is fundamental in order to improve catalytic properties of zeolites. This knowledge is a first step in finding strategies to accelerate the initiation of the MTO reaction, to minimize the formation of byproducts, and to prolong catalyst lifetime.

3.4 Methods

Materials

H-ZSM-5 zeolite was provided by Clariant Produkte (Deutschland) GmbH. Methanol (≥99.9%) and DME (≥99.9%), were supplied by Sigma-Aldrich. The introduced deionized water was further purified by an EASYpure II RF-Compact-Waterfilter by Barnstead.

Catalytic testing

All catalytic results were obtained using a fixed bed quartz reactor with an internal diameter of 6 mm at 748 K and ambient pressure. The catalyst particles (200-280 µm) were homogeneously diluted with silicon carbide (ESK-SiC) in the range of 355-500 µm to ensure temperature uniformity in the catalytic bed. Catalysts were activated at 748 K for 1 h under N_2 atmosphere before the reaction.

Methanol and water vapor at partial pressures up to 180 mbar were fed by passing N_2 through saturators which were tempered by a VWR circulation thermostat at temperatures up to 333 K. Higher partial pressures were reached by addition of the respective fluid by a Shimadzu HPLC - pump combine with an aDROP direct evaporator ("µSteam"). DME was introduced by a Bronkhorst MFC and diluted with N_2.

The reactor effluents were transferred via a heated line into a gas chromatograph (HP 5890) equipped with a HP-PLOTQ capillary column. The product distributions are given on a carbon basis.

Formaldehyde was quantified by condensing the reaction effluent into two bottles at 275 K for 30 min TOS with subsequent stoichiometric Hantzsch reaction as described by Nash [37] and depicted in Reaction 6.

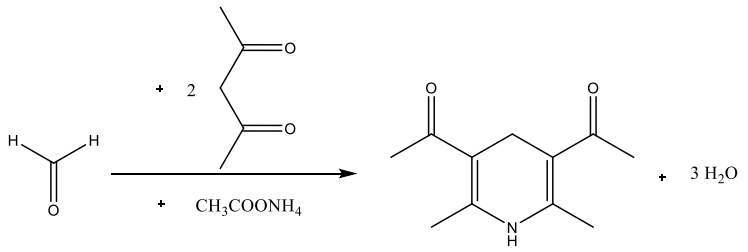

(Rxn. 6)

A Varian Cary 50 UV-Vis Spectrophotometer was used to determine the formaldehyde concentration via the absorption of the formed 3,5-diacetyl-1,4-dihydro-2,6-lutidine. In order to compare the resulting values with the yields of other products determined by GC, it was calculated an average value of formaldehyde yield for 30 min periods.

3.5 References

1. Meisel, S. L., Gasoline from methanol in one step. *CHEMTECH; (United States)* **1976**, Medium: X; Size: Pages: 86-89.
2. Chang, C. D., Hydrocarbons from Methanol. *Catalysis Reviews* **1983,** *25* (1), 1-118.
3. Mokrani, T.; Scurrell, M., Gas Conversion to Liquid Fuels and Chemicals: The Methanol Route - Catalysis and Processes Development. *Catalysis Reviews* **2009,** *51* (1), 1-145.
4. Tian, P.; Wei, Y.; Ye, M.; Liu, Z., Methanol to Olefins (MTO): From Fundamentals to Commercialization. *ACS Catalysis* **2015,** *5* (3), 1922-1938.
5. Olsbye, U.; Svelle, S.; Bjørgen, M.; Beato, P.; Janssens, T. V. W.; Joensen, F.; Bordiga, S.; Lillerud, K. P., Conversion of Methanol to Hydrocarbons: How Zeolite Cavity and Pore Size Controls Product Selectivity. *Angewandte Chemie International Edition* **2012,** *51* (24), 5810-5831.
6. Chen, K.; Damron, J.; Pearson, C.; Resasco, D.; Zhang, L.; White, J. L., Zeolite Catalysis: Water Can Dramatically Increase or Suppress Alkane C–H Bond Activation. *ACS Catalysis* **2014,** *4* (9), 3039-3044.
7. De Wispelaere, K.; Wondergem, C. S.; Ensing, B.; Hemelsoet, K.; Meijer, E. J.; Weckhuysen, B. M.; Van Speybroeck, V.; Ruiz-Martínez, J., Insight into the Effect of Water on the Methanol-to-Olefins Conversion in H-SAPO-34 from Molecular Simulations and in Situ Microspectroscopy. *ACS Catalysis* **2016,** *6* (3), 1991-2002.
8. Martinez-Espin, J. S.; Mortén, M.; Janssens, T. V.; Svelle, S.; Beato, P.; Olsbye, U., New insights into catalyst deactivation and product distribution of zeolites in the methanol-to-hydrocarbons (MTH) reaction with methanol and dimethyl ether feeds. *Catalysis Science & Technology* **2017**.
9. Martínez-Espín, J. S.; De Wispelaere, K.; Janssens, T. V. W.; Svelle, S.; Lillerud, K. P.; Beato, P.; Van Speybroeck, V.; Olsbye, U., Hydrogen Transfer versus Methylation: On the Genesis of Aromatics Formation in the Methanol-To-Hydrocarbons Reaction over H-ZSM-5. *ACS Catalysis* **2017**, 5773-5780.
10. Svelle, S.; Kolboe, S.; Swang, O.; Olsbye, U., Methylation of alkenes and methylbenzenes by dimethyl ether or methanol on acidic zeolites. *The Journal of Physical Chemistry B* **2005,** *109* (26), 12874-12878.
11. Liu, Y.; Müller, S.; Berger, D.; Jelic, J.; Reuter, K.; Tonigold, M.; Sanchez-Sanchez, M.; Lercher, J. A., Formation Mechanism of the First Carbon–Carbon Bond and the First Olefin in the Methanol Conversion into Hydrocarbons. *Angewandte Chemie* **2016,** *128* (19), 5817-5820.
12. Chowdhury, A. D.; Houben, K.; Whiting, G. T.; Mokhtar, M.; Asiri, A. M.; Al-Thabaiti, S. A.; Basahel, S. N.; Baldus, M.; Weckhuysen, B. M., Initial Carbon–Carbon Bond Formation during the Early Stages of the Methanol-to-Olefin Process Proven by Zeolite-Trapped Acetate and Methyl Acetate. *Angewandte Chemie* **2016,** *128* (51), 16072-16077.
13. Wu, X.; Xu, S.; Zhang, W.; Huang, J.; Li, J.; Yu, B.; Wei, Y.; Liu, Z., Direct Mechanism of the First Carbon–Carbon Bond Formation in the Methanol-to-Hydrocarbons Process. *Angewandte Chemie* **2017,** *129* (31), 9167-9171.
14. Svelle, S.; Joensen, F.; Nerlov, J.; Olsbye, U.; Lillerud, K.-P.; Kolboe, S.; Bjørgen, M., Conversion of methanol into hydrocarbons over zeolite H-ZSM-5: Ethene formation is mechanistically separated from the formation of higher alkenes. *Journal of the American Chemical Society* **2006,** *128* (46), 14770-14771.
15. Bjørgen, M.; Svelle, S.; Joensen, F.; Nerlov, J.; Kolboe, S.; Bonino, F.; Palumbo, L.; Bordiga, S.; Olsbye, U., Conversion of methanol to hydrocarbons over zeolite H-ZSM-5: On the origin of the olefinic species. *Journal of Catalysis* **2007,** *249* (2), 195-207.
16. Pérez-Uriarte, P.; Ateka, A.; Gamero, M.; Aguayo, A. T.; Bilbao, J., Effect of the Operating Conditions in the Transformation of DME to olefins over a HZSM-5 Zeolite Catalyst. *Industrial & Engineering Chemistry Research* **2016,** *55* (23), 6569-6578.

17. Chang, C. D.; Silvestri, A. J., The conversion of methanol and other O-compounds to hydrocarbons over zeolite catalysts. *Journal of Catalysis* **1977,** *47* (2), 249-259.
18. Yashima, T.; Sato, K.; Hayasaka, T.; Hara, N., Alkylation on synthetic zeolites: III. Alkylation of toluene with methanol and formaldehyde on alkali cation exchanged zeolites. *Journal of Catalysis* **1972,** *26* (3), 303-312.
19. Liu, Y.; Kirchberger, F. M.; Müller, S.; Eder, M.; Tonigold, M.; Sanchez-Sanchez, M.; Lercher, J. A., Critical role of formaldehyde during methanol conversion to hydrocarbons. *Nature Communications* **2019,** *10* (1), 1462.
20. Hwang, A.; Bhan, A., Bifunctional Strategy Coupling Y2O3-Catalyzed Alkanal Decomposition with Methanol-to-Olefins Catalysis for Enhanced Lifetime. *ACS Catalysis* **2017,** *7* (7), 4417-4422.
21. Standl, S.; Hinrichsen, O., Kinetic Modeling of Catalytic Olefin Cracking and Methanol-to-Olefins (MTO) over Zeolites: A Review. *Catalysts* **2018,** *8* (12), 626.
22. Kubelková, L.; Nováková, J.; Jírů, P., Reaction of Small Amounts of Methanol on Hzsm-5, Hy and Modified Y Zeolites. In *Studies in Surface Science and Catalysis*, Jacobs, P. A.; Jaeger, N. I.; Jírů, P.; Kazansky, V. B.; Schulz-Ekloff, G., Eds. Elsevier: 1984; Vol. 18, pp 217-224.
23. Hutchings, G. J.; Gottschalk, F.; Hunter, R., Comments on "kinetic model for methanol conversion to olefins" with respect to methane formation at low conversion. *Industrial & Engineering Chemistry Research* **1987,** *26* (3), 635-637.
24. Plessow, P. N.; Studt, F., Unraveling the Mechanism of the Initiation Reaction of the Methanol to Olefins Process Using ab Initio and DFT Calculations. *ACS Catal* **2017,** *7* (11), 7987-7994.
25. Arora, S. S.; Bhan, A., The critical role of methanol pressure in controlling its transfer dehydrogenation and the corresponding effect on propylene-to-ethylene ratio during methanol-to-hydrocarbons catalysis on H-ZSM-5. *Journal of Catalysis* **2017,** *356*, 300-306.
26. Townsend, D.; Lahankar, S.; Lee, S.; Chambreau, S.; Suits, A.; Zhang, X.; Rheinecker, J.; Harding, L.; Bowman, J., The roaming atom: straying from the reaction path in formaldehyde decomposition. *Science* **2004,** *306* (5699), 1158-1161.
27. Schulz, H., "Coking" of zeolites during methanol conversion: Basic reactions of the MTO-, MTP- and MTG processes. *Catalysis Today* **2010,** *154* (3–4), 183-194.
28. Jones, A. J.; Iglesia, E., Kinetic, Spectroscopic, and Theoretical Assessment of Associative and Dissociative Methanol Dehydration Routes in Zeolites. *Angewandte Chemie International Edition* **2014,** *53* (45), 12177-12181.
29. Pope, C. G., Water adsorption on ZSM-5 and its aluminum free analog, silicalite. *Journal of Colloid and Interface Science* **1987,** *116* (1), 221-223.
30. Piccini, G.; Alessio, M.; Sauer, J., Ab initio study of methanol and ethanol adsorption on Brønsted sites in zeolite H-MFI. *Physical Chemistry Chemical Physics* **2018,** *20* (30), 19964-19970.
31. Martinez-Espin, J. S.; De Wispelaere, K.; Erichsen, M. W.; Svelle, S.; Janssens, T. V.; Van Speybroeck, V.; Beato, P.; Olsbye, U., Benzene co-reaction with methanol and dimethyl ether over zeolite and zeotype catalysts: Evidence of parallel reaction paths to toluene and diphenylmethane. *Journal of Catalysis* **2017,** *349*, 136-148.
32. Tajima, N.; Tsuneda, T.; Toyama, F.; Hirao, K., A New Mechanism for the First Carbon−Carbon Bond Formation in the MTG Process: A Theoretical Study. *Journal of the American Chemical Society* **1998,** *120* (32), 8222-8229.
33. Wu, X.; Xu, S.; Wei, Y.; Zhang, W.; Huang, J.; Xu, S.; He, Y.; Lin, S.; Sun, T.; Liu, Z., Evolution of C–C Bond Formation in the Methanol-to-Olefins Process: From Direct Coupling to Autocatalysis. *ACS Catalysis* **2018,** *8* (8), 7356-7361.
34. Ilias, S.; Bhan, A., Tuning the selectivity of methanol-to-hydrocarbons conversion on H-ZSM-5 by co-processing olefin or aromatic compounds. *Journal of Catalysis* **2012,** *290*, 186-192.
35. Ilias, S.; Bhan, A., Mechanism of the Catalytic Conversion of Methanol to Hydrocarbons. *ACS Catalysis* **2013,** *3* (1), 18-31.

36. Müller, S.; Liu, Y.; Kirchberger, F. M.; Tonigold, M.; Sanchez-Sanchez, M.; Lercher, J. A., Hydrogen Transfer Pathways during Zeolite Catalyzed Methanol Conversion to Hydrocarbons. *Journal of the American Chemical Society* **2016,** *138* (49), 15994-16003.
37. Nash, T., The colorimetric estimation of formaldehyde by means of the Hantzsch reaction. *Biochemical Journal* **1953,** *55* (3), 416-421.

3.6 Supporting information

Figure S.1: Quotient $(P_{MeOH})^2/(P_{DME}\cdot P_{H2O})$ at different partial pressures in the equilibrium.

Feeding pressure [mbar] DME/H_2O	**Partial pressure (eq.) DME/MeOH/H_2O [mbar]**	**$(P_{MeOH})^2/(P_{DME}\cdot P_{H2O})$[a]**
90/729	45/90/684	0.241 ± 0.018
90/365	54/72/329	0.278 ± 0.010
90/180	67/47/157	0.198 ± 0.006
90/90	73/34/73	0.201 ± 0.004
130/65	113/34/48	0.204 ± 0.005
65/130	49/32/113	0.180 ± 0.003

[a] The fluctuation of equilibrium constant values is speculated to be the consequence of deviation from ideal gas, which is the pre-assumption in our calculation of partial pressure.

Figure S.2: Conversion of DME with and without the presence of methane (diluted in N_2, 748 K, W/F = 0.007 $min\cdot kg_{cat}/mol_{CH2\ from\ DME}$)

Feed-composition	**$C_3^=$ yield [C%]**
90 mbar DME in N_2	0.003
90 mbar DME + 167 mbar CH_4 in N_2	0.003

Figure S.3: Formation rate of methane/formaldehyde for different feed compositions and with varying DME partial pressures. Reaction at 748 K.

Partial pressure (feed) DME/MeOH/H_2O [mbar]	**Partial pressure (equilibrated) DME/MeOH/H_2O [mbar]**	**CH_4 formation rate [$mol_{methane} \cdot kg_{cat}^{-1}\ min^{-1}$]**
30/0/0	30/0/0	0.075
45/0/0	45/0/0	0.113
90/0/0	90/0/0	0.207
180/0/0	180/0/0	0.349
90/0/90	73/34/73	0.094
130/0/65	113/34/48	0.131
65/0/130	49/32/113	0.053
90/0/730	45/90/684	0.028
90/0/365	54/72/329	0.040
90/0/180	67/47/157	0.064

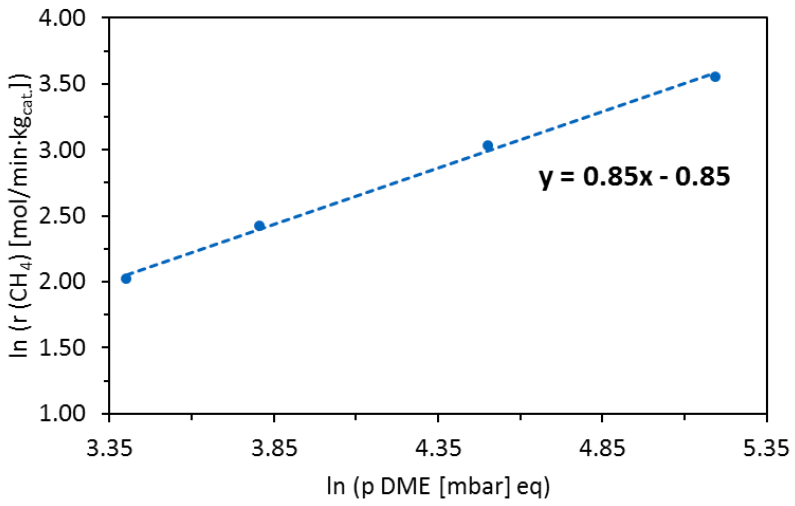

Figure S.4: Dependence of the logarithmic methane formation rate on the logarithmic DME partial pressure.

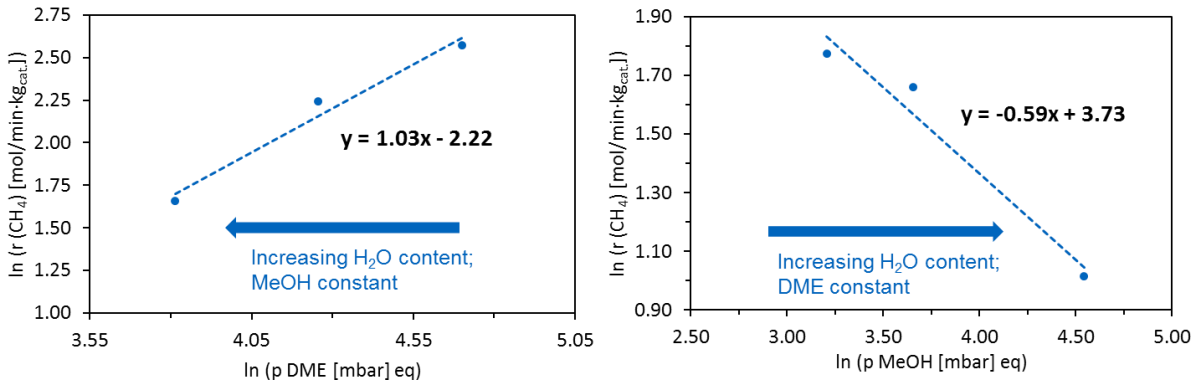

Figure S.5: Dependence of the logarithmic methane formation rate on the logarithmic DME partial pressure (A) and the logarithmic MeOH partial pressure (B). The changing water partial pressure is indicated by blue arrows.

S.6. Calculation of the coverage of BAS (i = H_2O, MeOH):

$$\Theta_i = \frac{K_i \cdot P_i}{1 + K_i \cdot P_i} \qquad \text{(S. Eq. 1)}$$

$$K_i = e^{-\frac{\Delta H_i - \Delta S_i \cdot T}{R \cdot T}} \qquad \text{(S. Eq. 2)}$$

With $\Delta H_{H2O} = -65\ kJ/mol$ and $\Delta S_{H2O} = -110\ J \cdot K/mol$[1] can the maximum coverage of BAS with adsorbed water be calculated as 4 % (for a water partial pressure of 684 mbar). In case of MeOH the coverage for a maximum partial pressure of 180 mbar is with 0.003 % even lower ($\Delta H_{MeOH} = -84\ kJ/mol$ and $\Delta S_{MeOH} = -185\ J \cdot K/mol$[2]).

S.7. Equations leading to the formation rate of methane:

$$r_{CH4} = k_{DME} \cdot \Theta_{CH3} \cdot P_{DME} + k_{MeOH} \cdot \Theta_{CH3} \cdot P_{MeOH} \qquad \text{(S. Eq. 3)}$$

The above equation is the methane formation rate (Equation 5 in main text). Using Equations 3 and 4, the coverage of methoxy, θ_{CH_3}, is expressed as

$$\Theta_{CH3} = \frac{P_{MeOH}}{P_{H2O} \cdot K_{H2O} + P_{MeOH}} \qquad \text{(S. Eq. 4)}$$

Substituting θ_{CH_3} in S. Equation 3 by that in S. Equation 4 gives

$$r_{CH4} = \frac{P_{MeOH}}{P_{H2O} \cdot K_{H2O} + P_{MeOH}} \cdot (k_{DME} \cdot P_{DME} + k_{MeOH} \cdot P_{MeOH}) \qquad \text{(S. Eq. 5)}$$

Noting that P_{H_2O} can be expressed by P_{MeOH} and P_{DME} based on the equation 2 in the main text:

$$P_{H2O} = \frac{{P_{MeOH}}^2}{P_{DME} \cdot K_{Eq}} \qquad \text{(S. Eq. 6)}$$

Then the S. Equation 5 is reformulated into

$$r_{CH4} = \frac{1}{\frac{P_{MeOH} \cdot K_{H2O}}{P_{H2O} \cdot K_{Eq}} + 1} \cdot (k_{DME} \cdot P_{DME} + k_{MeOH} \cdot P_{MeOH}) \qquad \text{(S. Eq. 7)}$$

Under dry DME reaction, the pressure of MeOH is close to zero, which makes the methane rate as

$$\lim_{MeOH \to 0} r_{CH4} = \lim_{MeOH \to 0} \frac{1}{\frac{P_{MeOH} \cdot K_{H2O}}{P_{H2O} \cdot K_{Eq}} + 1} \cdot (k_{DME} \cdot P_{DME} + k_{MeOH} \cdot P_{MeOH}) = k_{DME} \cdot P_{DME} \qquad \text{(S. Eq. 8)}$$

The S. Equation 8 is the Equation 7 in the main text.

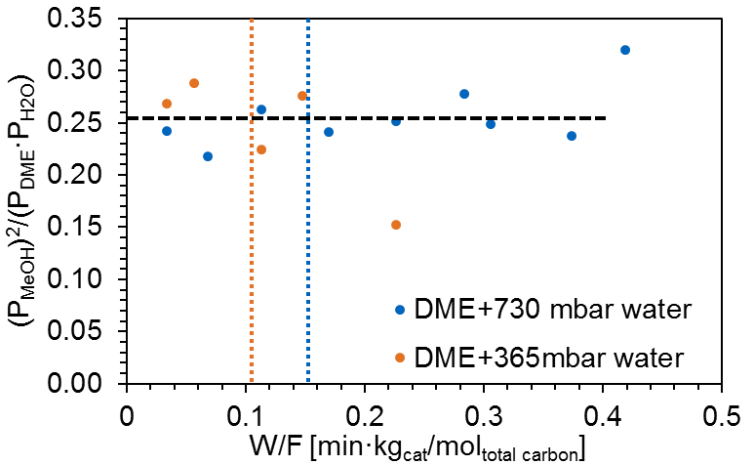

Figure S.7: Quotient $(P_{MeOH})^2/(P_{DME} \cdot P_{H2O})$ versus the contact time for the DME/H_2O ratio of 1:8.10 and 1:4.05.

Support-References:

1. C. G. Pope, Journal of Colloid and Interface Science, 1987, **116**, 221-223.
2. G. Piccini, M. Alessio and J. Sauer, Physical Chemistry Chemical Physics, 2018, 20, 19964-19970

3.7 Associated Content

Publication

This chapter is based on an article planned for submission (Felix M. Kirchberger, Yue Liu, Markus Tonigold, Maricruz Sanchez-Sanchez, Johannes A. Lercher)

Contributions

F.M.K. did main contributions in kinetic experiments, data analysis and manuscript preparation, Y.L. did the majority of characterization and contributed to data analysis; Y.L., M.T., M.S.-S. and J.A.L. conceived the research; The manuscript was written through contributions of all authors. All authors have given approval to the final version of the manuscript.

Acknowledgements

The authors acknowledge the support of the Bavarian Ministry of Economic Affairs and Media, Energy and Technology and Clariant Produkte (Deutschland) GmbH. Laura Tebcharani, Moritz Eder, Markus Pschenitza and Greta Zambo are thanked for their helpful assistance in the experimental work.

4. Evaluation of hydrogen transfer processes during the conversion of DME into hydrocarbons over Ga-modified MFI

Abstract: The presence of Ga on MFI zeolites significantly increases the selectivity towards aromatics during the conversion of DME into hydrocarbons while the overall activity on DME conversion is slightly reduced. If the catalyst is reduced prior to its exposure to hydrocarbons, the effect on aromatics yield can be further increased. This is attributed to a higher coverage of BAS by reduced Ga, forming sites that are highly active in dehydrogenation. Hydrogen transfer pathways, which produce the majority of aromatics over unmodified MFI, are not significantly influenced by the presence of Ga. The improvement in catalytic behavior achieved in Ga-MFI catalysts after reduction is reversed in the presence of water. This is attributed to the reoxidation and/or redistribution of Ga species by H_2O at high and full oxygenate conversions.

4.1 Introduction

The conversion of methanol and the respective ether dimethyl ether (DME) into a wide variety of hydrocarbons over zeolites has created attention since its first description in 1976.[1] The on-purpose production of specific groups of chemicals like methanol to olefins (MTO),[2-4] methanol to gasoline (MTG)[5-7] or methanol to aromatics (MTA)[8-10] are intensively researched.

Dehydrogenation and hydrogen transfer reactions between hydrocarbons are important mechanistic steps in acid catalyzed processes like catalytic cracking,[11-13] alkylation[14] or methanol conversion to hydrocarbons (MTH).[15-16] The rates of hydrogen transfer reactions affect product distribution, i.e. the formation of aromatics, alkanes or molecular hydrogen. Moreover, the extent of hydrogen transfer processes is connected to catalyst deactivation because of the formation of polyaromatic side products that block pores and active sites.[17-20] Recent mechanistic studies have aimed on minimizing the formation of aromatics[16] and other elementary steps leading to coke formation,[21-22] as ways to increase catalyst lifetime and olefin selectivity in MTO processes. When the target product is aromatics, the increase in yields must be achieved without significant decrease of the lifetime of the catalyst. Doping H-ZMS-5 catalyst with hydrogenating metals such as Ag, Ni, Cu, Zn[6, 8-9, 23] and Ga[24-26] has successfully increased aromatic yields up to a range of 50-70 wt.%. The majority of these studies are conducted over MFI-type zeolites with low Si/Al ratios (11.5-45) and metal loadings between 0.5 and 50 wt.%, with reaction conditions adjusted to allow high yields of aromatics.

Ga-exchanged H-ZSM-5 has been recently subject of study for the dehydrogenation and aromatization of light alkanes.[27-30] The positive effect of reducing the catalyst to improve its alkane dehydrogenation potential was already studied in the 1990s.[29-30] Recently both Mansoor et al.[28] and Schreiber et al.[27] proposed active site structures to explain the increase of dehydrogenation rates. Although the nature of the active Ga species is still under debate, the activity enhancement is attributed to the reduction of Ga^{3+} to Ga^{+}. In Fig. 1, it is shown the proposal by Schreiber et al.,[27] where Ga^{+} exchanged on one BAS creates a Lewis-Brønsted acid pair in combination with another adjacent BAS. The proposal by Schreiber et al. is based on the fact that the maximum dehydrogenation activity is reached for a one to one ratio of Ga-modified BAS to protonated BAS.

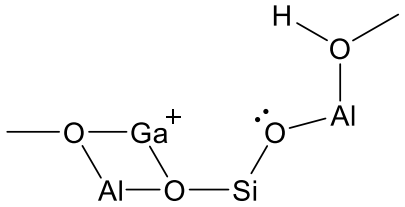

Figure 1: Structural representation of the combination of exchanged Ga^{+} and a protonated BAS as Lewis- Brønsted acid pair.[27]

Reduction of the catalyst before exposition to MeOH or DME is also described in recent MTA publications.[31] Similar, to the works on alkane dehydrogenation,[27-28] an important role of the metal to BAS ratio on the aromatic yield in MTA has also been reported.[31-33] It is an obvious necessity that originating from a C:H-ratio of 1:2 after dehydrogenation of MeOH or DME, hydrogen has to be removed from carbon in order to produce aromatics. It should be noted that the formation of light alkanes – the hydrogen rich byproduct of aromatics formation of hydrogen transfer between olefins - is economically undesirable, therefore a route of forming aromatics that only entails the production of H_2 as a byproduct is highly attractive. Consequently, active sites for dehydrogenation are essential for an efficient MTA catalyst, but it is also a crucial question if the sites will be stable and as active under MTH conditions as in alkane dehydrogenation.

In this work, we investigate the reaction pathways in MeOH/DME conversion leading to formation of aromatics in a reduced Ga-modified H-ZSM-5 catalyst. The stability of the catalyst and its performance under MTH conditions is tested along the catalyst bed. Comparisons with reference catalysts H-ZSM-5 and unreduced Ga-ZSM-5 provide further insight into the different dehydrogenation pathways working in Ga modified H-ZSM-5 and show ways to improve selectivity to aromatics on MTA catalysts without causing fast deactivation.

4.2 Results and discussion

4.2.1 Influence of Ga modifications on activity and selectivity

4.2.1.1 Modification of MFI with Ga and effect on acid properties

The study of HT and dehydrogenation processes was performed on an MFI with Si/Al = 45 with a molar ratio of Ga to Al of 0.45. This formulation ensures a molar ratio of Ga-species to BAS close to 1:2 and consequently a ratio of 1:1 of protonated BAS to Ga-modified BAS after reduction of the catalyst. According to previous findings,[27] this catalyst formulation is expected to yield high activity in dehydrogenation and, thus, a high selectivity to aromatics in MTA. As a reference, the unmodified MFI zeolite and the zeolite after incipient wetness impregnation with $Ga(NO_3)_3$ solution were also tested and characterized. Table 1 shows nomenclature and preparation conditions for each of the samples.

Table 1: Nomenclature of tested samples.

Sample label	Preparation procedure
MFI	MFI (Si/Al = 45)
GaMFI	MFI (Si/Al = 45), Ga content: Ga/Al = 0.45
GaMFI H_2-treated	MFI (Si/Al = 45), Ga content: Ga/Al = 0.45, reduced in H_2 atmosphere at 773 K (60 min)

Table 2 summarizes the acid properties of the samples under study. It can be seen that the introduction of Ga caused an increase of Lewis acidity in the catalyst (strong LAS increased by 350 % and weak LAS by 140 %). The H_2-treatment caused a further increase of only the weak LAS by 130 %. The latter observation agrees well with the increase on Ga dispersion under reductive atmosphere, which is expected to increase the number of metal surface sites.[30-31] Conversely, BAS concentration decreases significantly after exchange with Ga, and a further decrease is achieved by H_2-treatment. In particular, the number of strong BAS – responsible for the activity in MTH - decreases after both preparation steps to a value of 40% of the BAS concentration in the parent MFI. These results agree well with the hypothesis that reduction of Ga-species further increase the exchange of protons in H-ZSM-5 by Ga^+-species.[27-28, 31]

Table 2: Concentration of BAS and LAS (both divided in total and strong sites) of the tested samples using IR spectroscopy of adsorbed pyridine.

	BAS total [µmol/g]	LAS total [µmol/g]	BAS Strong [µmol/g]	LAS Strong [µmol/g]
MFI	360	45	330	21
GaMFI	280	153	238	96
GaMFI H_2-treated	209	225	127	92

4.2.1.2 Catalytic performance of Ga-modified MFI in MTA

For evaluation of the activity of a catalyst in the MeOH/DME conversion, it is necessary to take into account not only the performance under a fully developed dual cycle mechanism, but also in the first part of the catalytic bed (equivalent to low contact times). In this region, the formation rate of the first C-C bonds is very slow and conversion of MeOH/DME is very low. Only at longer contact times the concentrations of hydrocarbons in the micropores autocatalyze the reaction and fast methylation occurs. For this reason, the conversion vs contact time graphs are typically showing an S-shape like in Fig. 2. The first derivative of this curve represents the methanol (or DME) consumption rate at a given contact time. The presence of water has been shown to affect the methanol consumption rates.[16, 22, 34-35] In order to minimize these water effects, the mechanistic study reported here is conducted using DME as reactive component. This ensures a relatively low water content in the reaction mixture, although it should be noted that, as the reaction progresses, increasing concentrations of H_2O – generated by the conversion of DME to hydrocarbons – are verified along the catalytic bed. Inevitably, also a certain amount of MeOH (from DME hydration over the catalyst) is present together with DME and H_2O.

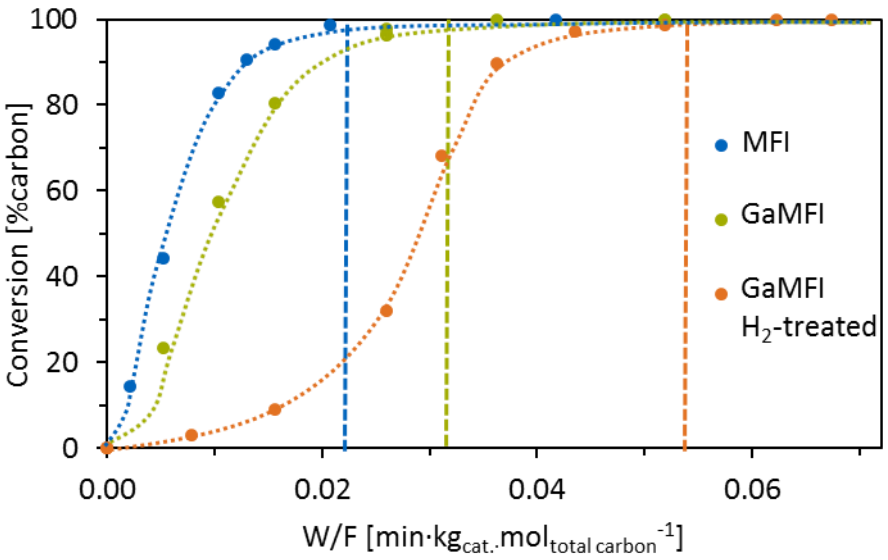

Figure 2: Conversion of DME and MeOH versus the contact time. The initial DME partial pressure is kept constant at 90mbar under N_2 dilution and ambient pressure, Temperature = 748 K.

In Fig. 2, it can be seen that Ga-modification without H_2-pretreatment has only a minor effect on the activity of the MFI catalyst. The presence of exchanged Ga causes a shift of the full conversion line towards higher contact times. This shift is translated into the necessity of a ca. 30 % increase in the catalyst mass in order to reach full conversion on GaMFI. This observation is in good agreement with the decrease in concentration of BAS caused by modification with Ga (Table 2), because BAS are the active sites for C-C bond formation and methylation reactions.[21, 36-37]
The activity in MeOH/DME conversion of Ga-MFI is remarkably reduced after H_2-pretreatement. Based on the contact time curve in Fig. 2, an increase of ca. 130 % of catalyst mass would be necessary to reach full conversion on H_2 treated GaMFI. Examining the first derivative of the curves in Fig. 2, it can be observed that the decrease in overall activity of H_2 treated GaMFI is the consequence of lower rates in the reactions involved in the initiation period, in which the first C-C-bonds are formed, and the subsequent methylation reactions. It can be stated that the activity of the H_2 treated GaMFI compared to the GaMFI – represented by the lower derivative of the curve in Fig. 2 – is lower mainly during the initiation period and until ca. 50 % of the oxygenates are converted. At higher conversion levels the methylation rates of these two samples seem comparable. The decrease in total activity is again in good agreement with our analysis of the concentration of acid sites in Table 2, where a marked decrease of BAS is verified after reduction. As proposed by Schreiber[27] and Gao,[31] upon H_2-treatment protons on BAS get replaced by Ga-species (Ga^+ or GaO^+) which are considered inactive for MeOH/DME conversion.

The evolution of the aromatics yield of the different samples is investigated with increasing contact time, to show the influence of the presence of Ga on the resulting product distribution. As expected, a clear increase of the fraction of the carbon that is converted into aromatics can be observed in the order MFI < GaMFI < GaMFI H_2-treated (Fig. 3). At a constant W/F-value of 0.10 $min \cdot kg \cdot mol^{-1}$, sufficiently high to ensure that all samples have reached full conversion, the aromatic yield is 7.5 C% in MFI, 15 C% in GaMFI and 23.5 C% in the GaMFI H_2-treated. A more revealing insight into the selectivity towards aromatics is provided by examining the aromatics formation rate. In Fig. 3, the derivative of the aromatics yield versus the contact time represents the formation rate of aromatics in $\% \cdot mol_{total\ carbon} \cdot kg_{cat}^{-1} \cdot min^{-1}$. In case of all three samples two main regimes can be differentiated: fast formation of aromatics before full conversion (i.e., in presence of MeOH/DME) and slow formation of aromatics beyond the contact time point of full conversion (hydrocarbon interconversions). The fast aromatic formation rate at partial conversions can be at first explained by the methanol induced hydrogen transfer (MIHT) pathway proposed by Müller et al.,[15] which is expected to dominate as long as MeOH and/or DME is present. It is interesting to note that at partial conversions, the aromatics formation rate increases in the order

MFI < GaMFI < GaMFI H_2-treated. In the full conversion regime, the aromatics formation rate observed for the two Ga-modified samples is about a factor of two faster than the parent MFI. Interestingly, the rate of formation of aromatics in this regime is similar in GaMFI and GaMFI H_2-treated catalysts, in spite of their different catalytic behavior at low conversions. This seems to indicate that the hydrogen treatment does not significantly affect the activity in hydrogen transfer between hydrocarbons, which is the dominant reaction pathway for formation of aromatics at full conversion.

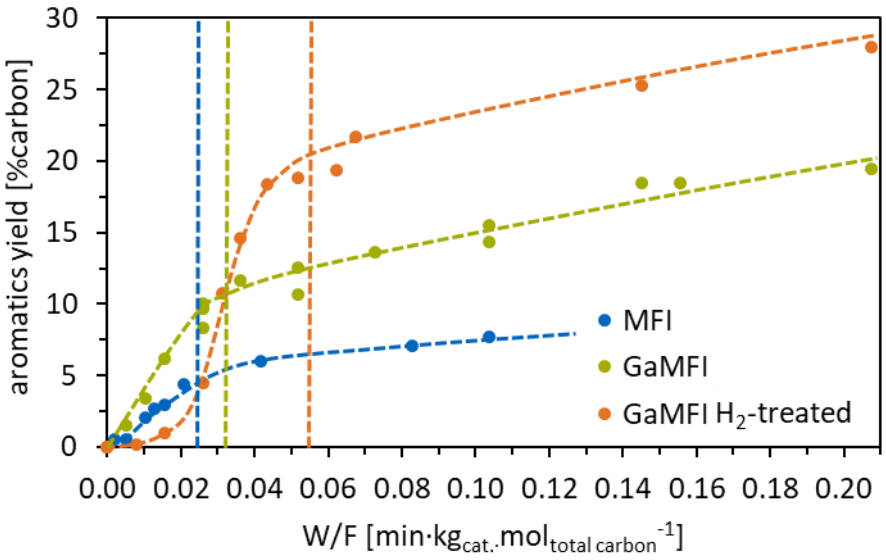

Figure 3: Yield (in %carbon) of aromatics versus the contact time. Dashed lines indicate the contact time when full conversion is reached. The initial DME partial pressure is kept constant at 90mbar under N_2 dilution and ambient pressure, Temperature = 748 K.

Propylene is the most abundant olefin product and thus the yield of propylene is used to follow the formation of olefins with increasing W/F (Fig. 4). A significant decrease of olefin yield from MFI to the GaMFI H_2-treated can be observed, correlating with the increase in aromatic yield. It can be furthermore observed that all samples display a maximum of propylene yield at contact times close after full conversion. This can be explained by the transition from C_{3-5} olefin formation via methylation in the olefin cycle[38-39] to consumption of olefins in hydrocarbon interconversion reactions - such as hydride transfer - once MeOH/DME is not available. All these reactions of olefin formation (by methylation) and consumption (by formation of aromatics and alkanes via HT) are catalyzed by BAS.[15, 37] Thus, the fact that the general shape of the olefin yield vs contact time does not change with Ga modification – for all samples the maximum propylene yield is observed at ca. 1.4 times the contact time necessary to reach full conversion - supports the hypothesis that presence of the Ga does not affect BAS catalyzed reactions (although it affects the concentration of available BAS for such reactions).

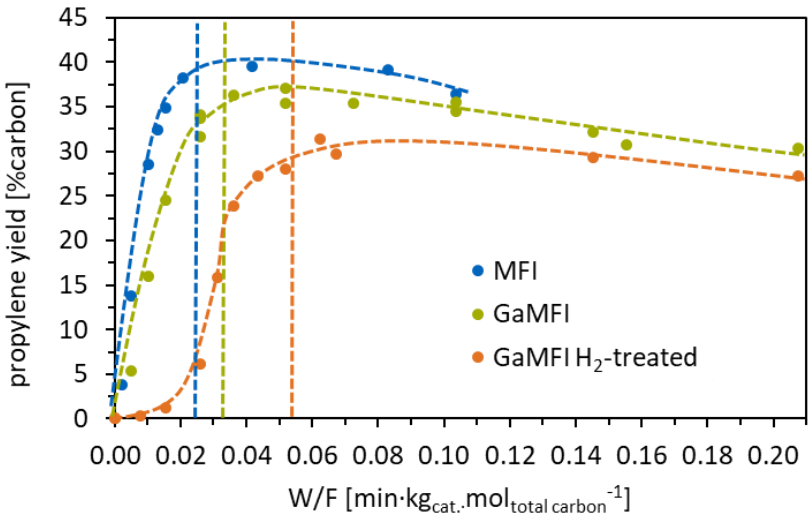

Figure 4: Yield (in %carbon) of propene versus the contact time. Dashed lines indicate the contact time when full conversion is reached. The initial DME partial pressure is kept constant at 90mbar under N_2 dilution and ambient pressure, Temperature=748 K.

Aromatics are formed over MFI zeolites via HT processes. These reactions are predominantly occurring between olefins at high or full conversions (olefin-induced hydrogen transfer, OIHT) and, at low conversions, between MeOH/DME and olefins (methanol-induced hydrogen transfer, MIHT). Stoichiometric amounts of H-rich byproducts (usually in the form of light alkanes) are formed together with aromatics as a result of the hydrogen transfer reactions. Remarkably, the yield of alkanes does not change significantly with Ga modification, as can be seen in Fig. 5. Therefore, the, in terms of H_2 balance, additional selectivity to aromatics achieved by Ga-modified samples observed in Fig. 3 must be associated to dehydrogenation reactions.

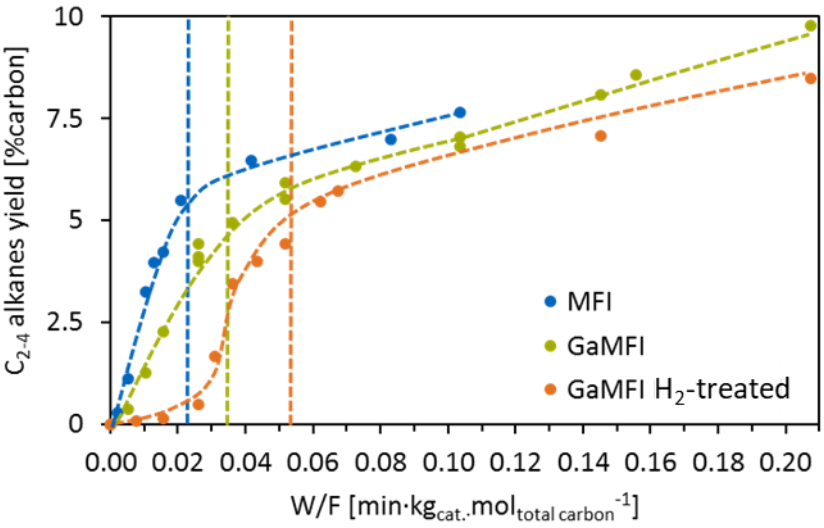

Figure 5: Yield (in %carbon) of C_{2-4} alkanes versus the contact time. Dashed lines indicate the contact time when full conversion is reached. The initial DME partial pressure is kept constant at 90 mbar under N_2 dilution and ambient pressure, Temperature = 748 K.

4.2.2 Contribution of different hydrogen transfer pathways on the formation of aromatics

There are 4 different reaction pathways for the formation of aromatics from MeOH/DME feeds on acid zeolites. As already mentioned, the main pathways for formation of aromatics from olefins in acid zeolites are the methanol induced hydrogen transfer (MIHT) and the olefin induced hydrogen transfer (OIHT) routes, both leading to concomitant formation of C_{2-4} alkanes. The MIHT is significantly faster than the OIHT when oxygenates are available[15] and it does not exist in the absence of them beyond the point of full MeOH/DME conversion. Consequently, we approximate the formation rate of alkanes at partial conversions to the MIHT rate, and to the OIHT rate at full conversions. A third pathway recently proposed in acid zeolites is the hydrogen transfer between oxygenates resulting in the formation of methane and HCHO that consecutively react via Prins-type reactions to the formation of aromatics.[40] Although the rate of this hydrogen transfer reaction is very low,[40] it is of significance during the initiation period of MTH, where only C_1 species are available for reaction, and the CH_4 formed by this pathway in first layers of the catalytic bed must be taken into account in H_2 balances. Finally, the introduction of dehydrogenation activity on a zeolite via metal or metal cation modifications provides a fourth route of formation of aromatics, as shown in Scheme 1. This last pathway is the desired one, as no carbon atoms are lost due to the formation of unwanted byproducts.

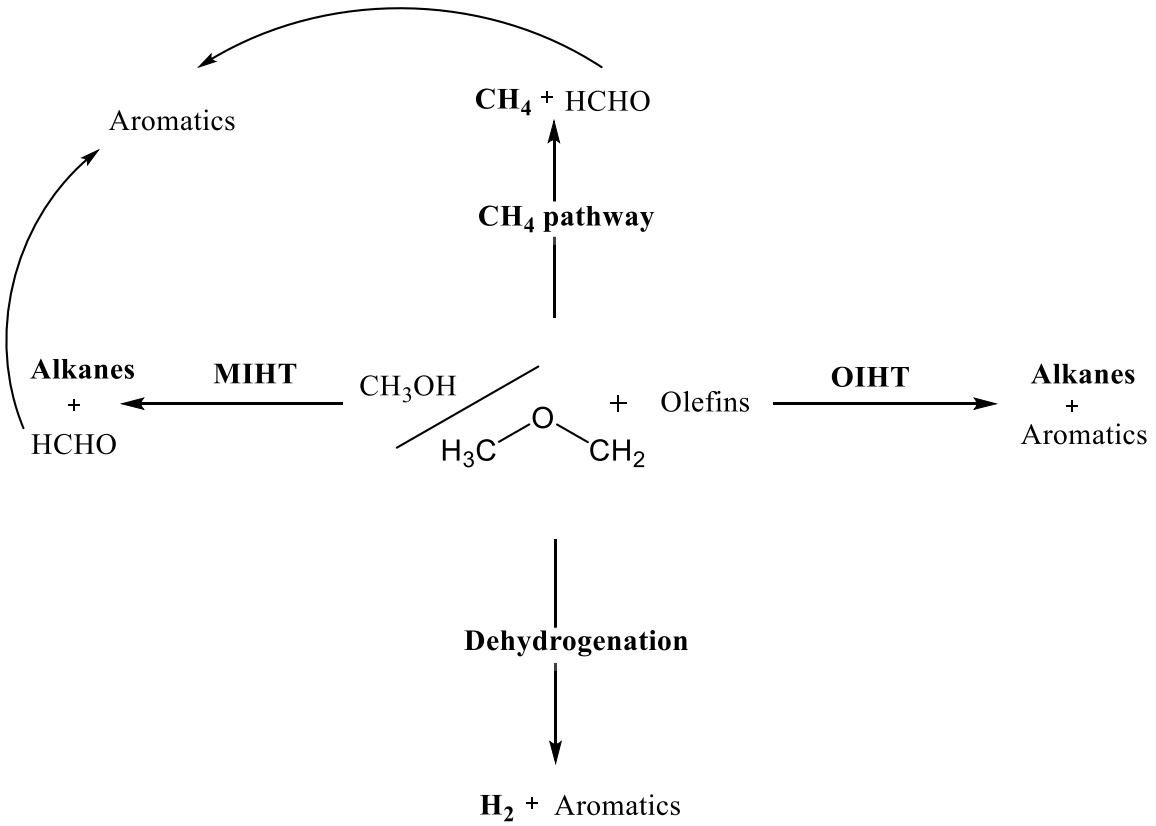

Scheme 1: Pathways of Hydrogen transfer/Dehydrogenation reactions enabling the formation of hydrogen poor carbon species. Decomposition of MeOH into methane and hydrogen poor C_1 species (CH_4 pathway), olefin induced hydrogen transfer (OIHT), dehydrogenation and methanol induced hydrogen transfer (MIHT) reactions.

In order to maximize the amount of produced aromatics and to understand the role of Ga-modification, it is crucial to evaluate to which degree the different pathways shown in Scheme 1 contribute to the overall yield. We perform such evaluation by following the respective hydrogen rich species which are produced by each pathway. These H-rich species, namely alkanes and H_2, can be considered end products, because of their low reactivity under MTH reaction conditions. First it is necessary to evaluate how much hydrogen is available in the reaction mixture that could be theoretically converted into H_2, CH_4 or C_{2-4} alkanes. We assume that all O atoms in the feed are ultimately converted into H_2O in the MTH reactions, and that water molecules once formed will not participate again in reactions with hydrocarbons. The remaining CH_2-units, once the H_2 necessary to form H_2O has been subtracted, define the C:H ratio as 1:2 for all hydrocarbon interconversions. In other words, the molar amount of H_2-units available can be calculated based on the molar carbon flow introduced as MeOH (or DME equivalents) in the system. Note that both the MIHT and the OIHT pathways produce alkanes as hydrogen rich products and, therefore, we have lumped them together as “alkane pathway”. Thus, in order to establish quantitative comparisons between the routes producing different hydrogen rich carbon species, we define the equivalent of H_2 molecules based on the deviation of H/C ratio from the average ratio of 2:1 for

instance, one molecule of CH_4 (H/C = 4) has an excess of 2 H atoms and is equivalent to one molecule of H_2.

The values for the rate of formation of the different H-rich products (expressed as H_2 equivalents) are calculated from the first derivative of the respective yield vs contact time curves (Fig. 6) and the values obtained are summarized in Table 3. Fig. 6A shows the overall contribution of the 4 different pathways in Scheme 1 on the aromatic formation rates in the MTA reaction on GaMFI H_2-treated. Fig. 6B-D show the H_2 transferred yields via the different pathways over the three tested catalysts, based on the H-acceptor reference molecules: alkanes for MIHT and OIHT, methane for HT between C_1-species, and H_2 for Ga catalyzed dehydrogenation.

Table 3: Rate of the different H-transferring pathways over MFI, Ga-modified MFI and the Ga-modified MFI after pretreatment with hydrogen.

	H-transfer rate [%H_2·mol·min^{-1}·kg$_{cat}^{-1}$]			
pathways	**Methane**	**MIHT**	**OIHT**	**H_2**
MFI	52[a]	73	8	0
GaMFI	111[a]	55	8	29
GaMFI H_2-treated	107[a]	63	7	290[b]
				33[c]

A: Initial rates
B: Max. rate between 10 - 70 C% conversion
C: Rate at full DME conversion

The alkane pathway (Fig. 6B) shows for all samples a contact time curve similar to the one described by Müller et al.[15] At the initial stage, alkanes are not formed because the concentration of olefins available is still too low. In case of GaMFI H_2-treated the MIHT pathway reaches its maximum rate in the contact time range from 0.025 to 0.055 min·kg·mol^{-1}. At full conversion, MIHT is suppressed and OIHT is the only pathway responsible for the formation of alkanes. This pathway is known to have low rates in comparison to MIHT,[15] thus the overall yield of alkanes at total conversion does not significantly increase with contact time. The rate of formation of alkanes at full conversion is similar for all samples (Fig. 6B, Table 3). The MIHT rates differ slightly between the 3 samples but do not show a correlation with the catalyst parameters (Table 2). Based on these observations, we conclude that the presence of Ga does not significantly affect MIHT and OIHT pathways. The shift towards longer contact times of the curve for the GaMFI H_2-treated sample is attributed to its lower concentration of BAS (Table 2) and subsequent overall lower activity (Fig. 2).

The methane formation signalizes the contribution of hydrogen transfer between C_1 oxygenates and consecutive formation of aromatics via Prins-type reactions with HCHO.[40] The rate of formation of CH_4 is high at low conversions and decreases with decreasing MeOH/DME partial

pressure at higher contact times (Fig. 6C). After full MeOH/DME conversion the amount of formed methane slightly decreases in case of the Ga-containing samples and especially over the GaMFI H_2-treated. This can be attributed to activation of methane over the Ga-sites to form gallium-methyl species[41] and consecutive reactions of methylation of existing aromatics together with additional H_2 formation.[41-42] The formation of methane (Fig. 6C) takes place on all 3 samples, although the rate is about a factor of 2 higher for the Ga-modified samples (Table 3). In any case, the extent of the contribution of this pathway to the total yield of aromatics is ultimately subordinated to the contact time at which significant amounts of olefins are formed and methylation reactions take over. This is so, because formation of CH_4 and HCHO is only significant in the initiation stage, where only C_1-species are available as hydrogen acceptors. This way, the lower overall MTH activity of GaMFI H_2-treated sample translates into a larger fraction of the catalytic bed in which HCHO can be formed and thus a higher concentration of HCHO is available on the catalyst for the formation of aromatics via Prins-type reactions.[40]

The dehydrogenation over GaMFI H_2-treated (Fig. 6D) follows an S-shape comparable to the conversion of MeOH/DME (Fig. 2) but with an initial slope different from 0, indicating that this catalyst is also able to dehydrogenate C_1 substrates during the initiation period. Beyond the point of full MeOH/DME conversion, the dehydrogenation rate decreases and remains constant independently of the contact time. It should be noted that dehydrogenation is the main aromatic formation pathway in the full conversion range for the H_2-treated Ga-MFI catalyst, as can be seen in Fig. 6A. Conversely, the reference unmodified MFI does not produce any measurable amount of H_2 under the reaction conditions. GaMFI shows a constant dehydrogenation rate at contact times beyond full MeOH/DME conversion. Interestingly, the dehydrogenation rate of GaMFI H_2-treated, while being one order of magnitude higher in the W/F range from 0.02 to 0.04 min·kg·mol^{-1} drops to a value similar to the rate in the untreated GaMFI when DME/MeOH conversion exceeds 90 C% (at 0.4 min·kg·mol^{-1}) (Table 3).

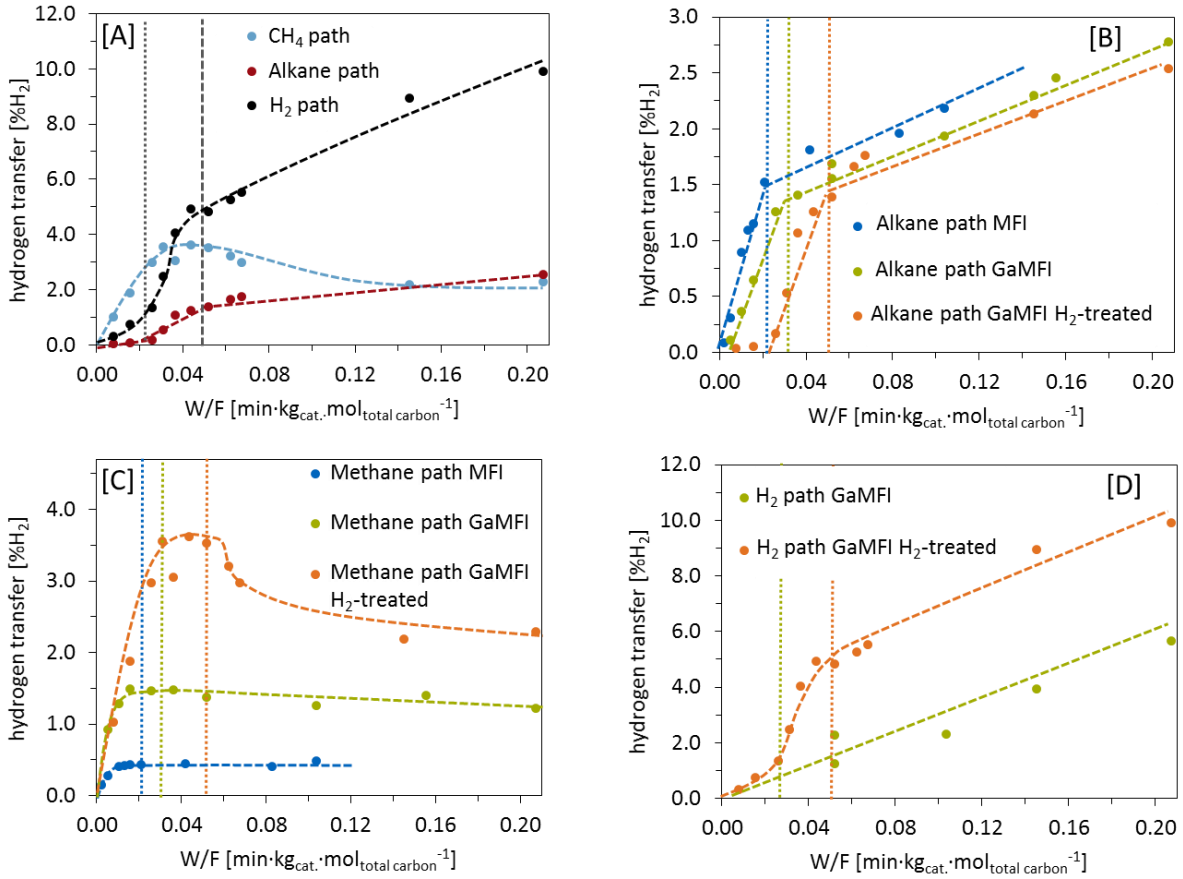

Figure 6: A: H-acceptor yields expressed as transferred H_2 equivalents (in % of the total available H_2 units in the available hydrocarbons) versus contact time over GaMFI H_2-treated. The grey dotted line marks the contact time necessary for 10 C% DME/MeOH conversion the dashed line the point of full conversion. B-D: Transferred hydrogen molecules versus contact time separated per pathway (alkane path (B), methane path (C) and the dehydrogenation path (D)) for MFI (blue), GaMFI (green) and GaMFI H_2-treated (orange). In case of the dehydrogenation path, the amount of H_2 produced over MFI is below the detection limit (< 0.5 %H_2). Dotted lines indicate the contact time when full conversion is reached. The initial DME partial pressure is kept constant at 90mbar under N_2 dilution and ambient pressure, Temperature = 748 K.

Comparing the three pathways for GaMFI H_2-treated catalyst, it is concluded that the MIHT and OIHT pathways are only a minor contribution to the formation of aromatics on this catalyst. For instance, at the chosen W/F-reference contact time of 0.1 min·kg·mol^{-1}, only ~ 15% of the overall amount of hydrogen have been transferred via this pathway (Table 4). Conversely, a ~ 63 % fraction of H_2-equivalents is transferred via hydrocarbon dehydrogenation under the same conditions. The methane pathway seems to be highly relevant in the first part of the catalyst bed, where initiation reactions are taking place. An influence of Ga species on the rates for this pathway can be also observed, although further analysis of its significance is out of the scope of this work. In any case, there is no further contribution of this pathway past the point of 50 C% conversion, as can be seen by the near 0 or slightly negative slope of methane formation in Fig. 6C.

The extent of the contribution of the aromatic formation pathways in Scheme 1 to the total aromatic formation reveals significant differences between MFI, GaMFI, and H_2-treated Ga-MFI. A comparison in terms of aromatics yields and H_2-acceptor yields is offered in Table 4. In the parent MFI zeolite, alkanes are the predominant form of H-acceptor species, with over 80 % of the transferred hydrogen following the MIHT + OIHT pathways at W/F=0.1 min·kg·mol^{-1}. The rest of the contributions comes from the formation of methane. For the GaMFI, all pathways contribute to a similar extent – 38 % dehydrogenation, 34 % MIHT+OIHT and 28 % Methane - at the chosen contact time. At full conversion, the dehydrogenation rate on GaMFI is over 3 times higher than the OIHT rate. This indicates that the formation of aromatics via dehydrogenation is dominant in the presence of Ga. Interestingly, in the full conversion region the rates of OIHT and dehydrogenation on H_2-treated GaMFI are identical to rates on untreated GaMFI (Table 3). This observation will be further discussed in the next section.

Table 4: Yields of aromatics and the different hydrogen rich species over three catalyst at a chosen W/F value of 0.1 min·kg$_{cat}$·mol^{-1}. The initial DME partial pressure is kept constant at 90 mbar under N_2 dilution and ambient pressure, Temperature = 748 K.

	At W/F= 0.1 [min·kg·cat·mol^{-1}]				
			Y H-acceptor [%H_2]		
	X [C%]	Y aromatics [C%]	Methane	Alkanes	H_2
MFI	100	7.5	0.50	2.20	0.00
GaMFI	100	15.0	1.48	1.80	2.00
GaMFI H_2-treated	100	23.5	2.55	1.75	7.40

4.2.3 Role of different acid sites in HT transfer pathways

Having shown the contributions of the different HT pathways to the formation of aromatics over the GaMFI H_2-treated and the MFI and untreated GaMFI reference catalysts, we investigate next the participation of the different active sites in the different pathways.

The lower concentration of BAS in GaMFI and in the H_2-pretreated GaMFI clearly causes an overall lower activity of the samples during the initiation period (Fig. 2). However, these changes in acid site concentration do not have a significant effect for BAS-catalyzed reactions at full MeOH/DME conversion.

It was proposed by Müller et al.[15] that the rate determining step of the MIHT is catalyzed on LAS. However, in spite of the clear increase in LAS concentration obtained by introduction of Ga (Table 2), relatively similar rates of alkane formation via MIHT were obtained for all 3 samples (Fig. 6B and Table S1). This indicates a mild effect of Ga species on MIHT rates, probably because the additional LAS introduced by Ga are of different nature than the LAS examined on MFI studies.

We also did not observe any significant differences in the OIHT rates by Ga modification. This is not surprising, as the HT reactions in this pathway are solely catalyzed by BAS.[15, 38] On the other hand, the concentration of BAS in the H_2-treated GaMFI is ca. 50 % of the concentration in the parent MFI (Table 2) and, therefore, a lower OIHT rate was to be expected on this sample. The lower concentration of BAS in Ga-MFI and in the H_2-pretreated GaMFI clearly causes an overall lower activity of the samples during the initiation period (Fig. 2). However, these changes in acid site concentration do not have a significant effect for BAS-catalyzed reactions at full MeOH/DME conversion.

The rate of the methane formation is roughly doubled in presence of Ga as can be seen by the increase in the initial slope in Fig. 6C (numerical values in Supporting Table S1). However it does not seem to be relevant if the sample is reduced before reaction or not. The decomposition of oxygenates into methane, formaldehyde and CO is in most MTH studies attributed to the BAS,[21-22, 43] but there are also studies showing that these reaction steps can occur on Lewis acidic metal oxides[44]. Based on the increase of LAS while the BAS decrease in the presence of Ga (Table 2), we speculate that both Ga and Al-related LAS might participate in the formation of CH_4, compensating the lower BAS concentration on Ga-modified samples.

Finally, regarding the dehydrogenating pathway, it is clear that MFI does not generate a measurable amount of hydrogen, while both Ga modified samples show dehydrogenation activity. In particular, the H_2-treated GaMFI catalyst shows a dehydrogenation rate 3.5 times higher than

the untreated GaMFI averaged until full conversions, and its maximum rate in this region is even one order of magnitude higher. This difference, however, is difficult to explain and it is likely related to the addition of several effects. Among them, the dehydrogenation of part of the CH_4 formed (as shown in Fig. 6C) might be of considerable significance at contact times in the range of 0.02 to 0.04 $min \cdot kg \cdot mol^{-1}$. As CH_4 is formed at very short contact times, it is available for dehydrogenation before large amounts of aliphatics are present. Thus, the ability to activate CH_4 via dehydrogenation leads to an increased H_2 formation rate over H_2-treated GaMFI during the initiation period. All in all, what can be said without speculation is that, once that most of MeOH/DME is converted, the influence of the H_2 pretreatment cannot be seen any more in the dehydrogenation rates. Furthermore the pre-reduction treatment is expected to have a positive effect on the dehydrogenation activity. While it is reported that Lewis acid gallium oxide – as present in GaMFI – can be the active site for the dehydrogenation[45] step, the findings of Schreiber et al.[27] and Gao et al.[31] show an enhanced dehydrogenation rate as result of pre-reducing the catalyst. This effect is explained by the proximity of strong BAS and Lewis-acidic Ga-sites blocking BAS as depicted in Fig. 1. This hypothesis is supported by the findings depicted in Fig. 6D as the GaMFI H_2-treated shows a significantly higher initial rate compared to the GaMFI. The formation of Ga-blocked BAS is also supported by the significant decrease in BAS (Table 2) and is thereby an evidence for the proposed two-site dependent mechanism. The fact that after full MeOH/DME conversion, no difference between the GaMFI and the GaMFI H_2-treated is observed, could point to a loss of these paired sites at higher contact time which is discussed in the next section.

4.2.4 Changes in the state of the Ga-active site

In the light of the results obtained from the analysis of the different HT and dehydrogenation pathways, the question arises about the origin of the catalytic improvement of Ga-modified MFI after H_2-treatment. Analysis of the different dehydrogenation pathways and the rates at different contact times as in Fig. 6 have shown that that there is not any significant difference in HT and dehydrogenation rates over GaMFI and GaMFI H_2-treated samples once full oxygenate conversion is reached. Thus, also the aromatics formation rate (Fig. 3) is similar for both samples under these conditions. This could be due to the changes in Ga-related active sites introduced by H_2 treatment, are reversible under reaction conditions of full conversion by, for instance, re-oxidation in H_2O and/or redispersion of Ga-species.

In order to study the changes in the Ga-species originated from H_2O, IR measurements of a Ga-MFI sample before and after H_2 treatment are compared with the same region after H_2O treatment (30 mbar of H_2O at 748 K for 30 min) (Table 5, spectra in Support S2). It can be seen a decrease of the relative value of BAS concentration (based on SiAlOH band deconvolution) of 68 % on GaMFI after exposure to H_2. This result is in good agreement with the results of pyridine adsorption (Table 2). When the GaMFI is exposed to H_2 first and then to H_2O, its BAS concentration increases again up to 95 % of the initial value.

The activity of a GaMFI was also compared to the same sample after H_2 treatment and after H_2 and consecutive H_2O treatment. As can be seen in Fig. 2, the overall activity in MTH of Ga-MFI is significantly lower after reductive treatment, but it is restored if exposed to water after reduction (S3). Based on this observation, we conclude that the blockage of BAS by reduced Ga-species is partially reversed by introduction of water. We hypothesize that the water formed during the conversion of DME is able to regenerate the BAS. Thus, under dry conditions, a significant difference in reactivity between the GaMFI and the GaMFI H_2-treated is verified at the beginning of the catalyst bed, originating the differences in selectivity and activity observed in Fig. 2-6. Schreiber et al. proposed the presence of water will result in reestablishing protons on the before blocked BAS while forming of Ga_xO_y species and H_2.[27] At high or full MeOH/DME conversions, the H_2O content in the gas phase is significant, because it is a byproduct of the MTH reaction. Thus, this water effect could explain the increase of BAS concentration observed after exposure to water and the fact that the catalytic performances of GaMFI H_2 treated becomes similar to untreated GaMFI at high conversions.

Table 5: BAS concentration of GaMFI as determined in an in situ IR cell after being exposed to H_2 or H_2 and water. The BAS concentration is determined via the SiAlOH-band deconvolution in N_2-atmosphere.

Exposure to	Fraction of initial BAS concentration [%]
H_2 [169mbar,150 min, 773K]	68
H_2 [169mbar,150 min, 773K] + H_2O [30mbar,40 min, 748K]	95

In order to prove this hypothesis also under MTH conditions, water was co-fed along with DME over the GaMFI H_2-treated, in concentrations similar to those achieved in the catalyst after full conversion of DME. The catalytic tests (Fig. 7) show that in presence of H_2O the catalyst mass necessary to overcome the initiation period (i. e., to reach 5 C% conversion) is reduced by 25 % (from W/F 0.0215 to 0.0155 min·kg·mol^{-1}). As mentioned above, this overall increase of activity in presence of water might be related to an increase in BAS. Note that, for the untreated GaMFI sample, the effect of cofeeding water is small and, if anything, it slightly decreases the overall activity, in good agreement with reported H_2O effects on MTO over H-MFI[22, 35]. On the other hand, the selectivity towards aromatics, decreased over the GaMFI H_2-treated in presence of H_2O: Instead of 3.3 C% only 2.9 C% are found at 25 C% conversion (compared to 1.6 C% over GaMFI). This increase of activity together with the lower aromatic selectivity points also to the regeneration of part of the covered BAS in the presence of H_2O.

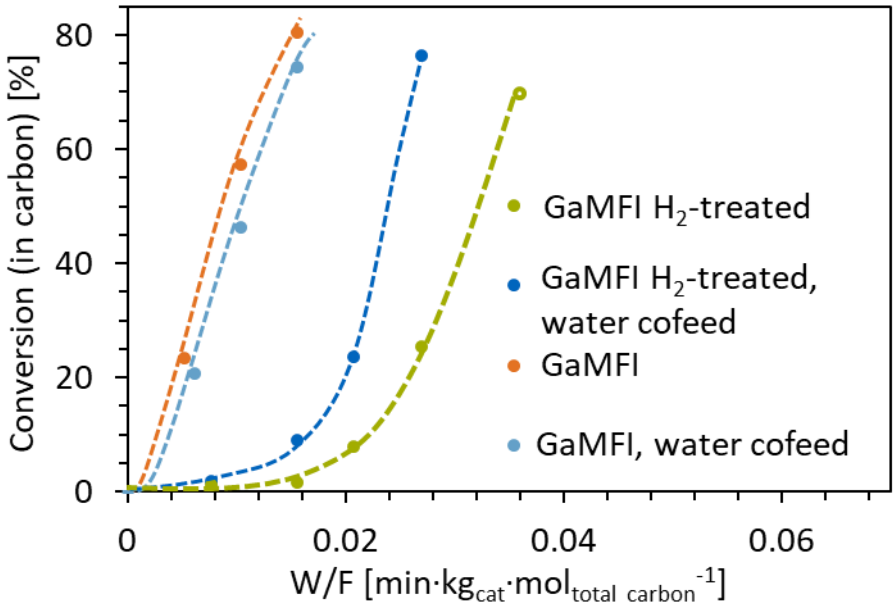

Figure 7: Conversion of DME and MeOH versus contact time over GaMFI and H_2 treated GaMFI. Orange: 90 mbar DME in N_2 over GaMFI, light blue: 90 mbar DME and 45 mbar H_2O in N_2 over GaMFI. Green: 90 mbar DME in N_2 over GaMFI, dark blue: 90 mbar DME and 45 mbar H_2O in N_2 over GaMFI. Reaction temperature = 748 K. The hollow point in the GaMFI H_2 treated is calculated based on the results of measurements with GaMFI H_2-treated at slightly different conditions.

The fact that the conversion curves of the two samples under water co-feed do not fully converge could be due to an only partial regeneration of the BAS in presence of H_2O and hydrocarbons. It is hypothesized that the adsorption of hydrocarbons on Ga and BAS hinders the migration of Ga out of the zeolite pores and thereby stabilize partially the reduced catalyst in contrast to exposing it to pure water atmosphere (Table 5, S3). Thus, the GaMFI H_2-treated in presence of H_2O and hydrocarbons will not show the exact same activity as the untreated GaMFI.

To sum up, we conclude that the benefit of the H_2-treatment depends heavily on the contact time and thus reaction zone in MTH. At partial conversion or close to full conversion, treating a Ga-MFI with H_2 achieves to more than double the yield of aromatics, because both faster dehydrogenation rates and slower (BAS related) methylation rates are verified. If large contact times are used that provide a significant fraction of the catalytic bed dedicated to further converting hydrocarbons into aromatics in absence of oxygenates, the relevance of the H_2 pretreatment decreases.

4.3 Conclusions

The addition of Ga via incipient wetness impregnation on MFI increases the selectivity of the catalyst towards aromatics while having a minor negative effect on the catalysts ability to convert DME. This effect is mainly based on the introduction of dehydrogenation functionality of the Lewis acidic Ga sites while the contribution of BAS catalyzed hydrogen transfer processes producing alkanes is not significantly affected. The presence of Ga moreover doubles the formation rate of methane during the initiation period. This reaction is associated to the generation of HCHO intermediate[40] and subsequent formation of aromatics in later sections of the catalytic bed.

The additional functionalities introduced by Ga-modification are shown here to be highly beneficial for the conversion of DME into aromatics without converting large quantities of carbon into undesired alkanes.

Reduction of Ga with hydrogen before reaction causes a significant decrease of BAS, resulting in a further decrease of DME conversion capability. This is attributed to the blocking of BAS by further dispersion of reduced Ga-species. The such created sites increase the dehydrogenation rate. In combination this leads to an increase of aromatics selectivity of about a factor of four until full conversion is reached. In sections of the catalyst bed after full MeOH/DME conversion, we do not observe any influence of the hydrogen treatment on the dehydrogenation or hydrogen transfer rates. This is attributed to either a decrease of the Ga-species dispersion and subsequent decrease on the concentration of BAS-Ga sites, and/or reoxidation of part of Ga^{+} species to Ga^{3+} by the water formed from the dehydration of MeOH/DME conversion. However, overall yields of aromatics and H_2 are significantly higher in H_2-treated GaMFI, as an accumulated consequence of the higher dehydrogenation yields at lower contact times. Based on these findings the use of MeOH as feed or even co-feeding water in order to increase the selectivity to aromatics[16] seems not advisable in combination with pre-reducing the catalyst but explains why this procedure is so beneficial in alkane dehydrogenation. In a water free hydrocarbon environment, the formed pairs of Ga-BAS and BAS are expected to be stable over the full length of the catalyst bed and thereby increase the dehydrogenation activity.

These findings provide an insight into the mechanism of the formation of aromatics from DME over Ga containing zeolites. The relevance of the different reaction pathways along the catalyst bed has been elucidated. Investigating changes of the catalyst properties under reducing atmosphere prior to the catalytic reaction and the durability of these changes under reaction conditions provide a manual for when and how to pretreat catalyst for optimized performance.

4.4 Methods

4.4.1 Materials

H-ZSM-5 zeolite was provided by Clariant Produkte (Deutschland) GmbH. DME (≥ 99.9 %), was supplied by Sigma-Aldrich. The introduced deionized water was further purified by an EASYpure II RF-Compact-Water filter by Barnstead. Ga was loaded on the zeolites via incipient wetness impregnation from a $Ga(NO_3)_3$ solution (purity > 99 %, provided by Sigma Aldrich) as described by Schreiber et al.[27]

4.4.2 Catalytic testing

All catalytic results were obtained using a fixed bed quartz reactor with an internal diameter of 6 mm at 748 K and ambient pressure. The catalyst particles (200-280 µm) were homogeneously diluted with silicon carbide (ESK-SiC) in the range of 355-500 µm to ensure temperature uniformity in the catalytic bed. Catalysts were activated at 748 K for 1 h under N_2 atmosphere before the reaction or in case of the H_2-pretreatment activated for 0.5 h under N_2 atmosphere and for 1 h under H_2 atmosphere at 773 K.

DME, N_2 and H_2 were introduced by a Bronkhorst MFC.

The reactor effluents were transferred via a heated line into a gas chromatograph (HP 5890) equipped with a HP-PLOTQ capillary column. The product distributions are given on a carbon basis. Hydrogen was detected by a Pfeiffer Omnistar GSD 320 mass spectrometer and is given as percentage of the overall included amount of H_2-units in hydrocarbons.

In all reactions DME and MeOH are lumped as reactants for the calculation of the overall conversion

4.5 References

1. Meisel, S., Gasoline from methanol in one step. *CHEMTECH;(United States)* **1976,** *6* (2).
2. Olsbye, U.; Svelle, S.; Bjørgen, M.; Beato, P.; Janssens, T. V. W.; Joensen, F.; Bordiga, S.; Lillerud, K. P., Conversion of Methanol to Hydrocarbons: How Zeolite Cavity and Pore Size Controls Product Selectivity. *Angewandte Chemie International Edition* **2012,** *51* (24), 5810-5831.
3. Tian, P.; Wei, Y.; Ye, M.; Liu, Z., Methanol to Olefins (MTO): From Fundamentals to Commercialization. *ACS Catalysis* **2015,** *5* (3), 1922-1938.
4. Sun, X.; Mueller, S.; Liu, Y.; Shi, H.; Haller, G. L.; Sanchez-Sanchez, M.; van Veen, A. C.; Lercher, J. A., On reaction pathways in the conversion of methanol to hydrocarbons on HZSM-5. *Journal of catalysis* **2014,** *317*, 185-197.
5. Anderson, M. W.; Klinowski, J., Solid-state NMR studies of the shape-selective catalytic conversion of methanol into gasoline on zeolite ZSM-5. *Journal of the American Chemical Society* **1990,** *112* (1), 10-16.
6. Zaidi, H.; Pant, K., Catalytic conversion of methanol to gasoline range hydrocarbons. *Catalysis Today* **2004,** *96* (3), 155-160.
7. Bjørgen, M.; Joensen, F.; Holm, M. S.; Olsbye, U.; Lillerud, K.-P.; Svelle, S., Methanol to gasoline over zeolite H-ZSM-5: Improved catalyst performance by treatment with NaOH. *Applied Catalysis A: General* **2008,** *345* (1), 43-50.
8. Conte, M.; Lopez-Sanchez, J. A.; He, Q.; Morgan, D. J.; Ryabenkova, Y.; Bartley, J. K.; Carley, A. F.; Taylor, S. H.; Kiely, C. J.; Khalid, K., Modified zeolite ZSM-5 for the methanol to aromatics reaction. *Catalysis Science & Technology* **2012,** *2* (1), 105-112.
9. Niu, X.; Gao, J.; Miao, Q.; Dong, M.; Wang, G.; Fan, W.; Qin, Z.; Wang, J., Influence of preparation method on the performance of Zn-containing HZSM-5 catalysts in methanol-to-aromatics. *Microporous and Mesoporous Materials* **2014,** *197*, 252-261.
10. Xin, Y.; Qi, P.; Duan, X.; Lin, H.; Yuan, Y., Enhanced performance of Zn–Sn/HZSM-5 catalyst for the conversion of methanol to aromatics. *Catalysis letters* **2013,** *143* (8), 798-806.
11. Townsend, A. T.; Abbot, J., Catalytic cracking of tetralin on HY zeolite. *Applied Catalysis A: General* **1992,** *90* (2), 97-115.
12. Mostad, H. B.; Riis, T. U.; Ellestad, O. H., Catalytic cracking of naphthenes and naphtheno-aromatics in fixed bed micro reactors. *Applied Catalysis* **1990,** *63* (1), 345-364.
13. Liu, C.; Deng, Y.; Pan, Y.; Gu, Y.; Qiao, B.; Gao, X., Effect of ZSM-5 on the aromatization performance in cracking catalyst. *Journal of Molecular Catalysis A: Chemical* **2004,** *215* (1), 195-199.
14. Boronat, M.; Viruela, P.; Corma, A., Theoretical Study of Bimolecular Reactions between Carbenium Ions and Paraffins: The Proposal of a Common Intermediate for Hydride Transfer, Disproportionation, Dehydrogenation, and Alkylation. *The Journal of Physical Chemistry B* **1999,** *103* (37), 7809-7821.
15. Müller, S.; Liu, Y.; Kirchberger, F. M.; Tonigold, M.; Sanchez-Sanchez, M.; Lercher, J. A., Hydrogen Transfer Pathways during Zeolite Catalyzed Methanol Conversion to Hydrocarbons. *Journal of the American Chemical Society* **2016,** *138* (49), 15994-16003.
16. Martinez-Espin, J. S.; Mortén, M.; Janssens, T. V.; Svelle, S.; Beato, P.; Olsbye, U., New insights into catalyst deactivation and product distribution of zeolites in the methanol-to-hydrocarbons (MTH) reaction with methanol and dimethyl ether feeds. *Catalysis Science & Technology* **2017,** *7* (13), 2700-2716.
17. Schulz, H., "Coking" of zeolites during methanol conversion: Basic reactions of the MTO-, MTP- and MTG processes. *Catalysis Today* **2010,** *154* (3–4), 183-194.

18. Müller, S.; Liu, Y.; Vishnuvarthan, M.; Sun, X.; van Veen, A. C.; Haller, G. L.; Sanchez-Sanchez, M.; Lercher, J. A., Coke formation and deactivation pathways on H-ZSM-5 in the conversion of methanol to olefins. *Journal of Catalysis* **2015,** *325*, 48-59.
19. Martínez-Espín, J. S.; De Wispelaere, K.; Janssens, T. V. W.; Svelle, S.; Lillerud, K. P.; Beato, P.; Van Speybroeck, V.; Olsbye, U., Hydrogen Transfer versus Methylation: On the Genesis of Aromatics Formation in the Methanol-To-Hydrocarbons Reaction over H-ZSM-5. *ACS Catalysis* **2017**, 5773-5780.
20. Schmidt, J. E.; Poplawsky, J. D.; Mazumder, B.; Attila, Ö.; Fu, D.; de Winter, D. A. M.; Meirer, F.; Bare, S. R.; Weckhuysen, B. M., Coke Formation in a Zeolite Crystal During the Methanol-to-Hydrocarbons Reaction as Studied with Atom Probe Tomography. *Angewandte Chemie International Edition* **2016,** *55* (37), 11173-11177.
21. Liu, Y.; Müller, S.; Berger, D.; Jelic, J.; Reuter, K.; Tonigold, M.; Sanchez-Sanchez, M.; Lercher, J. A., Formation Mechanism of the First Carbon–Carbon Bond and the First Olefin in the Methanol Conversion into Hydrocarbons. *Angewandte Chemie* **2016,** *128* (19), 5817-5820.
22. Kirchberger, F. M.; Liu, Y.; Tonigold, M.; Sanchez-Sanchez, M.; Lercher, J. A., Mechanistic origin of reactivity differences between methanol and dimethyl ether in their zeolite catalyzed conversion to hydrocarbons. *in preperation* **2019**.
23. Zhang, G. Q.; Bai, T.; Chen, T. F.; Fan, W. T.; Zhang, X., Conversion of methanol to light aromatics on Zn-modified nano-HZSM-5 zeolite catalysts. *Industrial & Engineering Chemistry Research* **2014,** *53* (39), 14932-14940.
24. Freeman, D.; Wells, R. P. K.; Hutchings, G. J., Conversion of Methanol to Hydrocarbons over Ga2O3/H-ZSM-5 and Ga2O3/WO3 Catalysts. *Journal of Catalysis* **2002,** *205* (2), 358-365.
25. Lopez-Sanchez, J. A.; Conte, M.; Landon, P.; Zhou, W.; Bartley, J. K.; Taylor, S. H.; Carley, A. F.; Kiely, C. J.; Khalid, K.; Hutchings, G. J., Reactivity of Ga 2 O 3 clusters on zeolite ZSM-5 for the conversion of methanol to aromatics. *Catalysis letters* **2012,** *142* (9), 1049-1056.
26. Lai, P.-C.; Chen, C.-H.; Hsu, H.-Y.; Lee, C.-H.; Lin, Y.-C., Methanol aromatization over Ga-doped desilicated HZSM-5. *RSC Advances* **2016,** *6* (71), 67361-67371.
27. Schreiber, M. W.; Plaisance, C. P.; Baumgärtl, M.; Reuter, K.; Jentys, A.; Bermejo-Deval, R.; Lercher, J. A., Lewis–Brønsted Acid Pairs in Ga/H-ZSM-5 To Catalyze Dehydrogenation of Light Alkanes. *Journal of the American Chemical Society* **2018,** *140* (14), 4849-4859.
28. Mansoor, E.; Head-Gordon, M.; Bell, A. T., Computational Modeling of the Nature and Role of Ga Species for Light Alkane Dehydrogenation Catalyzed by Ga/H-MFI. *ACS Catalysis* **2018,** *8* (7), 6146-6162.
29. Price, G. L.; Kanazirev, V., Ga2O3/HZSM-5 propane aromatization catalysts: formation of active centers via solid-state reaction. *Journal of Catalysis* **1990,** *126* (1), 267-278.
30. Price, G. L.; Kanazirev, V.; Dooley, K. M.; Hart, V. I., On the mechanism of propane dehydrocyclization over cation-containing, proton-poor MFI zeolite. *Journal of Catalysis* **1998,** *173* (1), 17-27.
31. Gao, P.; Wang, Q.; Xu, J.; Qi, G.; Wang, C.; Zhou, X.; Zhao, X.; Feng, N.; Liu, X.; Deng, F., Brønsted/Lewis Acid Synergy in Methanol-to-Aromatics Conversion on Ga-Modified ZSM-5 Zeolites, As Studied by Solid-State NMR Spectroscopy. *ACS Catalysis* **2018,** *8* (1), 69-74.
32. Pinilla-Herrero, I.; Borfecchia, E.; Holzinger, J.; Mentzel, U. V.; Joensen, F.; Lomachenko, K. A.; Bordiga, S.; Lamberti, C.; Berlier, G.; Olsbye, U.; Svelle, S.; Skibsted, J.; Beato, P., High Zn/Al ratios enhance dehydrogenation vs hydrogen transfer reactions of Zn-ZSM-5 catalytic systems in methanol conversion to aromatics. *Journal of Catalysis* **2018,** *362*, 146-163.
33. Freeman, D.; Wells, R. P.; Hutchings, G. J., Methanol to hydrocarbons: enhanced aromatic formation using a composite Ga2O3–H-ZSM-5 catalyst. *Chemical Communications* **2001,** (18), 1754-1755.

34. Chen, K.; Damron, J.; Pearson, C.; Resasco, D.; Zhang, L.; White, J. L., Zeolite Catalysis: Water Can Dramatically Increase Or Suppress Alkane C–H Bond Activation. *ACS Catalysis* **2014,** *4* (9), 3039-3044.
35. De Wispelaere, K.; Wondergem, C. S.; Ensing, B.; Hemelsoet, K.; Meijer, E. J.; Weckhuysen, B. M.; Van Speybroeck, V.; Ruiz-Martínez, J., Insight into the Effect of Water on the Methanol-to-Olefins Conversion in H-SAPO-34 from Molecular Simulations and in Situ Microspectroscopy. *ACS Catalysis* **2016,** *6* (3), 1991-2002.
36. Chang, C. D., Hydrocarbons from Methanol. *Catalysis Reviews* **1983,** *25* (1), 1-118.
37. Haw, J. F.; Song, W.; Marcus, D. M.; Nicholas, J. B., The mechanism of methanol to hydrocarbon catalysis. *Accounts of chemical research* **2003,** *36* (5), 317-326.
38. Ilias, S.; Bhan, A., Mechanism of the Catalytic Conversion of Methanol to Hydrocarbons. *ACS Catalysis* **2013,** *3* (1), 18-31.
39. Ilias, S.; Bhan, A., Tuning the selectivity of methanol-to-hydrocarbons conversion on H-ZSM-5 by co-processing olefin or aromatic compounds. *Journal of Catalysis* **2012,** *290*, 186-192.
40. Liu, Y.; Kirchberger, F. M.; Müller, S.; Eder, M.; Tonigold, M.; Sanchez-Sanchez, M.; Lercher, J. A., Critical role of formaldehyde during methanol conversion to hydrocarbons. *Nature Communications* **2019,** *10* (1), 1462.
41. Luzgin, M. V.; Gabrienko, A. A.; Rogov, V. A.; Toktarev, A. V.; Parmon, V. N.; Stepanov, A. G., The “Alkyl” and “Carbenium” Pathways of Methane Activation on Ga-Modified Zeolite BEA: 13C Solid-State NMR and GC-MS Study of Methane Aromatization in the Presence of Higher Alkane. *The Journal of Physical Chemistry C* **2010,** *114* (49), 21555-21561.
42. Choudhary, V. R.; Kinage, A. K.; Choudhary, T. V., Direct aromatization of natural gas over H-gallosilicate (MFI), H-galloaluminosilicate (MFI) and GaH-ZSM-5 zeolites. *Applied Catalysis A: General* **1997,** *162* (1), 239-248.
43. Nováková, J.; Kubelková, L.; Dolejšek, Z., Primary reaction steps in the methanol-to-olefin transformation on zeolites. *Journal of Catalysis* **1987,** *108* (1), 208-213.
44. Tindall, I. F.; Vickerman, J. C., The adsorption and reactions of methanol on clean and oxidised aluminium surfaces. *Surface Science* **1985,** *149* (2), 577-591.
45. Zheng, B.; Hua, W.; Yue, Y.; Gao, Z., Dehydrogenation of propane to propene over different polymorphs of gallium oxide. *Journal of Catalysis* **2005,** *232* (1), 143-151.

4.6 Supporting information

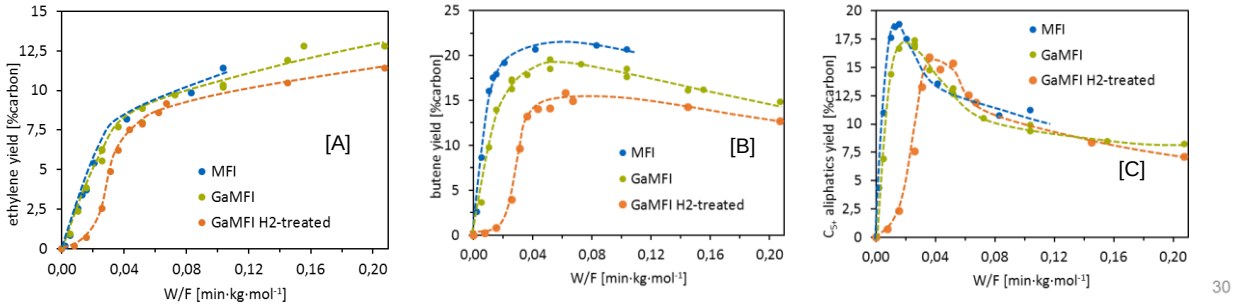

S1: Yield (in %carbon) of ethylene (A), butene (B) and C_{5+} aliphatics (C) versus the contact time.

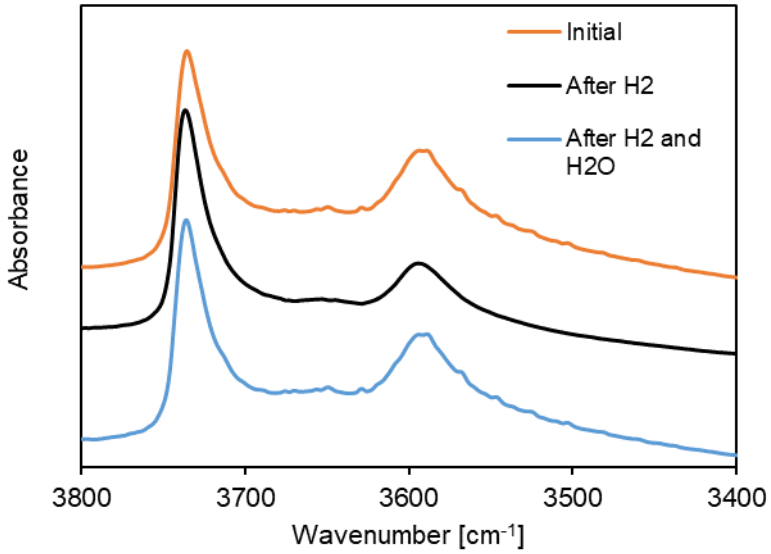

S2: Stacked IR spectra of GaMFI (orange), GaMFI after treatment with H_2 (169 mbar,150 min, 500 °C) (black) and GaMFI after treatment with H_2 (169 mbar,150 min, 500 °C) and afterwards H_2O + H_2O (30 mbar,40 min, 475 °C) (blue). The concentration of BAS is determined by integration of the signal at 3590 cm^{-1}.

S3: Conversion and yield of aromatics of GaMFI and after being exposed to H_2 or H_2 and water. The catalytic tests are conducted at 90 mbar DME partial pressure under N_2 dilution and ambient pressure. Temperature = 748 K.

Exposure to	Conversion [C%]	Aromatics Yield [C%]
-	96.4	10.2
H_2 [1013 mbar, 60 min, 773 K]	32.1	4.5
H_2 [1013 mbar, 60 min, 773 K] + **H_2O** [101 mbar, 30 min, 748 K]	90.9	7.5

4.7 Associated Content

Publication

This chapter is based on an article planned for submission (Felix M. Kirchberger, Yue Liu, Markus Tonigold, Maricruz Sanchez-Sanchez, Johannes A. Lercher)

Contributions

F.M.K. did main contributions in catalyst preparation, kinetic experiments, data analysis and manuscript preparation, Y.L. did the majority of characterization and contributed to data analysis; Y.L., M.T., M.S.-S. and J.A.L. conceived the research; The manuscript was written through contributions of all authors. All authors have given approval to the final version of the manuscript.

Acknowledgements

The authors acknowledge the support of the Bavarian Ministry of Economic Affairs and Media, Energy and Technology and Clariant Produkte (Deutschland) GmbH. Clara Eisebraun, Moritz Eder, Hanna Türk and Philipp Fischer are thanked for their helpful assistance in the experimental work.

5. Summary and Conclusion

Methanol and dimethyl ether are converted into hydrocarbons via multiple acid catalyzed reaction steps. Activity, product distribution and catalyst lifetime strongly depend on hydrogen transfer reactions involved in the overall MTH mechanism. Hydrogen transfer leads to the direct formation of non-olefinic byproducts or to the formation of highly reactive intermediates. Therefore, this thesis aims at the elucidation of hydrogen transfer reactions and the consecutive reactions of their products during the conversion of methanol and dimethyl ether over MFI zeolites.

It could be shown that formaldehyde – a product of MeOH/DME dehydrogenation – is present during the initiation and autocatalytic stages of the MTH process in concentrations up to 0.3 C%. It plays a major role in the formation of the first olefins, which occurs via condensation reactions to yield acetic acid or methyl acetate. These intermediates form ethylene or propylene by decarboxylation. In the autocatalytic stage, formaldehyde reacts with olefins via Prins reactions forming dienes and finally aromatics and coke. These reaction pathways were elucidated by using ^{13}C-labled formaldehyde. Additionally, it could be shown that the rate of the Prins reaction is one order of magnitude higher than hydrogen transfer between olefins over MFI catalysts, but still two orders of magnitude lower than the methylation reactions.

Methane was identified as the hydrogen acceptor and end-product of the hydrogen transfer reactions in the initiation stage and formation of first carbon-carbon bonds. Methane formation rate was therefore used to indirectly quantify the hydrogen transfer rates. Thereby the linear correlation between hydrogen transfer and carbon-carbon bond formation could be shown, which supports the crucial nature of hydrogen deficient species as formaldehyde or CO for the initiation of MTH conversion. Furthermore, it was found that dimethyl ether is one order of magnitude more reactive than MeOH in this hydrogen transfer step. This higher reactivity of DME explains the superior performance of H-ZSM-5 catalyst when pure DME is used. Conversely, there was not observed any significant differences between the net methylation rate of DME and MeOH. The overall lower methylation rates of MEOH-rich feeds are thus the consequence of the inhibiting effect of H_2O, as it reduces the number of available BAS-methoxy species for methylation.

In order to maximize the aromatics yield during the conversion of MeOH/DME to hydrocarbons, a sample was modified with a dehydrogenating center such as gallium ions. It was shown that Ga incorporation in MFI blocks part of the BAS of the zeolite while introducing additional LAS. Gallium containing MFI show a significant dehydrogenation activity and an increased activity for HT between C_1-species. Conversely the HT in presence of olefins - which produces the majority of aromatics in unmodified MFI - is not significantly altered. The dehydrogenation activity can be

enhanced by reducing the Ga-modified catalyst before exposing it to MeOH/DME. This effect is attributed to an additional dispersion of gallium and further blocking of acid sites. The effect of Ga reduction was shown to be reversible in the presence of water which makes the pre-treatment of the catalyst less relevant for later sections of the catalyst bed close to full MeOH/DME conversion and beyond, because water is produced during MTH and thus present on the catalytic bed.

In summary, the findings reported in this thesis provide a further insight in the reaction mechanisms responsible for initiating carbon-carbon bonds as well as for the formation of the different products during the MTH process. This information can help to choose catalyst properties and reaction conditions that optimize product selectivities and catalyst lifetime.